Immunogenicity of antigen-displaying virus-like particles and their use as a potential vaccine against prion diseases

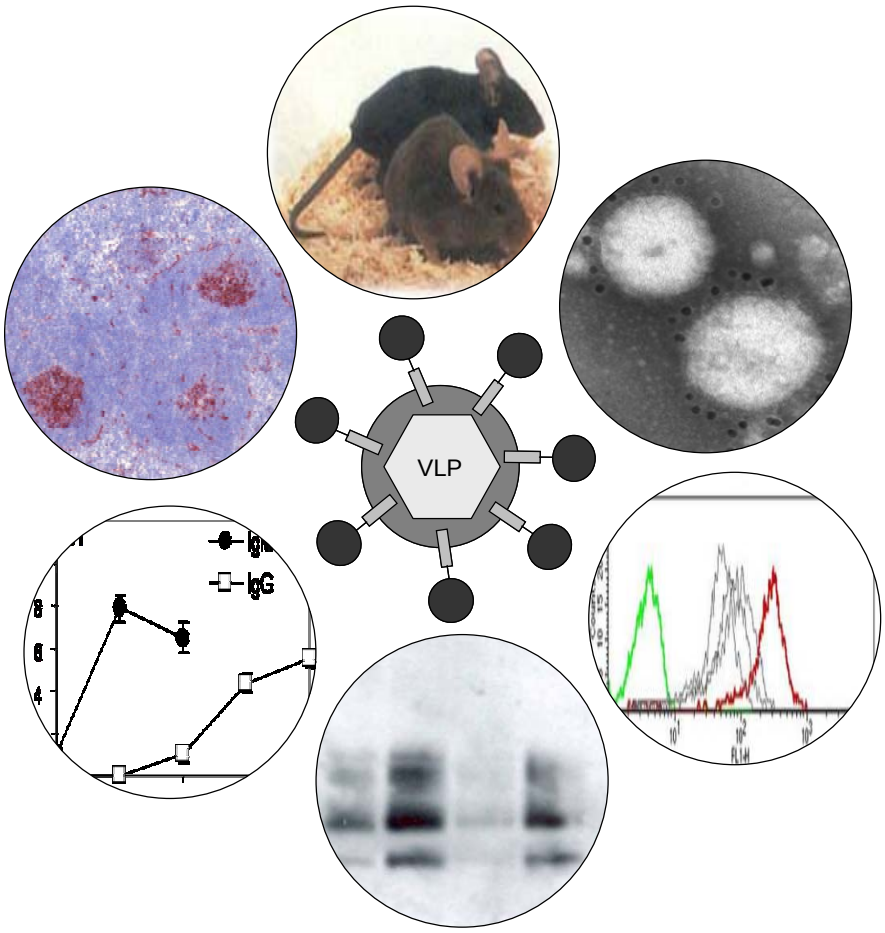

Patricia Bach

Immunogenicity of antigen-displaying virus-like particles and their use as a potential vaccine against prion diseases

Dissertation zur Erlangung
des naturwissenschaftlichen Doktorgrades
der Bayerischen Julius-Maximilians-Universität Würzburg

vorgelegt von

Patricia Bach

aus Offenbach am Main

Würzburg, 2007

Eingereicht am: 24.07.2007

Mitglieder der Prüfungskommission:

Vorsitzender: Prof. Dr. M. J. Müller

Gutachter: Prof. Dr. M. A. Klein

Gutachter: Prof. Dr. T. Raabe

Tag des Promotionskolloquiums: 12.12.2007

Doktorurkunde ausgehändigt am:

Für meine Eltern

„Zwei Dinge sind zu unserer Arbeit nötig: Unermüdliche Ausdauer und die Bereitschaft, etwas, in das man viel Zeit und Arbeit gesteckt hat, wieder wegzuwerfen."

Albert Einstein
deutscher Physiker und Nobelpreisträger

Table of contents

1 Introduction

1.1 The immune system protects hosts against infection with pathogens

1.1.1 Innate and adaptive immunity

The immune system represents a defense mechanism that protects an organism against many microbial infections by recognizing and eliminating pathogens. Furthermore, in case of some infections, the immune system has the remarkable capacity to maintain lifelong memory responses that protect against reinfection. The “innate” immune response serves as a first line defense against microorganisms. Immune cells contributing to “innate” immunity comprise natural killer (NK) cells, macrophages and different types of granulocytes. These immune cells non-specifically eliminate pathogens and infected cells by phagocytosis and destruction of infected cells. Innate immune cells of the host express pathogen recognition receptors (PRR) that are triggered by pathogen associated molecular patterns (PAMP). PRRs comprise different types of receptor families, such as Toll-like receptors (TLRs), RIG-like receptors, NOD-like receptors and presumably other yet unknown systems [Meylan et al., 2006]. TLRs are the best studied pattern-recognition receptors that bind a multitude of PAMPs. 12 members of the TLR familiy exist that are triggered by PAMPs such as LPS, double-stranded (ds) RNA, single-stranded (ss) RNA, prokaryotic DNA containing CpG motives and many others [Takeda et al., 2003; Akira et al., 2004; Kawai et al., 2006].

In contrast, the “adaptive” immune system has the ability to specifically recognize single pathogen species and to mount specific memory responses. Specific immunity is conferred by B and T lymphocytes. Similarly to all other immune cells, B cells differentiate from a common precursor in the bone marrow. Mature B cells recirculate and populate secondary lymphoid organs. Upon direct binding of antigen to the B cell receptor (BCR) and subsequent BCR crosslinking, B cells are activated and secrete immunoglobulins that show

the identical specificity as the BCR. In contrast, T cells derive from a T cell precursor that migrates from bone marrow to the thymus where T cells rearrange the T cell receptor (TCR). After positive and negative selection, mature T cells leave the thymus and populate secondary lymphoid organs. Unlike the BCR, the TCR recognizes protein fragments, i.e. peptides, displayed on self-molecules of the major histocompatibility complex (MHC). T lymphocytes are classified according to their surface receptor expression patterns and functions into two major subsets, $CD8^+$ cytotoxic T lymphocytes (CTL) that mediate lysis of infected cells and $CD4^+$ T helper (Th) cells which activate other immune cells. Within $CD4^+$ T helper cells, Th1, Th2, Th17, and Treg can be discriminated. Th1 cells participate in cell mediated immunity by controlling elimination of intracellular pathogens, whereas Th2 cells primarily participate in clearance of extracellular pathogens and provide help for B cells. Th17 cells have recently been identified as a unique IL-17 producing T cell subset that develops upon IL-23 stimulation and that promotes inflammatory processes [Tato et al., 2006]. $CD4^+$ T cells constitutively expressing CD25 on their surface can exhibit regulatory functions (Treg cells). The forkhead box transcription factor (Foxp3) is specifically expressed by Treg cells and plays a major role in the regulation of Treg development and function [Fontenot et al., 2005]. These cells are necessary for maintaining self-tolerance in new borns and for avoiding autoimmunity in adults [Shevach, 2000].

1.1.2 The induction of antibody responses

Upon pathogen encounter, antibody responses are usually induced and lifelong protective immunity is often maintained. Whereas T lymphocytes confer cellular immunity and exhibit effector functions, B lymphocytes contribute to humoral immune responses. Antibodies can control pathogens by various different mechanisms: binding of antibodies to viruses or intracellular bacteria prevents pathogens from entering cells, i.e. pathogens are directly neutralized. Furthermore, extracellularly replicating bacteria that are coated by antibodies can be efficiently eliminated by phagocytic cells which recognize the Fc-part

(constant region) of bound antibody, a process called opsonization. Finally, antibodies can trigger activation of the complement system. After binding of antibodies to the pathogen's surface and formation of a complement-antibody complex, serum complement components are activated through the classical pathway. The complement system comprises nearly 30 soluble plasma proteins that can be activated directly by pathogens or indirectly by antibodies bound to the surface of pathogens. Triggering of complement initiates a cascade of proteolytic cleavage reactions that finally results in formation of a complex formed by the final components of the cascade that perforates the pathogen's membrane and leads to direct killing of certain microorganisms.

In the periphery, pathogens are taken up by dendritic cells (DC). This antigen uptake activates DC and is followed by DC migration into the draining lymph nodes (LN). During migration, DCs undergo maturation that is characterized by upregulation of MHC class II and induction of the costimulatory molecules CD80 and CD86. In the LN, DCs present the processed antigen to lymphocytes. When DCs enter the T cell zone of LN, antigen-specific T cells bind antigen-derived peptides presented by MHC. For full T cell activation, in addition to the antigen-dependent TCR-MHC interaction, the CD28 receptor, which is constitutively expressed by T cells, has to interact with CD80 and/or CD86 on DC. Following activation, $CD4^+$ T cells proliferate and differentiate into Th cells, which move around to screen for antigen-specific B cells.

Upon antigen encounter, B cells migrate to the border between the B and T cell zone, and interact with T helper cells. Then, stimulated lymphocytes migrate to the T cell zone, proliferate and build "primary foci" where B cells also differentiate to plasmablasts. In addition, some B cells migrate to primary lymphoid follicle where they continue to proliferate and form germinal centers (GC).

1.1.3 Germinal Centers

Germinal centers (GC), which are also known as secondary follicles, are the sites of massive B cell proliferation and differentiation. Several studies showed

that BCR hypermutation and selection of high affinity BCR take place in GC [Jacob et al., 1991; Berek et al., 1991]. Furthermore, immunoglobulin subclass switch from IgM to IgG, IgA or IgE isotypes is initiated within the GC [Wolniak et al., 2004]. The switch is controlled by Th cells or by DC-derived cytokines [Schneider, 2005]. Following selection, B cells leave GC and differentiate either into memory B cells or to plasma cells [MacLennan, 1994; Nossal, 1994]. Memory B cells are primarily found in secondary lymphoid organs, whereas plasma cells home to the bone marrow to produce high levels of IgG.

In the GC, B cells undergo several important modifications. Firstly, low affinity B cells enter the follicle and proliferate in the dark zone. In this phase, B cells are also called centroblasts. After proliferation, the V-region DNA sequences of BCR undergo “somatic hypermutation”. Hypermutated B cells move into the light zone where they are called centrocytes. These centrocytes express surface Ig and are selected by a dense network of follicular dendritic cells (FDC) that continuously present antigen to activated B cells for high affinity binding. This process is called “affinity maturation” Certain GC B cells whose BCR lost specific binding during somatic hypermutation or evolved auto-specificity, are counter-selected and undergo apoptosis [Wolniak et al., 2004].

Within secondary lymophoid organs, B cells are present in the marginal zone (MZ). MZ B cells are specialised to quickly carry out T cell-independent (TI) IgM responses [Fagarasan et al., 2000; Gatto et al., 2004] and to initiate the early plasmablast wave during the first three days of an antibody response against TI antigens [Martin et al., 2000]. Generally, TI antigens are classified into two groups, TI-1 and TI-2 antigens. TI-1 antigens, such as LPS, are randomly organized structured antigens which have inherent mitogenic activity, whereas TI-2 antigens, such as bacterial capsular polysaccharides, have highly repetitive structures and activate B cells via multiple epitopes and BCR crosslinking. Due to their limited size, viruses can even reach the follicles to directly trigger follicular B cells [Gatto et al., 2004]. In general, GCs are found in both follicular and marginal zone B cell blasts. However, the majority of marginal zone B cells remain in the marginal zone as plasma cells to facilitate IgM and IgG-mediated opsonization of circulating pathogen. IgM antibody responses usually show a

very short serum half-life. Therefore, the IgM to IgG subclass switch is required to maintain elevated serum titers of neutralizing antibodies that confer long term protection. T cell-dependent (TD) rapid isotype class switch was shown to be essential for survival of a VSV infection [Thomsen et al., 1997]. The importance of the induction of various different IgG isotypes during viral infection is controversially discussed. In mice, viral infections frequently elict IgG2a responses [Coutelier et al., 1987].

1.2 Interferons

Interferon (IFN) was originally discovered on the basis of its antiviral activity [Isaacs et al., 1987]. IFNs are classified into two types, type I IFN that include IFN-α, IFN-β and IFN-ω and type II IFN, also termed IFN-γ. Type I IFN s directly induced upon virus infection of cells, whereas IFN-γ is synthesized only by certain cells of the immune system, including natural killer cells (NK), CD4 Th1 cells and CD8 suppressor cells [Bach et al., 1997]. Both types of IFN show primary sequence homology and use distinct cell surface receptors [Chen et al., 2004; Pestka et al., 2004]. Type I IFN includes small isogenic proteins encoded by up to 13 different IFN-α genes, depending on the species, and one IFN-β gene.

Type I IFN bind to a common surface receptor, the type I Interferon Receptor (IFNAR) [Branca et al., 1981]. The heterodimeric IFNAR is composed of two subunits, IFNAR1 and IFNAR2 [Lutfalla et al., 1992] which are members of the class II cytokine receptor family. Both subunits participate in ligand binding and intracellular signaling. In a first step, IFN binds to IFNAR2 that subsequently recruits IFNAR1 to form a complex that mediates signaling [Lamken et al., 2004].

Mice that are deficient in type I IFN receptor ($IFNAR^{-/-}$) are highly susceptible to infection with different viruses [Muller et al., 1994]. Furthermore, they are unable to establish an antiviral state, demonstrating that type I IFN plays an important role in host response to viral pathogens. Within the first hours after virus infection, a number of pathogen-associated molecular patterns (PAMPs) trigger

innate immunity, and cytokines, such as type I IFN, are produced that ensure initial survival of the host [Kawai et al., 2006].

Whereas virtually all tissues cell types express IFNAR and thus respond to type I IFN by the expression of a wide array of IFN-inducible genes [Samuel, 2001], only few cells are specialized to produce large amounts of type I IFN upon *in vivo* infection [Barchet et al., 2002; Colonna et al., 2004; Asselin-Paturel et al., 2005; Cao et al., 2007]. Upon infection with vesicular stomatitis virus (VSV), a specialized DC subset with a plasma cell-like morphology, so-called plasmacytoid DCs (pDCs), represents one major source of type I IFN [Barchet et al., 2002]. Apart from pDCs, myeloid DCs (mDCs) may also produce type I IFN upon virus infection [Barchet et al., 2005].

1.2.1 The Impact of type I IFN stimulation on immune responses

In addition to anti-viral activity [Samuel, 2001] type I IFN shows pleiotrophic effects such as anti-proliferative effects [Petricoin, III et al., 1997], apoptotic effects [Marrack et al., 1999] and effects on the expression of cytokines and cytokine receptors [Holan et al., 1991; Strengell et al., 2004]. Furthermore, it was reported that type I IFN exerts direct and indirect effects on lymphocytes and might have an impact on antibody responses. Many indirect effects of type I IFN are presumably mediated by the activation of APCs [Le Bon et al., 2001] which in turn secrete various cytokines, such as IL-15, that can act on lymphocytes [Zhang et al., 1998].

About T cells, it was recently described that type I IFN has a direct effect on $CD8^+$ T cells to promote clonal expansion [Aichele et al., 2006] and formation of memory T cells by enhancing cell survival [Kolumam et al., 2005]. *In vivo*, type I IFN plays a critical role in cross-priming of $CD8^+$ T cells [Le Bon et al., 2003].

Several lines of evidence pointed towards the impact of type I IFN on antibody responses. In *in vitro* studies, B cells treated with suboptimal anti-IgM showed an enhanced IgM production upon costimulation with IFN-α/β [Braun et al., 2002]. More strikingly, *in vivo* experiments established an adjuvant effect of IFN-α/β leading to improved antibody responses. In this context, it was shown

that IgG responses towards an influenza subunit vaccine [Proietti et al., 2002] and against the soluble protein chicken gamma globulin (CGG) [Le Bon et al., 2001; Le Bon et al., 2006] were enhanced by type I IFN stimulation. In the latter model, Le Bon et al. demonstrated that injection with CGG devoid of adjuvans induced only very weak antibody responses, whereas coinjection of CGG and IFN-α/β induced significant CGG-specific IgM and IgG responses. Under these conditions, IFN-α/β stimulation of DCs, as well as of B and T cells, played a critical role [Le Bon et al., 2001; Le Bon et al., 2006; Le Bon et al., 2006a]. Furthermore, type I IFN was shown to promote plasma cell differentiation [Jego et al., 2003].

Depending on the virus infection analyzed, virus-induced type I IFN may or may not have an impact on anti-viral antibody responses. Van den Broek et al. demonstrated that after infection with the non-cytopathic lymphocytic choriomeningitis virus (LCMV), which induces significant type I IFN responses [Malmgaard et al., 2002], IFNAR$^{-/-}$ mice and wild-type (WT) controls mounted similar antibody responses against the nuclear protein (NP) of LCMV. These NP-specific antibody responses were not neutralizing and probably had no protective effect. Nevertheless, they showed a comparable magnitude and similar isotype pattern [van den Broek et al., 1995]. In contrast, after infection with a low pathogenic influenza virus strain that is similarly cleared in IFNAR$^{-/-}$ and WT mice, IFNAR signaling was one of the first direct stimulatory signals required for local lymph node B cells to mount antibody responses. In this model, IFNAR$^{-/-}$ mice, which showed a reduced frequency of influenza-specific B cells, produced a changed isotype pattern of influenza-specific antibodies. In addition, the differentiation of activated B cells to antibody-secreting plasma cells was hampered [Coro et al., 2006]. Recent VSV infection studies conducted in mice carrying adoptively transferred transgenic VSV-specific B cells suggested that IFNAR signaling of B cells enhanced plasma blast formation and increased IgM responses [Fink et al., 2006]. However, in these studies the adoptively transferred IFNAR-deficient B cells expressed a transgenic B cell receptor and competed with endogenous IFNAR-competent B cells. Therefore, the overall neutralizing antibody responses were rather similar, irrespective of

whether IFNAR deficient or IFNAR competent transgenic B cells were transferred.

1.3 Vesicular stomatitis virus (VSV)

Vesicular stomatitis virus (VSV) is a single-stranded (-) RNA virus of the genus Vesiculovirus and belongs to the family Rhabdoviridae [Dietschhold et al., 1996]. VSV shows bullet-shaped morphology and measures about 170 nm in length and 70 nm in width (Figure 1). VSV encodes 5 structural proteins (N, L, P, M and G). The envelope of VSV is based on the matrix (M) protein inserted in a host cell-derived lipid bi-layer. The externally oriented glycoprotein (VSV-G) forms the paracrystalline virion surface that is characterized by the tips of VSV-G which are arranged at a distance of 5-10 nm, each [Bachmann et al., 1995].

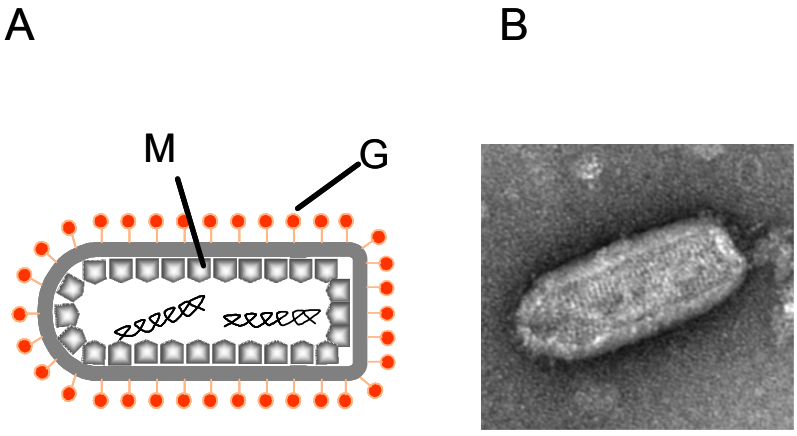

Figure 1 **Vesicular Stomatitis Virus (VSV). (A)** Schematic illustration of VSV showing the matrix (M) protein lining the envelope and the VSV-G (G) surface protein that surrounds the envelope. **(B)** Electron microscopic picture of VSV.

Several serotypes of VSV exist, including the experimentally used strains New Yersey (NY) and Indiana (IND). VSV shows a very broad host spectrum ranging from mammals and birds to insects. Main hosts are horses, cattle and swine. VSV causes a disease characterized by vesicular lesions in the mouth that led to the name of “vesicular stomatitis”. Inoculation of VSV in humans can cause an influenza-like disease. In mice, intravenous (i.v.) infection is tolerized up to a rather high dose of 10^8 plaque-forming units (PFU). The highly-repetitive pattern

of VSV-G protein results in BCR cross-linking of VSV-G specific B cells, and therefore provides a strong signal to induce early IgM responses without further need of T cell help [Bachmann et al., 1995]. VSV is therefore classified as a T cell-independent (TI-1) antigen [Ochsenbein et al., 1999].

The anti-VSV humoral response is directed nearly exclusively to one major determinant of VSV-G, probably because only the tip of VSV-G is accessible to antibodies [Bachmann et al., 1994; Roost et al., 1996; Kalinke et al., 1996].

Intravenous VSV infection of mice induces maximal type I IFN levels after approximately 12 h. At later time points, type I IFN levels decline and reach back-ground levels by day 2 [Barchet et al., 2002; Kamphuis et al., 2006]. Rapid type I IFN induction is critically required for the initial survival as demonstrated by VSV infected IFNAR$^{-/-}$ mice that succumb to low-dose infection within few days, whereas WT mice usually survive infections with up to 10^8 virus particles [Muller et al., 1994]. Furthermore, protection requires the induction of VSV neutralizing antibody responses as indicated by B cell-deficient mice that succumb to VSV infection between day 5 and 7 [Thomsen et al., 1997]. Finally, long-term protection is supported by the subclass switch of neutralizing IgM to IgG. This was demonstrated by mice depleted of CD4$^+$ T cells that mounted VSV neutralizing IgM responses, but did not show an IgG subclass switch and showed an increased sensitivity to lethal VSV infection [Bachmann et al., 1997].

1.4 Prion biology

1.4.1 Prion diseases

Prion diseases or transmissible spongiform encephalopathies (TSE) are fatal neurodegenerative disorders that affect humans and a wide variety of animals. Bovine spongiform encephalopathy (BSE) in cattle [Wells et al., 1987], scrapie in sheep and goats [McGowan, 1922], or Creutzfeldt-Jakob disease (CJD) [Creuzfeldt, 1920] in humans represent the most prominent types of TSEs (Table1). Prion diseases share important mechanistic aspects with more frequent neurodegenerative diseases such as Alzheimer´s disease and Parkinson´s disease, but they are unique in that they are transmissible within

and between species. Clinical features of TSEs are mental changes, ataxia and massive loss of neuronal function in the brain [Parry, 1983].

Table 1 Overview of TSE diseases in humans and animals

Disease	Natural host species	Transmission route or mechanism of pathogenesis	References
Bovine spongiform encephalopathy (BSE)	Cattel	Ingestion of BSE-contaminated meal	[Wells et al., 1987]
Chronic wasting disease (CWD)	Deer and elk	Transmission unknown	[Williams et al., 1980]
Creuzfeldt-Jakob disease (CJD)	Human	Sporadic, familial (Prnp germline mutation)	[Kretzschmar, 1993]
Feline spongiform encephalopathy (FSE)	Zoological and domestic cats	Ingestion of BSE-contaminated meat	[Bessen et al., 1994]
Gerstmann-Sträussler-Schenker syndrome (GSS)	Humans	Familial (*Prnp* germline mutation)	[Gerstmann et al., 1936]
Kuru	Human	Ingestion of ritualistic cannibalism	[Gajdusek, 1977]
Scrapie	Sheep and goats	Ingestion	[McGowan,1922]
Transmissible mink encephalopathy (TME)	Mink	Ingestion	[Marsh et al., 1993]
Variant Creuzfeldt-Jakob disease (vCJD)	Human	Ingestion of BSE-contaminated food	[Will et al., 1996]

For a long time it was believed that the infectious source of TSEs was a virus or a viroid [Sigurdsson, 1954; Thormar, 1971] until additional studies revealed that the scrapie agent is resistant to procedures that destroy nucleic acids such as treatment with nucleases and UV irradiation. These findings led to the suggestion that the infectious agent is devoid of nucleic acids [Alper et al.,

1967]. In 1967, J. S. Griffith postulated the hypothesis that the causative agent is a protein [Griffith, 1967]. 15 years later Stanley Prusiner showed that prion diseases are caused by an infectious agent named prion [Prusiner et al., 1982]. The term prion is the abbreviation for “proteinaceous infectious particle” and was defined as “small proteinaceous infectious particle”.

In the past decade, TSE diseases have achieved enhanced attention due to the appearance of BSE or ‘mad cow disease’ and vCJD in the UK, which strongly influenced medical, agricultural, economic and political issues worldwide. Currently, another prion disease of unknown origin, the chronic wasting disease (CWD), appears in wild and captive populations of deer and elk in North America [Williams, 2002; Williams et al., 2003]. The spread of prions entering an organism via the food chain has been shown to start out by the infection of immune and lymphoreticular cells and the subsequent infection of the peripheral and the central nervous system [Aguzzi et al., 2003].

1.4.2 The prion protein

The prion protein (PrP) is a cell-surface glycosylphosphatidylinositol (GPI) anchored protein [Stahl et al., 1991] that is widely expressed in mammals [Schatzl et al., 1995]. PrP comprises 253 amino acids (aa) and includes two signal sequences in the amino- and carboxy-terminal ends which are removed during post-translational modifications (Figure 2). The N-terminal region contains a segment of several octapeptide-repeat regions that preferentially binds copper [Hornshaw et al., 1995].

High expression levels of PrP are particularly found in the central nervous system and in cells of the immune system [Ford et al., 2002]. However, the exact physiological role of the cellular prion protein (PrP^{C}) is still unknown. Mice lacking PrP (*Prnp*$^{0/0}$) showed no obvious phenotype [Bueler et al., 1992; Bueler et al., 1993; Weissmann et al., 2003]. A comprehensive analysis of *Prnp*$^{0/0}$ mice revealed subtle phenotypes such as abnormalities in synaptic physiology [Collinge et al., 1994] and deviations in circadian rhythm and sleep [Tobler et al., 1996]. Furthermore, recent evidence pointed towards a role of PrP in

renewal of hematopoetic stem cells under stress [Zhang et al., 2006]. Interestingly, *Prnp*$^{0/0}$ mice are completely resistant to prion disease [Bueler et al., 1992; Bueler et al., 1993] indicating that PrP^{C} expression is essential for prion replication and disease development [Bueler et al., 1993].

The pathogenic PrP isoform is referred to as PrP^{Sc} and shows great resistance to radiation and nucleases [Alper et al., 1967]. The high proportion of ß-sheets in PrP^{Sc} renders it insoluble and markedly resistant to proteases [Cohen et al., 1998]. In contrast to PrP^{Sc}, the cellular PrP^{C} contains mostly alpha-helical structures and a small portion of flattened ß-sheet. Therefore, PrP^{C} is highly susceptible to proteinase K (PK) digestion, whereas PrP^{Sc} is largely resistant. Although PrP^{C} and PrP^{Sc} share an identical amino acid sequence, they differ in their secondary and presumably tertiary structure. So far, only the 3D structure of PrP^{C} was resolved, but not that of PrP^{Sc} [Riek et al., 1996].

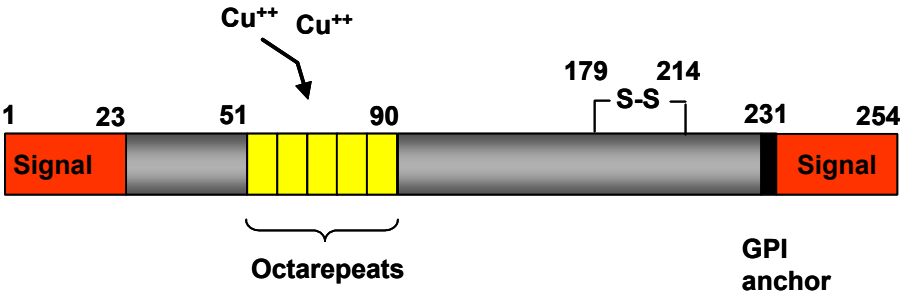

Figure 2 **Primary structure of the prion protein.** The cellular prion protein (PrP^{C}) is a glycosylphosphatidylinositol (GPI) anchored protein of 253 amino acid (aa) residues. It consists of a flexible N-terminal and a globular C-terminal domain. During PrP^{C} processing, a 22 aa N-terminal signal peptide is removed together with a 23 aa C-terminal signal sequence to promote attachment of the GPI-anchor at aa 231. The N-terminus possesses the copper-binding site of a series of 5 octarepeats. The C-terminus is highly structured and possesses two glycosylation sites (Asn-181 and Asn-197) and cysteine residues (aa 179 and aa 214) act as sites to form a disulfide bound.

The “protein-only“ hypothesis postulates that the disease-associated prion protein PrP^{Sc} is the causing agent of prion diseases and that it replicates by converting the abnormal PrP^{C} into the pathological PrP^{Sc} conformer [Prusiner et al., 1982; Stahl et al., 1991].

1.4.3 The prion hypothesis

The conversion of PrP^{C} to PrP^{Sc} has been proposed to be a self-propagating conversion, for which two models are being discussed (Figure 3). In the refolding model (A), the conformational change is kinetically controlled. A high activation energy barrier prevents spontaneous conversion of PrP^{C} to PrP^{Sc}, whereas the interaction with PrP^{Sc} induces a conformational change to yield PrP^{Sc} [Kocisko et al., 1994]. The seeding model (B) postulates an equilibrium between PrP^{C} and PrP^{Sc}, that strongly favours PrP^{C}. In that model PrP^{Sc} is only stabilized when it adds onto a crystal-like seed of PrP^{Sc}. The seeding model, also referred to as the nucleation model, has found convincing experimental support in case of yeast prions, and recently also for mammalian prions [Weissmann, 2004].

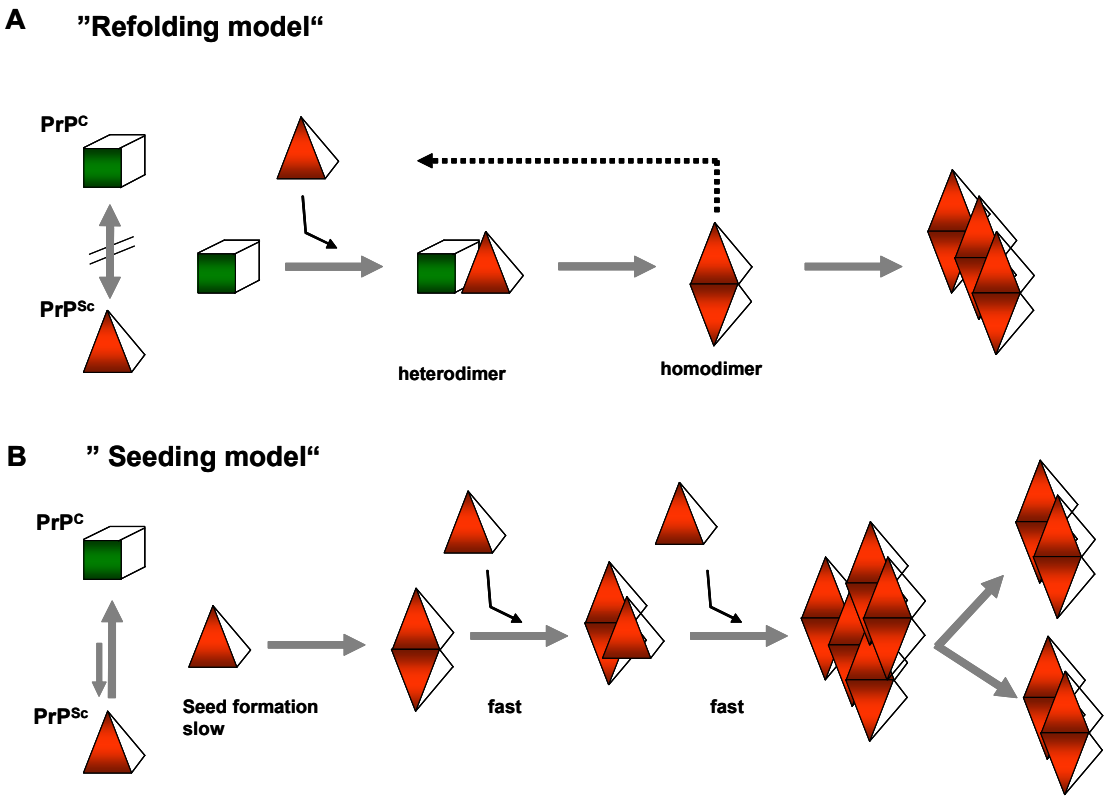

Figure 3 **Conversion models of PrP^{C} to PrP^{Sc}. (A)** The "refolding model" postulates an interaction between PrP^{C} and PrP^{Sc}, which is induced to transform itself into more PrP^{Sc}. **(B)** The "seeding model" postulates that PrP^{C} and PrP^{Sc} are in equilibrium, with PrP^{C} being strongly favoured. Only if several monomeric PrP^{Sc} forms a seed, more PrP^{Sc} can be recruited to form PrP^{Sc} aggregates (adapted from A.Aguzzi [Aguzzi et al., 2001]).

1.5 Active immunization against the prion protein, possible or impossible?

Prion biology is very different when compared with conventional pathogens. The difficulty of inducing anti-PrP^C antibodies is likely due to the fact that the prion protein is a self-antigen expressed on the surface of many host cells that confers immunologic self-tolerance. As the immune system evolved in a way that self-determinants normally are not attacked, it is not surprising that prion infection does not induce protective immunity. Furthermore, PrP^C specific immune response can not be easily stimulated by vaccination. If the induction of an immune response specifically against the pathogenic PrP^{Sc} was possible, it probably would cross-react with PrP^C that might lead to undesirable autoimmune reactions. *Prnp*$^{0/0}$ mice that are devoid of PrP^C can easily be immunized to mount PrP-specific antibody responses. Unfortunately, so far no antibody has been identified that reliably discriminates between PrP^C and PrP^{Sc}. Several groups worked first *in vitro* and later *in vivo* to establish the basis for therapeutic or prophylactic antibody therapies against prion diseases. Strategies for therapeutic vaccination rely on antibodies directed against PrP^C that would inhibit the conversion of PrP^C into PrP^{Sc} in the periphery before the pathogen can invade the central nervous system.

1.5.1 Passive immunotherapy of prion diseases

Several cell lines, including the murine neuroblastoma cell line N2a, can propagate scrapie prions (PrP^{Sc}) such as the Rocky Mountain laboratory (RML) strain. Prion infected cell lines have been used to identify prion neutralizing monoclonal antibodies (mAb) and to study mechanisms of antibody-mediated prion inactivation [Enari et al., 2001]. To elucidate mechanisms of antibody mediated inhibition of PrP^{Sc} formation, neutralizing activities of mAbs and antibody fragments have been assessed in cell culture systems persistently infected with prions [Enari et al., 2001; Peretz et al., 2001; Beringue et al., 2004; Perrier et al., 2004; Miyamoto et al., 2005]. Furthermore, several groups studied the effect of passive anti-PrP immunization on scrapie [Sigurdsson et al., 2003;

White et al., 2003; Feraudet et al., 2005]. White et al. tested two different monoclonal antibodies (mAb) by intraperitoneal (i.p.) administration in mice. When mAb treatment was started 30 days following scrapie infection, a time when peripheral prion accumulation reached plateau levels, splenic PrP^{Sc} was significantly reduced after 30 days of mAb therapy. Under continued mAb therapy mice survived for more than 500 days, whereas controls showed first signs of disease after approximately 195 days. Protective effects of passive immunization were only observed upon i.p. infection, whereas upon intracerebral (i.c.) exposure mAb treatment was ineffective. This was most likely due to the inability of mAbs to cross the blood-brain barrier. Overall, passive immunization against prion diseases showed significant prolongation of survival times and scrapie inhibition after peripheral prion infection. Continuous mAb treatment resulted in PrP^{Sc} clearance, even when massive prion replication had taken place in the periphery. A major obstacle of passive immunization strategies is to stably maintain protective anti-PrP antibody levels.

1.5.2 Tolerance and autoimmunity

Because somatic BCR and TCR rearrangement is a random process, a significant proportion of B and T cells potentially recognize self-antigens. The discrimination of “self” from “non-self” is a hall-mark of the immune system. Already in the twentieth century, Paul Ehrlich proposed the concept of “horror autotoxicus”. He concluded from his experiments that the immune system usually does not attack self-tissues [Ehrlich P. et al., 1957].

Generally, autoimmune diseases can be prevented by mechanisms that delete or inactivate self-reactive lymphocytes [Goodnow et al., 2005]. Immune cells that express self-reactive receptors can be triggered to die (clonal deletion). Alternatively, immune cells can ‘edit’ potentially hazardous receptors by recombination events or mutations to express receptors that are not self-reactive. Furthermore, several intrinsic and extrinsic factors reduce or suppress the ability of self-reactive lymphocytes to be activated (peripheral tolerance). This leads to an “anergic” state. In the end, extrinsic factors can also limit the

danger in the periphery, if potentially self-reactive lymphocytes escaped tolerance mechanisms.

In B lymphocytes two concepts of immune tolerance are proposed: In the first concept developing lymphocytes have to pass through a tolerance-susceptible stage. The encounter of antigen leads to deletion or functional inactivation of lymphocytes. However, those B cells which progress through this stage in the absence of antigen will loose tolerance sensitivity and acquire antigen-inducible functions [Nossal, 1994]. In the second concept, antigen encounter (signal 1) is generally tolerizing and B cells become only activated if a second costimulatory signal is provided by a helper T cell (signal 2) [Bretscher et al., 1970]. After all, B cell tolerance is a subject of controversy and there are arguments against an intrinsic B cell tolerance, where B cell unresponsiveness is mainly considered to be the result of insufficient T cell help or weak BCR cross-linking by antigens [Bachmann et al., 1997]. For B cell tolerance, the concentration of a self-antigen, multivalent presentation to a B cell and the affintiy of the B cell receptors play an important role. Some B cells with low affinity for self-antigens may be capable to secrete low affinity anti-self antibodies.

The presence of low concentration of self-antigens in a host leads to complete T cell tolerization, whereas B cells need a higher antigen dose for tolerization (Figure 4). The presence of high amounts of antigens (e.g. MHC molecules) induces complete T and B cell tolerance, whereas low self-antigen expression (e.g. the cellular PrP^{C} protein) probably does not completely tolerize B cells.

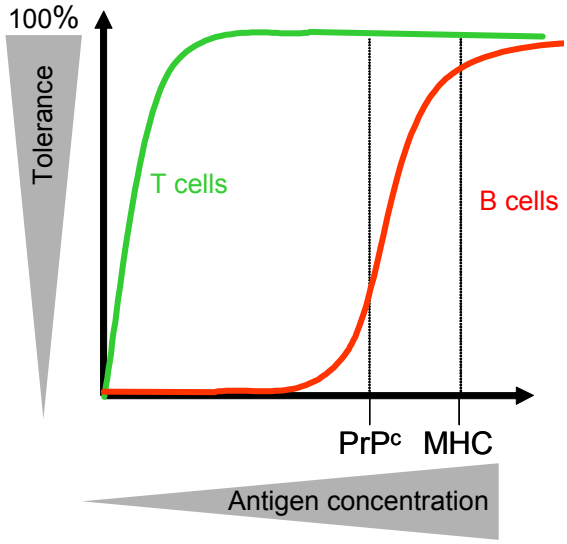

Figure 4 **Model of T cell versus B cell tolerance.** T cells show 100% tolerization when low concentrations of self-antigens are present in a host. In contrast, B cells need higher expression level amounts of self-antigens (e.g. MHC) for complete tolerization.

In general, the level of self-antigen expression required for the induction of B cell tolerance is higher than that required for the induction of T cell tolerance. Therefore, an important mechanism to prevent the immunoglobulin switch from of the M isotype (IgM) to potentially more harmful immunoglobulins of the G isotype (IgG) simply ensures absence of T cell help by the relative ease of inducing T cell tolerance.

Breaking tolerance to specific self-antigens may result in autoimmunity. The immune system may then attack self-tissues by inducing autoantibodies or recruiting lymphocytes that are reactive with host antigens. The aberrant immune response can cause autoimmune diseases. However, the mechanism is poorly understood. Many parameters, such as genetic predisposition, environmental factors, signaling defects or tissue damage are involved. Considering the specificity of autoimmune diseases, it is widely believed that inappropriate activation of self-reactive B or T lymphocytes takes place. One possible mechanism has been described as “molecular mimicry. In this model, an exogenous antigen which mimics a self-antigen can activate autoreactive T cells, thus causing autoimmunity. Alternatively, viral or microbial superantigens

can activate large numbers of T cells. Those viral or bacterial infections lead to local activation of antigen-presenting cells and can result in enhanced processing and presentation of self-antigens.

1.5.3 PrP-specific tolerance vs. immunity

Heppner et al. addressed the question whether in the presence of endogenous PrP, B cells develop which recognize PrP^C. To this end, a transgenic mouse model was generated in which the immunoglobulin heavy chain of a PrP-specific antibody was expressed [Heppner et al., 2001]. The expression of the transgenic immunoglobulin heavy chain caused a skewed B cell repertoire that resulted in spontaneous production of anti-PrP serum antibodies. Interestingly, the expression of PrP-specific serum antibodies was independent of whether endogenous PrP was present or not. This observation was in contrast to other transgenic immunoglobulin mouse models in which co-expression of the antigen and the corresponding B cell receptor caused deletion, anergy or editing of antigen-specific B cells [Goodnow et al., 1988; Nemazee et al., 1989; Hartley et al., 1991; Gay et al., 1993; Tiegs et al., 1993].

Interestingly, in double-transgenic mice overexpressing PrP, deletion of transgenic PrP-specific B cells was observed [Heppner et al., 2001]. This suggested that endogenous PrP expression was probably too low to induce complete B cell tolerance in mice. Furthermore, anti-PrP transgenic mice expressing endogenous PrP did not show obvious signs of autoimmunity. This was presumably due to the fact that the transgenic Ig was expressed as an IgM. Transgenic mice that were i.p. challenged with RML prions did not show PrP^{Sc} in the spleen until 234 days post infection, whereas control mice showed infectivity in spleen by day 50. This observation clearly showed that PrP^C-specific transgenic serum antibodies significantly delayed scrapie pathogenesis. However, when anti-PrP transgenic mice were administered with prions intracerebrally they were not protected.

The cellular and molecular basis of tolerance to PrP^C was addressed in a set of transgenic mouse lines expressing PrP in selected tissues. Transgenic mice

expressing PrP under the control of an oligodendrocyte and Schwann cell-specific promoter (MBP-PrP) mounted a significant anti-PrP^C humoral immune response when immunized with bacterially expressed PrP [Polymenidou et al., 2004]. All other transgenic mice behaved similar to wild-type mice and showed PrP-specific antibody responses that recognized PrP by ELISA, but failed to recognize the native form of PrP^C. Those data implicated that in mice which expressed PrP exclusively on oligodendrocytes and Schwann cells PrP-specific B cells were not tolerized. Unfortunately, MBP-PrP mice do not support prion propagation. Therefore, in these mice the protective efficacy of the PrP-specific antibody responses could not be assessed directly.

1.5.4 Strategies to overcome B cell self-tolerance

Considering the efficacy of passive anti-prion vaccination strategies, active immunization against PrP^C seemed to be a straight forward approach to prevent prion infection. However, the induction of PrP^C-specific immunity is hampered by immunologic tolerance phenomena. Various attempts have been undertaken to induce PrP-specific antibody responses. Most of these studies have been carried out in rodents, especially in mice, because in these models scrapie incubation periods are much shorter than in cattle or sheep. For immunization, PrP-specific peptides or bacterially expressed recombinant PrP together with various different adjuvants have been used [Hanan et al., 2001; Souan et al., 2001; Sigurdsson et al., 2002; Polymenidou et al., 2004; Rosset et al., 2004]. PrP antigens were also coupled to different immunogenic carriers [Koller et al., 2002; Arbel et al., 2003; Schwarz et al., 2003]. In most of these studies, however, only faint PrP-specific immune responses were induced that, at best, delayed disease onset by a couple of days. In another approach, PrP^C-specific antibody responses were induced by using dimeric PrP consisting of a tandem duplication of mouse PrP [Gilch et al., 2003]. Interestingly, such sera were effective in clearing PrP^{Sc} in a PrP^{Sc} inhibition *in vi*tro assay. However, mice immunized with the dimeric PrP showed only a minor delay of prion pathogenesis.

In summary, all active immunization studies undertaken so far revealed that normal mice mount rather low PrP-specific antibody responses that are not directed against the native form of PrP^C and thus can not significantly interfere with prion replication *in vivo*.

It has been proposed that the mammalian immune system evolved to recognize pathogens which often display repetitive determinants at a spacing of 50-100 Å [Bachmann et al., 1993; Bachmann et al., 1996]. Certain viruses (e.g. VSV) and bacteria that consist of strictly ordered components are better immunogens than suspensions of isolated components that show irregularly arranged determinants [Fehr et al., 1997]. In a study it was shown that autoantibodies were induced by papillomavirus or polyomavirus virus-like particles (VLP) coated with TNF-alpha [Chackerian et al., 2001]. The strongest autoantibody response was observed when VLP were coated with the highest density of self-antigen. This indicates that the density of self-antigens played a critical role [Chackerian et al., 2002]. In conclusion, is seems to be possible to overcome B cell tolerance by displaying relevant determinants on some highly immunogenic viral carrier.

1.5.5 Virus-like particles (VLP)

In previous decades, prophylactic vaccines have been developed against a variety of different infectious diseases. Attenuated and inactivated microorganisms as well as toxoids or protein subunits have been used for vaccination purposes (for review see [Deml et al., 2005]). Several groups have shown that especially VLP can be used to induce strong immune resonses against selected virus determinants. VLP lack the potential to proliferate and thus to express unwanted immuno-suppressive viral proteins. To date, numerous types of VLP have been produced utilizing the ability of more than 30 different viruses to self-assemble into highly organized particulate structures [Deml et al., 2005]. Most frequently used VLP are hepatitis B virus cores, displaying e.g. influenza, human immunodeficiency, polio- or hantavirus derived

determinants (reviewed in [Pumpens et al., 2001]). Furthermore, human immunodeficiency virus (HIV) Gag proteins were used as carriers to present foreign polypeptides and determinants [Deml et al., 2005]. Because the structure, morphogenesis and molecular mechanism of virus assembly are well understood, display scaffolds of phage particles such as the RNA phage Qβ were generated [Kozlovska et al., 1996]. Two groups of vectors that display foreign polypeptides were classified: type I and type II VLP. Both differ with respect to the kind of antigen presentation. Type I VLP display proteins that are fused to the Gag polyprotein, whereas type II VLP present the antigen at the outer particle surface [Deml et al., 2005]. Unlike other VLP, retrovirus-based VLP are enveloped particles that can easily incorporate complete polypeptides or proteins into the membrane. The incorporation of the foreign polypeptides or proteins can be achieved by using either the retrovirally derived envelope (Env) protein or by unspecific packaging of host membrane proteins into their envelope [Hammarstedt et al., 2000; Hammarstedt et al., 2004]. Furthermore, retrovirus-based VLP are highly immunogenic and facilitate introduction of antigens in the MHC class I and II processing and presentation pathway. Additionally, they act as “danger signals” to activate the innate immune system thus, initiating strong Th1-biased humoral and cellular immune responses [Deml et al., 2005].

2 Aims of this thesis

Several *in vitro* and *in vivo* studies suggested that active vaccination against prion diseases should be a feasible approach to prevent prion infection. However, in previous approaches the induction of anti-PrP^C immune responses was hampered by tolerance phenomena. PrP^C-specific tolerance is associated with the fact that PrP^C is an endogenous protein that is widely expressed in many tissues and does not confer “danger signals” upon immunization to induce the host immunity. The aim of this thesis was to analyze whether in analogy to conventional pathogens antibody responses can be induced against prions and if so, whether PrP^C-specific antibodies are protective.

For theoretical reasons, highly immunogenic antigens that do not replicate in the host represent ideal vaccine candidates for immunization studies. To assess the immunogenicity of VLP, in a first step VLP displaying the vesicular stomatitis virus (VSV) glycoprotein (VSV-G) on the surface (VLP-VSV) were generated and characterized by ELISA and electron microscopy. Upon immunization of mice with VLP-VSV, T help-independent VSV neutralizing IgM was induced. This IgM switched to IgG in a T help-dependent manner. Interestingly, the IgG subclass switch needed type I IFN receptor (IFNAR) signaling. Thus, VLP-VSV was highly immunogenic and induced VSV neutralizing antibody responses that in many aspects were reminiscent of antibody responses induced by live VSV.

In a second step, PrP^C-displaying VLP were developed. Since the C-terminal part of PrP^C was crucially involved in the conversion of PrP^C into PrP^{Sc}, PrP^C encoding amino acids 121-231 (PrP111) was displayed on VLP (VLP-PrP^{D111}). Upon VLP-PrP^{D111} immunization, PrP deficient (*Prnp*$^{0/0}$) mice mounted strong PrP^C-specific IgM and IgG antibody responses. Upon VLP-PrP^{D111} immunization of wild-type mice strong IgM but only very weak IgG antibody responses were induced that declined shortly after immunization. Those results showed that the T cell-dependent switch from the IgM to the IgG isotype of PrP^C-specific antibodies was less pronounced in wild-type mice than in *Prnp*$^{0/0}$ mice, probably due to T helper cell tolerance.

An important objective of this thesis was to circumvent tolerance to PrP^{C} in wild-type mice. This issue was addressed by a series of PrP-immunization approaches including VLP-PrP^{D111} emulsified in adjuvant or VLP priming/boosting strategies.

To trigger PrP^{C}-specific T cell help, VLP-PrP^{D111}-retroparticles expressing foreign T helper epitopes were generated and analyzed for the induction of PrP^{C}-specific antibodies in wild-type mice. Furthermore, the induction of anti-PrP^{C} antibody responses upon adoptive transfer of *Prnp*$^{0/0}$ "memory" B cells into wild-type mice was assessed. In this approach it was tested whether activated PrP^{C}-specific "memory" B cells were able to mount anti-PrP^{C} IgG antibody responses in wild-type recipient mice. Finally, the protective capacity of the different immunization protocols was evaluated.

3 Material and Methods

3.1 Materials

3.1.1 Mice

C57BL/6 mice were purchased from Charles River. Transgenic mice were bred under specific pathogen-free (SPF)-conditions in individually ventilated cages (IVCs) or filter-isolated cages at the mouse facility of the Paul-Ehrlich-Institut. Experimental animal work was conducted in compliance with the German federal and state legislation on animal experiments.

Table 2 Mouse strains used in this study

Mouse strain	Literature	Background
C57BL/6	Charles River or PEI	homozygous BL/6
IFNAR$^{-/-}$	[Muller et al., 1994]	homozygous BL/6
Tg20	[Fischer et al., 1996]	heterozygous SV129
Tg33	[Raeber et al., 1999]	heterozygous SV129
C57/BL6 *Prnp$^{0/0}$*	U. Kalinke, unpublished, PEI	homozygous BL/6
Prnp$^{0/0}$	[Bueler et al., 1992]	heterozygous SV129
CD4Cre$^{+/-}$ / CD19Cre$^{+/-}$ IFNAR$^{flox/flox}$	[Bach et al., 2007]	homozygous BL/6
CD19Cre$^{+/-}$ IFNAR$^{flox/flox}$	[Kamphuis et al., 2006]	homozygous BL/6
CD4Cre$^{+/-}$ IFNAR$^{flox/flox}$	[Kamphuis et al., 2006]	homozygous BL/6

3.1.2 Equipment

Table 3 Overview of Equipment

Equipment	Source
37°C room	PEI, Langen
Alarm clock	NeoLab, Heidelberg
Balance (LP 820)	Satorius AG, Göttingen
BD MoFLo Cell Sorter	Becton Dickinson Gmbh, Heidelberg
Biorad Protean II chamber	Biorad, München
Centrifuge (Biofuge fresco # 3328, Megafuge 1.0 # 2705)	Heraeus Sepatech, Osterode am Harz
Cooling block	Eppendorf AG, Hamburg
Cooling centrifuge (Varifuge 3.0 R,# 8078), Beckmann J6-HC, # JS-4.7	Heraeus Sepatech, Osterode am Harz; Beckman Coulter, Fullerton, California
ELISA reader, Sunrise	Tecan Deutschland GmbH, Crailsheim
FACScan	Becton Dickinson Gmbh, Heidelberg
Fast blot device	Biometra, Göttingen
Freezer	Liebherr, Biberach an der Riss
Gradiend former (Model 385)	Biorad, München
Incubators with supply of CO_2 (Cytoperm)	Heraeus, Hanau
LSR II	Becton Dickinson Gmbh, Heidelberg
Magnetic stirrer (Combimag Ret)	IKA, Werke GmbH, Staufen
Manual counter	IVO, Villingen-Schwenningen

Equipment	Source
Microscope	Axiovert 25, Axiolab, Zeiss, Jena
Microwave (9025E)	Privileg, Fürth
Mouse restrainer (3 cm tube diameter)	Harnischmacher, Kassel
Multichannel pipettes	Socorex, Schweiz
Novex Power Ease 500	Biorad, München
Overhead shaker (Heto Mastermix)	Holm and Halby, Brondby, Denmark
pH-Meter (761 Calimatic)	Knick, Egelsbach
Photometer (Ultraspec 3000)	Pharmacia Biotech, Freiburg
Pipetboy (Pipetboy acu)	IBS Integra Biosciences, Chur, Schweiz
Pipette (10 - 100 µl or 50 – 200 µl)	Eppendorf AG, Hamburg
Pipette 10 µl	Eppendorf AG, Hamburg
Power supply (Power Pac 300)	Biorad, München
Refrigerator	Liebherr, Biberach an der Riss
Set of surgical instruments	Hauptner/Herberholz, Solingen
Shaker	Infors AG, Sitzerland
Sterile work bench (Steril Gard II Advance) “The Baker Company”	Labotect, Göttingen
Table centrifuge (5415C)	Eppendorf AG, Hamburg
Transmission electron microscope EM 109 or 902	Carl Zeiss, Jena
Ultra low freezer (-80°C)	New Brunswick Scientific, UK

Equipment	Source
Ultrsonic homogenizer (Sonoplus)	Bandelin, Berlin
UV-irradiator (CL-1)	Herolab, Wiesloch
Vacuum pump (Vacusafe)	IBS Integra Biosciences, Chur, Schweiz
Vortexer	VWR, Darmstadt
Water bath	Gesellschaft für Labortechnik (GFL), Burgwedel

3.1.3 Consumables

Table 4 Overview of Consumables

Consumables	Source
96 well round/-flat/V-bottom cell culture plates	Nunc, Karlsruhe
Carbon-vaporised and flamed 400-mesh Cu/Rh grids	Plano, adapted in PEI microscopy facility
Cell scraper	Greiner Bio One, Essen
Chemiluminescence films	Amersham, Freiburg
Gloves	Braun, Melsungen
Combitips (1 ml, 2.5 ml, 5 ml,10 ml, 25 ml, 50 ml)	Eppendorf AG, Hamburg
Counting beads	Caltag Laboratories, Hamburg # PCB-100
Cover slip	VWR, Darmstadt
Cryo conservation tubes (1.2 ml, 2.5 ml)	Nunc, Karlsruhe

Consumables	Source
Cups (1.5 ml, 2 ml)	Eppendorf AG, Hamburg
Dialyse membrane: Spectra pore MWCO: 8.000	Spectrum, Broadwick, California
Erlenmeyer flask	Schott, Mainz
FACS tubes large/small (0.5 ml)	Becton Dickinson Gmbh, Heidelberg
Filicon (70 µm)	Becton Dickinson Gmbh, Heidelberg
Filter paper	Whatman, Schleicher & Schuell, Dassel
Glass capillaries	VWR, Darmstadt
Glass with a top (for anesthesia)	Schott, Mainz
Kodak Estar electron microscope film	Kodak, Stuttgart
LB-AMP-plates	PEI , Langen
Microscope slides	Labor Optic, Friedrichsdorf
Neubauer cell counting chamber	Labor Optik, Freidrichsdorf
Nickel-nitrilotriacetic acid (NTA) agarose resin	Qiagen, Hilden
Novex Tricine gels (10-20%)	Invitrogen, Karlsruhe
Nunc Maxisorb ELISA plates (96 well/384 well)	Nunc, Karlsruhe
NuPage Novex 12% Bis-Tris gel	Invitrogen, Karlsruhe
Omnican F (1 ml/0,01 ml) (High precision dosing syringe, 0.3 mm diameter canula integrated into syringe)	Braun, Melsungen
One way Mask (Coldex)	Procter and Gamble, Schwalbach

Consumables	Source
One way plastic pipettes (2 ml, 5 ml, 10 ml, 25 ml)	Greiner Bio One, Essen
Parafilm	American National Can Group, Chicago, USA
Petri dishes	Greiner Bio One, Essen
Pipette tips	Eppendorf AG, Hamburg
Poly Prep Chromatography colums	Biorad, München
PVDF-Membrane (Immobilon-P)	Millipore, Schwalbach
Snap freezing tube (13 x 32 mm with cap)	Kartell SPA, Milano
Sterile filters Qualilab (0.45 µm)	VWR, Darmstadt
Steritop filters GP 0.22 µm	Millipore GmbH, Schwalbach
Tissue culture flasks	Greiner Bio One, Essen
Tissue culture plates (6 well, 96 well)	TPP, Schweiz
Tumbler	Schott, Mainz
Vacutainer-Microtainer, Serum	Becton Dickinson Gmbh, Heidelberg via Döll Medizintechnik

3.1.4 Chemicals

Table 5 Overview of chemicals

Chemicals	Source
ABTS (2, 2'-azino-bis-(3-ethylbenziazoline-6-sulfonic acid)	Roche, Mannheim
Acetic acid	Merck KG, Darmstadt
Agarose	Invitrogen, Karlsruhe
Aluminium Hydroxide	Sigma-Aldrich, München
Ampicilline	Merck KG, Darmstadt
Aqua dest.	PEI, Langen
Bovine Serum Albumin (BSA)	Sigma-Aldrich, München
Bromphenol blue	Biorad, München
Chloroform	Merck KG, Darmstadt
Complete Freund's Adjuvant (CFA)	Sigma-Aldrich, München
Coomassie brilliant blue	Biorad, München
CpG 1668	Sigma-Aldrich, München
Crystal violet	Sigma-Aldrich, München
Desderman	Schülkes and Mayr, Norderstedt
Dimethylsulfoxyd (DMSO)	Sigma-Aldrich, München
DNA marker	Invitrogen, Karlsruhe
Double-distilled H_2O	PEI, Langen
Ethanol	Merck KG, Darmstadt
Ethidium bromide	Merck KG, Darmstadt
Ethylenediaminotetraacetate (EDTA)	Merck KG, Darmstadt

Chemicals	Source
FACS-Clean/-Rinse/-Flow	Becton Dickinson Gmbh, Heidelberg
FACS Lysing solution	Becton Dickinson Gmbh, Heidelberg
Fetal calf serum (FCS)	Biochrom, Berlin; Gibco Karlsruhe
Ficoll	Biochrom, Berlin
Glutamax	Gibco, Karlsruhe
Glutathione	Sigma-Aldrich, München
Glycerine	Merck KG, Darmstadt
Guanidinium Hydrochloride (GdmCl)	Sigma-Aldrich, München
H_2O_2	Merck KG, Darmstadt
HEPES 1M	PEI, Langen
Hydrochloric acid	Merck KG, Darmstadt
Immidazol	Merck KG, Darmstadt
Incomplete Freund's Adjuvant (CFA)	Sigma-Aldrich, München
Isofluran	Baxter, München
Isopropanol p.a.	Merck KG, Darmstadt
Isopropyl-ß-D-galactopyranoside (IPTG)	Sigma-Aldrich, München
Ketamine	Wirtschaftsgenossenschaft Deutscher Tierärzte (WDT), Garbsen
L-Glutamine	Gibco, Karlsruhe
Lipofectamine 2000	Invitrogen, Karlsruhe
Magnesiumchloride ($MgCl_2$)	Qiagen, Hilden

Chemicals	Source
Methanol	Roth, Karlsruhe
Methylamine tungestate (Wolframat)	Agar Scientific, Essex, England
Methylcellulose (Methocel MC)	Fluka, Taufkirchen
Milk powder	Roth, Karlsruhe
Multi Mark marker	Invitrogen, Karlsruhe
Paraformaldehyde (PFA)	Fluka, Taufkirchen
Peanut hemagglutinin (PNA)	Vector Laboratories, UK
Pefabloc (100 mg)	Roche, Mannheim
Penicillin/Streptomycin	Gibco, Karlsruhe
Proteinase K (20 µg/ml)	Roche, Mannheim
Rompun® TS (Xylazine)	Bayer , Leverkusen
Sodium azide (NaN_3)	Merck KG, Darmstadt
Sodium bicarbonate (7.5%)	Gibco, Karlsruhe
Sodium chloride (NaCl)	Merck KG, Darmstadt
Sodium dihydrogene phosphate (NaH_2PO_4)	Merck KG, Darmstadt
Sodium hydrogene carbonate ($NaHCO_3$)	Roth, Karlsruhe
Sodium hydrogene phosphate (Na_2PO_4)	Merck KG, Darmstadt
Sodium pyruvate ($C_3H_3NaO_3$)	Sigma-Aldrich, München
ß-mercaptoethanol	Sigma-Aldrich, München
Streptavidin-PE	Becton Dickinson Gmbh, Heidelberg

Chemicals	Source
SuperSignal Pico ECL	Pierce, Bonn
Terralin Liquid	Schülkes and Mayr, Norderstedt
Titer Max®	Sigma-Aldrich, München
Tris	Sigma-Aldrich, München
Trypan blue solution	Invitrogen, Karlsruhe
Trypsin-Melnik (2.5 M)	PEI, Langen
Tween 20	Fluka, Taufkirchen
Uranyl acetate	Merck AG,Darmstadt; prepared in PEI microscopy facility

3.1.5 Buffers and Media

Table 6 Overview of buffers and media

Buffer	Source
ABC/peroxidase	Dako Cytomation, Hamburg
BCA-Assay	Pierce, Bonn
C-type-RT Activity Assay	Cavidi Tech, Uppsala, Sweden
Dulbecco's modified Eagle's medium (DMEM)	Invitrogen, Karlsruhe
Dulbecco's modified Eagle's medium (DMEM) + 4.500 mg/l Glycose	Invitrogen, Karlsruhe
Earle's MEM	Biochrom, Berlin
LB AMP-Medium	PEI, Langen
MEM (10 x)	Gibco, Karlsruhe

Buffer	Source
Novex Tricine SDS Sample-buffer (2x)	Invitrogen, Karlsruhe
Novex Tricine SDS-running buffer (10x)	Invitrogen, Karlsruhe
NuPage MES SDS- running buffer (20x)	Invitrogen, Karlsruhe
PBS	Gibco, Karlsruhe
PBS Dulbecco (without Ca and Mg)	PEI, Langen
Qiagen plasmid kits	Qiagen, Hilden
Red blood cell lysing buffer	Sigma-Aldrich, München
SOC medium	Invitrogen, Karlsruhe
TBE (10x)	PEI, Langen
TBS-T (10x)	PEI, Langen
Tissue Freezing medium	Leica Microsystems, Bensheim

3.1.6 Prepared Buffers, Media and other reagents

Table 7 Prepared buffers, media and other reagents

Buffer	
Anesthesia (Ketamine/Rompun)	1 ml Ketamine 10%
	0.25 ml Rompun 2%
	5 ml 0.9% NaCl (sterile)
Blotting buffer (1x)	50 ml 10x Transferpuffer (10x)
	100 ml Methanol
	350 ml Aqua dest.

Buffer	
Buffer B	10 mM Tris-HCL, 100 mM Na_2PO_4 (pH 8.0)
Buffer D	10 mM Na_2PO_4 (pH 5.8)
Buffer G	6 M Guanidinium Hydrochloride (GdmCl) 5 mM Tris-HCl 100 mM Na_2PO_4 10 mM reduced Glutathione (pH 8.0)
Crystal violet	0.5% Crystal violet 5% Formaldehyde 0.8% NaCl Aqua dest.
DNA sampling buffer (6x)	0.25% Bromphenol blue, 30% Glycerine Aqua dest.
Dulbecco's modified Eagle's medium (DMEM)	Gibco, Invitrogen, Karlsruhe Supplement: 10% FCS 1% GlutaMax 1% Penicillin/Streptomycin
ELISA blocking buffer (Prepare immediately before use!)	5% BSA 0.1% Tween 20 PBS

Buffer	
ELISA coating buffer	3.18 g/l Na_2CO_3 5.88 g/l $NaHCO_3$ Aqua dest. Adjust to pH 9.6 with 0.1 M $NaHCO_3$
ELISA serum and antibody dilution buffer	1% BSA 0.1% Tween 20 PBS
FACS buffer, pH 8.0	PBS 2% BSA 0.03% NaN_3 20 mM EDTA
Lysis buffer	100 mM NaCl 0.5% NP-40 0.5% Sodium-Deoxycholate 10 mM Tris-HCl (pH 8.0)
MACS buffer, pH 7.3	PBS 2% FCS 2 mM EDTA
Methylcellulose 2%	Dissolve 15 g Methycellulose in 750 ml Aqua dest. under stirring at 4°C ON, autoclaving

Buffer	
PBS	10 mM NaCl 80 mM Na_2HPO_2 20 mM KH_2PO_4
Sample buffer (4x)	200 mM Tris/HCl (pH 6.8), 8% SDS, 0.4% Gromphenolblue, 40% Glycerin 4% ß-mercaptoethanol (freshly added)
ß-mercaptoethanol (280 mM) for VSV neutralizing assay	100 µl 14 M ß-mercaptoethanol (concentrated) 5 ml 0.9% NaCl
TBE (10 x)	890 mM Tris Base 890 mM Boric acid 25 mM EDTA, pH 8.0
TBS-T buffer	10 mM Tris pH 8 150 mM NaCl, 0.05% Tween 20
Transfer buffer (10x)	24 mM Tris 192 mM Glycine 20% Methanol

3.1.7 Bacteria, Viruses and Prion Inoculum

Table 8 Bacteria, Viruses and Prion Inoculum

Bacteria and Viruses	Source
E.coli XL2-blue	Stratagene, Amsterdam, The Netherlands
E.coli BL21 (DE3)	Invitrogen, Karlsruhe
RML 5.0	Obtained by Adriano Aguzzi
VSV-Indiana (Mudd-Summers isolate), wild type virus	Originally obtained from D. Kolakofsky, University of Geneva, Switzerland

3.1.8 Antibodies

Table 9 Antibodies used in this study

Primary Antibodies	Source
mAb anti-CD4 (GK-1.5)	Harlan Bioproducts, Indianapolis, USA
mAb anti-VSV-G IgG_{2a} (VI24), (stock, 1mg/ml)	Provided by Ulrich Kalinke
mAb mouse anti-mouse PrP IgG_1 (6H4)	Prionics, Zürich # 01-011
mAb mouse anti-p24 (880-A)	Chemicon, Hampshire, UK
Mouse anti-HA (clone 12CA5)	Roche, Mannheim
Mouse $IgG_{2a,}$ k-FITC (isotype control)	Biozol, Echingen # 0117-02
Polyclonal goat anti-p30	Quality, Biotech, New Jersey, USA
Polyclonal rabbit anti-mouse PrP	Labordiagnostic, Leipzig # 940.2101.4

Primary Antibodies	Source
Polyclonal rabbit anti-VSV-G	Kindly provided by Bernhard Odermatt, Zürich
Rat anti-mouse CD21-FITC	Becton Dickinson Gmbh, Heidelberg # 553318
Rat anti-mouse CD23-APC	Caltag Laboratories, Hamburg # MCD2305
Rat anti-mouse CD8-FITC (for sorting experiments)	NatuTec, Frankfurt # CTS11362F
Rat anti-mouse CD19-PE (for sorting experiments)	NatuTec, Frankfurt # CTS11439PE
Rat anti-mouse CD3-PE	Caltag Laboratories, Hamburg # RM 3404-3
Rat anti-mouse CD45R/B220-PE Cy5.5	Caltag Laboratories, Hamburg # RM2618
Rat anti-mouse CD4-FITC (for sorting experiments)	NatuTec, Frankfurt # CTS11107F
Rat anti-mouse CD4-PE	Becton Dickinson Gmbh, Heidelberg # 55 36 52
Rat anti-mouse CD8-FITC	Biozol, Echingen # 1550-02 S
Rat IgG_{2a}-PE Cy5.5 (isotype control)	Caltag Laboratories, Hamburg # R2a18
Rat mAb clone FDC-M1	Becton Dickinson Gmbh, Heidelberg

Secondary Antibodies	Source
Donkey anti-mouse IgG-FITC	Dianova, Hamburg # 715-095-150
Donkey anti human IgG-HRP	Dianova, Hamburg # 709-035-149
Goat anti-mouse IgG 10 nm gold	Dianova, Hamburg, provided by PEI microscopy facility

Secondary Antibodies	Source
Goat anti-mouse IgG_1-HRP	Southern Biotech, Burmingham, Alabama # 1070-05
Goat anti-mouse IgM/IgG labeled with 5 nm gold	Biocell, provided by PEI microscopy facility
Goat anti-mouse IgM-FITC	Caltag, Hamburg # M31501
Goat anti-rabbit IgG labeled with 10 nm gold	Biocell, provided by PEI microscopy facility
Polyclonal Rabbit anti-goat-HRP	Dako Cytomation, Hamburg # P0449
Rabbit anti-mouse IgG_{2a}-HRP	Zymed Invitrogen, Karlsruhe # 61-0220
Rabbit anti-mouse IgM, G+A-HRP	Zymed Invitrogen, Karlsruhe # 61-6420
Rabbit anti-mouse IgM-HRP	Zymed Invitrogen, Karlsruhe # 61-6820

3.1.9 Plasmids and vectors

All plasmids used are described in detail in the Appendix.

Table 10 Origin of plamids and vectors used in this study

Plasmids and vectors	Source
pCMVΔR8.2 human immunodeficiency virus *gag/pol* genes (HIVgp)	Kindly provided by Christian Buchholz, PEI [Naldini et al., 1996]

Plasmids and vectors	Source
pHIT60 murine leukaemia virus (MLV)-based *gag/pol* expression plasmid	Plasmid factory [Soneoka et al., 1995]
pMDG VSV-G protein	Kindly provided by Christian Buchholz, PEI [Naldini et al., 1996]
pDPrP111 murine Prion protein (mPrP)121-231aa	Kindly provided by Daphne Nikles, PEI
pD-EGF human epidermal growth factor (hEGF) fused to PDGFR-TMD	Kindly provided by Christian Buchholz, PEI [Merten et al., 2003]
pRSETa procaryotic expression vector	Invitrogen Catalog, Karlsruhe # V351-20
pRSETa mPrP (121-231aa)	Kindly provided by K.Wüthrich, Zurich
pDisplay (pD) vector platelet derived growth factor receptor (PDGFR)	Invitrogen Catalog, Karlsruhe # V660-20

All DNA restrictions were performed using commercially available restriction endonucleases from New England Biolabs (NEB) according to the manufacturer's instructions.

3.1.10 Software

Table 11 Software

Software	Source
BD FACS DIVA Software	Becton Dickinson Gmbh, Heidelberg

Software	Source
Graph Pad Prism	Graph Pad Software Inc, San Diego, USA
CellQuest Pro software	Becton Dickinson Gmbh, Heidelberg
Vector NTI Advance 9.0	Invitrogen, Karlsruhe

3.2 Methods

3.2.1 Molecular biology

3.2.1.1 Transformation of competent bacteria

Transformation of E. coli (BL21 (DE3) or XL2 blue) is the method of choice to amplify plasmid DNA through cellular replication. For this purpose, 100 µl competent cells were thawed on ice and approximately 50 ng DNA were added. After further incubation on ice for 30 min, a heat shock at 42°C for 45 sec was performed in a thermoblock. After 2 min incubation on ice, 900 µl of prewarmed (37°C) SOC medium was added to the cells and incubated for 60 min at 37°C. The bacteria suspension was plated onto LB-AMP-plates and incubated over night at 37°C.

3.2.1.2 Plasmid preparation

Preparation of plasmids from bacteria was performed using the Qiagen plasmid kits according to the manufacturer's instructions. The basic principle of this method is binding of DNA to anion exchange columns. Thus, all cellular compounds such as proteins can be washed away, whereas the DNA is retained within the columns. For purification of low amounts of DNA (Miniprep), 3 ml over night cultures were inoculated using LB-AMP-Medium. The next day, bacteria were harvested at 16,000 x g for 30 sec. The resulting pellet was lysed using solutions delivered by the manufacturer (P1 & P2). Chromosomal DNA and cellular fragments were excluded by centrifugation (16,000 x g for 10 min). Subsequently, the supernatant was applied to anion exchange columns according to the manual. For extraction of larger amounts of DNA (Maxiprep), 200 ml LB-AMP-Media were inoculated and cultivated over night. Bacterial yield was performed at 6000 x g for 15 min. Afterwards, cells were lysed and the remaining cell debris and chromosomal DNA was removed by centrifugation (15,000 x g for 30 min, 4°C). The resulting supernatant was subsequently purified via an anion exchange column according to the manufacturer's

instructions. Finally, concentration and purity of the DNA was determined photometrically.

3.2.2 Cell culture

3.2.2.1 Cells and media

Table 12 Overview of cells and media

Cells	Source
N2a #58-22L	Obtained from S.Lehmann, France [Nishida et al., 2000]
HEK 293FT cells	Originally obtained from American Type Culture Collection (ATCC)
Vero cells (African green monkey cell line)	Originally obtained from ATCC

Human embryonic kidney (HEK) 293FT cells were cultivated in DMEM supplemented with 10% FCS, 1% Glutamax and antibiotics (100 units/ml penicillin, 50 mg/ml streptomycin).
N2a #58-22L cells were grown in Dulbecco´s Modified Eagles Medium (DMEM) plus 4500 mg/l Glucose, supplemented with 10% FCS, 1% Glutamax and antibiotics (100 units/ml penicillin, 50 mg/ml streptomycin).
Vero cells were cultivated in Modified Eagles Medium (MEM) supplemented with 5% FCS and 1% Glutamax.

All cell lines were cultivated in an incubator at 37°C, 5% CO_2 and saturated water atmosphere. Cells were trypsinised (0.25% trypsin in PBS) for passaging. A fraction of the resulting suspension was seeded into new culture flasks and fresh medium was added.

3.2.2.2 Freezing and thawing of cultured cells

For storage, cells were kept at -80°C. Long term storage was performed in liquid nitrogen.

Freezing

Cells were trypsinized and resuspended in appropriate medium. After centrifugation (300 x g for 5 min at 4°C) cells were resuspended in freezing medium (90% DMEM, 10% DMSO), divided into cryotube aliquots of approximately 5 x 10^6 cells and frozen at -80°C.

Thawing

Cryotubes were incubated in a water bath at 37°C until the ice thawed. Then the cell suspension was immediately transferred into a falcon tube with 15 ml prewarmed medium. To remove the cytotoxic DMSO, cells were subsequently centrifuged (300 x g for 5 min at RT), resuspended in fresh medium and seeded into appropriate culture flasks.

3.2.2.3 Manual counting of cells

After shaking of cell suspension, 50 µl were taken and mixed 1:1 in a 96-well microtiter plate together with trypan blue solution. Dilutions of 1:10 to 1:50 were prepared for analysis in a Neubauer counting chamber and covered with a slip. Vital lymphocytes - as characterized by pale grey colour - were counted manually per microscope in the four large squares at the corners of the chamber grid. Cell numbers were calculated using the following formula:

Cells/ml = $n/4$ x dilution x 10^4 x volume [ml] of total suspension
n = counted cells in four squares

3.2.3 Protein biochemistry

3.2.3.1 SDS-polyacrylamide-gelelectrophoresis

The SDS-polyacrylamide-gelelectrophoresis (SDS-PAGE) (modified after [Laemmli, 1970]) allows to separate protein mixtures according to their apparent molecular weight. The basic principle includes binding of multiple molecules of the negatively charged detergent sodium dodecylsulfate (SDS) via hydrophobic interactions to denatured protein molecules. That way, the latter ones acquire an excess of negative charges on their surface and can thus be applied to electrophoresis. For this purpose, samples are loaded on polyacrylamid gels which act like molecular sieves, similarly to agarose gels. Samples were mixed with the appropriate amount of sample buffer (4x) and loaded either on 10-12% Tricine gels or Nu page 12% Bis-Tris gel, within a Biorad Protean II chamber.
SDS-PAGE was performed according to the manufacturer's instructions using a Power Ease 500 Power supply with the appropriate running buffer.

The MultiMark marker was used as protein standard.

MultiMark marker size standards (kD):
250, 148, 60, 42, 30, 22, 17, 6, 4

Coomassie staining of SDS-gels

After electrophoretic separation of proteins via SDS-PAGE, the bands were stained by incubating the gel for 15 min in a solution of Coomassie brilliant blue. Excessive dye was removed with a mixture of acetic acid and methanol until distinct protein bands were visible.

3.2.3.2 Western blot analysis

The Western blot technique is a method which enables the transfer of proteins on membranes. This transfer, also termed blot, enables the specific visualization of proteins of interest by immunostaining. Usually, proteins which have been separated by SDS-PAGE are applied to Western blot analysis.

Samples were separated on appropriate SDS gels and then transferred to a PVDF membrane within a Fastblot-device, according to the manufacturer's instructions. For this, membranes were shortly incubated in methanol and blotted in transfer buffer. After blotting at 15 V for 45 min, unspecific binding sites were blocked with 5% milk powder in TBS-T for 2 h. For specific protein staining, antibodies were diluted in 2% milk powder in TBS-T. Staining of PrP was performed using the anti-PrP monoclonal antibody 6H4 (1:5000) ON at 4°C. The membranes were washed three times with TBS-T before they were incubated for 1 h at RT with the secondary antibody horseradish peroxidase (HRP)-conjugated rabbit anti-goat IgG (1:10000 in TBS-T). After washing as described above, bands were visualized using the chemoluminescence kit according to the manufacturer's instructions. The two reagents contain a HRP substrate that emits light during conversion into the product. Hence the signal can be visualized by using chemiluminescence films. The signal was collected for 5-60 min, depending on the signal intensities.

3.2.3.3 *In vitro* PrP-neutralizing assay

Antibody treatment of cells

First, $1x10^5$ N2a #58-22L cells/well were seeded into 6 well plates. At day 2, 4 and 6 cells were treated with different concentrations of antibodies (6H4 or mouse sera) diluted in 1.5 ml of appropriate medium. Seven days after antibody treatment cells were lysed.

Preparation of cell lysates

For preparation of cell lysates, cells were lysed with 75 µl/well of lysis buffer for 5 min at 4°C and subsequently centrifuged for 3 min at 2400 x g at 4°C. Supernatants were stored at -80°C. Protein concentration was determined by a BCA assay according to the manufacturer's instructions.

Proteinase K digestion

Digestion with Proteinase K (PK) was performed using 20 µg/ml PK. 200 µg of protein was incubated with the appropriate amount of PK (2.6 µl in 20 µl sample volume; 20 µg/ml final concentration) at 37°C for 30 min. The reaction was stopped by addition of 1 mM Pefablock (final concentration) and centrifugation for 45 min, 4°C, 16,000 x g. After removal of supernatant 20 µl of lysis buffer was added to the pellet, mixed with 4 x sample buffer plus 1% ß-mercaptoethanol and incubated at 95°C for 10 min. Usually 100-200 µg of cell lysates were then loaded onto the SDS gel.

3.2.3.4 Expression and purification of recombinant mouse PrP amino acid 121-231

The expression plasmid pRSETa mPrP(121-231) fused to an N-terminal histidine tag (obtained from K.Wüthrich Zürich, Sitzerland) was transformed into E. coli BL21 (DE3) as described in 3.2.1.1. Protein purification was performed with a modified protocol according to Zahn [Zahn et al., 1997]. Bacteria were grown to an OD_{600} of 0.5 and then induced with 1 mM isopropyl-ß-D-galactopyranoside (IPTG). Cells were harvested 6 h after induction and centrifuged for 10 min, 6000 x g. The pellet was resuspended in 10 ml denaturating buffer G. After sonification on ice (8 x 60 sec) and subsequent centrifugation for 10 min, 5400 x g at 4°C, the soluble protein fraction was added on a nickel-nitrilotriacetic acid (NTA) agarose resin (6 ml) in a chromatography colum. For efficient protein binding, the agarose resin was incubated for 1 h at RT on an overhead shaker. Subsequently, the resin was washed three times with 10 ml of buffer G. In a next step, buffer G was exchanged with 25 ml to buffer B (in ratio 1:1) via a gradient former for protein refolding and washed additionally with 10 ml of buffer B. The protein was eluted with 50 mM immidazol in buffer B (4 ml). After a short incubation time (10 min), the residual protein was eluted from the resin by using 4 ml 150 mM immidazol dissolved in buffer B. In a final step the recombinant $mPrP^{REC121-231}$ protein was dialyzed via a dialyze membrane (MWCO: 8000) over night at 4°C in buffer D (100 ml).

3.2.4 Electron microscopy

3.2.4.1 Immungold-labelling

For detection of PrP or VSV-G displayed on retrovirus particles, virions concentrated from the cell supernatant were used. For immunonegative staining, 10 µl of concentrated particle suspension was adsorbed to glow discharged carbon coated formvar grids for 2 min. In case of VSV stain, purified VSV (stock 10^{12} PFU) was applied in a volume of 5 µl to the grids. After rinsing in PBS, grids were incubated with appropriate antibodies for 15 min at RT.

Table 13 Primary antibodies for immunogold-labelling

Primary antibodies	dilution
Polyclonal anti-VSV-G rabbit antiserum	1:1000
6H4 antibody	1:500

Grids were washed two times with PBS and incubated with the appropriate secondary antibody (1:50) for 15 min, respectively.

Table 14 Secondary antibodies for immunogold-labelling

Secondary antibodies	dilution
Goat anti-mouse IgM/IgG 5nm gold (PrP)	1:50
Goat anti-mouse IgG 10nm (PrP)	1:50
Goat anti-rabbit IgG 10nm gold (VSV-G)	1:50

Finally, immunolabled virus-like particles were washed two times with PBS and one time with Aqua dest. before particles were negatively stained with 2% uranylacetate or methylwolframat for 10 sec. Electron micoscopic preparations

were examined in a transmission electron microscope EM 109 or 902 and micrographs were taken on Kodak Estar electron microscope film.

3.2.5 Virological methods

3.2.5.1 Cell transfection and production of VLP

To express plasmids within eukaryotic cells, transfection using Lipofectamine 2000 was performed. The corresponding method is based on a complex formation between plasmid DNA and liposomes which subsequently fuse with the cellular membrane. Hence, the DNA is taken up by endocytotic mechanisms. For the generation of VLP, 3 x 10^6 cells were seeded into a T175 flask at the day before transfection. After cultivation over night, the transfection was performed as follows: Plasmid mixture with combined plasmids (Table 15) was diluted in 2 ml serum free DMEM. In parallel, 90 µl Lipofectamine 2000 was suspended in another 2 ml serum free DMEM (without any supplements). After incubation for 5 min at RT, both samples were mixed. This solution was incubated for further 20 min. Afterwards medium was exchanged against the transfection mixture (4 ml + 8 ml serum free DMEM) and the cells were incubated for 4 h at 37°C. After 4 h of incubation the transfection mixture was exchanged against DMEM containing serum. Cell culture supernatants were harvested 48 h after transfection, filtered through a sterile 0.45 µm filter and particles were concentrated by low speed centrifugation (16 h- 24 h, 2500 x g, 4°C). In case of VLP-PrP^{D111}, HIV-PrP^{D111}, or VLP-EGF^{D} particles, cell culture supernatants were harvested twice, 48 and 72 hours after transfection.

For standard particle preparations, twelve T175 flasks were transfected. After low-speed concentration, harvested particles were resuspended in 1 ml PBS Dulbecco + 1% FCS and divided into 20 aliquots of 50 µl. VLP were used for electron microscopy and immunization experiments. For quantification of particle numbers ELISA tests were performed as described in Chapter 3.2.8.2.

Table 15 Plasmid concentration for transfection of one T175 cell culture flask

Particles	pHIT60	pCMV∆R8.2	pmDG	pDEGF	pDPrP111
VLP-VSV	12.5 µg		5.0 µg		
VLP-PrP^{D111}	15.0 µg				15.0 µg
VLP-EGF^{D}	15.0 µg			15.0 µg	
VLP-PrP$^{D111/VSV}$	12.5 µg		5.0 µg		12.5 µg
HIV-PrP^{D111}		15.0 µg			15.0 µg

3.2.5.2 Reverse Transcriptase (RT) activity assay

The Reverse Transcriptase assay is based on detecting the activity of the viral enzyme reverse transcriptase (RT), which converts retroviral genomic RNA into double stranded DNA during the viral life cycle. The RT test solutions are commercially available. For detection of MLV particles the C-type RT test was used. All RT tests were performed by the group of Christian Buchholz (PEI, Langen).

Since the average amount of RT per particle has been evaluated [Pyra et al., 1994], it is possible to calculate particle values present per sample using the following equation:

$n_{CP} = 3 \times 10^9$ [p/units] × RT-value [units]

3.2.5.3 Viruses

Vesicular stomatitis virus serotype Indiana (VSV-IND, Mudd-Summers isolate) was originally obtained from D. Kolakofsky, University of Geneva, Switzerland, and was grown on BHK cells in MEM supplemented with 5% FCS to obtain virus stocks containing 10^9 PFU/ml. UV inactivation was performed with an UV irradiator on ice at 300 mJ, 45 sec. For immunizations into mice, VSV was diluted in PBS + 0.1% BSA.

3.2.5.4 VSV neutralization assay

Vero cells were seeded at a density of 2 x 10^5 cells/ml in 100 µl/well, MEM 5% FCS, using 96-well flat bottom cell culture plates. The plates were kept in the incubator to grow to confluency.

On day 2, anti-VSV mouse sera were reduced for the determination of IgG by adding 10 µl 280 mM ß-mercaptoethanol to 10 µl of the serum samples. The reduced sera were incubated for 1 h at RT. Untreated sera were used for determination of total Ig (IgM+IgG). Next, the sera were prediluted 1:40 by adding 380 µl MEM 5% FCS to the reduced sera and 390 µl MEM 5% FCS to the untreated sera. In order to destroy the complement system, the prediluted sera were heat-inactivated for 30 min at 56°C.

For serial dilutions of the sera, lines 2-12 of new 96-well plates were filled with 100 µl MEM 5% FCS. Subsequently, 200 µl heat-inactivated serum dilutions were added to the first line of the wells and 1:2 titration steps were made. Next, 100 µl VSV were added at a concentration of 10^3 PFU/ml to all wells already containing 100 µl antibody dilution. These plates were left to incubate for 90 min at 37°C without stapling.

Then, the medium of the confluently grown Vero cell culture plates was flicked off and 80 µl of the serum-VSV mixture was transferred onto the Vero cell layers by pipetting from front to back. The plates were incubated for 1 h at 37°C and methylcellulose 1 x MEM was adapted to 37°C. The plates were overlayed with 100 µl 1% methylcellulose 1x MEM (I) and incubated over night at 37°C.

On day 3, the medium was flicked off and the cultures were overlayed with crystal violet and incubated for 1 h at RT. Finally, the dye was carefully removed and the plates were washed extensively. The plates were air dried and the plaques were counted. The serum dilution reducing the number of plaques by 50% was taken as titer [Charan et al., 1986].

(I) Preparation of 1% methylcellulose in 1 x MEM

15 g methocel was dissolved in 750 ml double-distilled H_2O (2%) ON under stirring in the cold room. After autoclaving, a methylcellulose block was formed that dissolved at RT within 24 h. 250 ml of 2% methocel were mixed with 50 ml 10 x MEM. 30 ml 7.5% sodium bicarbonate was added. A final 1 x concentration of 0.44% was reached by filling up to 500 ml with 170 ml double-distilled H_2O.

3.2.6 Mouse experiments

3.2.6.1 Mouse anesthesia

One mouse was set into the glass prepared with approximately 1 ml Isofluran and observed for progressive stages of induction of anesthesia. The operation stage of anesthesia was achieved after usually 10 sec, when the mice started to breath profoundly and more slowly. The mice were then immediately taken out and manipulations could be performed for approximately 20-30 sec.

For general anesthesia mice were i.p. injected with 100 µl Ketamin/Rompun per 10 g body weight.

3.2.6.2 Immunization and infection of mice

Mice were warmed up in their cages for 10 min by an infra-red lamp. Subsequently, mice were introduced into restrainers and injected intravenously (i.v.) with 200 µl of appropriate antigen (VLP or VSV) diluted in PBS 0.1% BSA into the lateral tail vein using a 0.3 mm syringe.

For immunizations in the presence of various adjuvants, PrP-displaying virus-like particles were emulsified in an equal volume of CpG1668 (50 µg/mouse, 1:2), Titer Max (1:2), Alum (1:2) or complete/incomplete Freund's adjuvant (CFA/IFA) (1:2) immediately before subcutaneous administration (100 µl total volume), respectively. For boosting upon priming with VLP-PrP^{D111} in CFA, IFA was used.

For intracerebral (i.c.) infections, mice were first anesthetized i.p. with Ketamin/Rompun and afterwards inoculated i.c. with 1:10000 diluted RML 5.0

(stock: 10% homogenate in 0.32 M sucrose) in PBS containing 5% BSA. The inoculum was given in a 30 µl volume by i.c. injection using a 0.3 mm syringe into the right parietal lobe at a depth of 4 to 5 mm.
The prion inoculum used in these experiments was RML 5.0, which was derived by fivefold serial passage in CD-1 mice of a Chandler mouse-adapted scrapie strain (obtained from the group of A. Aguzzi, Zurich).
For i.p. infection experiments, mice were injected with 100 µl of a 10000-fold dilution of the inoculum RML 5.0 diluted in PBS 5% BSA.

3.2.6.3 Blood sampling for serum analysis

Mice were anesthetized and bled with capillary behind the eye (retroorbital bleeding). Blood was collected in heparinized micotainer tubes for FACS staining or for serum sampling in serum vacutainers.

3.2.6.4 Isolation of splenocytes

Mice were anesthetized and sacrificed by atlanto-occipital dislocation. The bodies were bathed in 70% ethanol for disinfection and with a pair of scissors and tweezers the spleen was prepared. The organ was put into a petri dish, squeezed with a 5 ml plastic pipette after opened the splenic capsule. Splenocytes were filtered through a 70 µm Filicon and caught in a 15 ml Falcon tube. After centrifugation for 5 min, 300 x g, at 4°C, the pellet was resuspended in 5 ml red blood lysing solution for 2 min at RT followed by a centrifugation step (5 min, 300 x g at 4°C). Finally, the cell pellet was resupended in FACS buffer. Cells are ready for cell staining.

3.2.6.5 Depletion of $CD4^+$ T cells

Three and one day before immunization with VLP-VSV or VSV, mice were injected i.p. with a dose of 500 µg of GK1.5 mAb per injection. Depletion efficiency, as determined by FACS analysis of peripheral blood, typically exceeded 99.9%.

3.2.7 Immunohistology

Freshly removed organs were immersed in Tissue Freezing Medium and snap frozen for several minutes in liquid nitrogen. Further steps were performed by the group of B.Odermatt, Zurich.

In brief, tissue sections of 5 μm thickness were cut in a cryostat, placed on siliconized glass slides, air dried, fixed with acetone for 10 min, and stored at -70°C. Immunohistological stainings were performed as described previously [Bachmann et al., 1996] except for detection of germinal center cells, which was done by using biotinylated PNA (1:50). For staining of follicular dendritic cells (FDC), rehydrated tissue sections were incubated with rat monoclonal antibodies clone FDC- M1 (1:50). Staining was revealed by the ABC/peroxidase method according to the manufacturer's instructions

3.2.8 ELISA analysis

3.2.8.1 Analysis of VSV-specific serum binding

Purified VSV-IND was prediluted 1:10000 in coating buffer (0.1 M $NaHCO_3$, pH 9.6) and coated in 0.1 M $NaHCO_3$, pH 9.6 on 96 well Nunc Maxisorp ELISA plates (100 µl/well). The plates were incubated over night at 4°C. The virus dilution was carefully flicked off and the plates were washed two times with 150 µl/well of PBS, 0.1 % Tween 20. To saturate unspecific protein binding, 100 µl/well of 5% BSA in PBS, 0.1% Tween 20 was added. After incubation for 2 h at RT, VSV-coated plates were washed two times with 150 µl/well as described above. Next, 150 µl of serum samples diluted in PBS, 0.1% Tween 20 were serially 3-fold diluted (20xlog3) and added to the VSV-coated plates. The mAb VI24 (1:2000) was used as a positive control. After 2 h incubation at RT, the VSV coated plates were washed three times with 150 µl/well PBS 0.1% Tween 20. To detect VSV-specific antibodies, 80 µl/well HRP-coupled detection antibodies (anti-IgG_{2a} 1:1000, diluted in 1% BSA, PBS, 0.1% Tween 20) was added and the plates were incubated for 1 h at RT. In the meantime, aliquots of ABTS, the substrate of HRP, were thawed and activated by supplementing

20 µl 30% H_2O_2 to 11 ml ABTS aliquots. Then, the incubated plates were washed three times and 100 µl/well of the substrate (0.5 mg/ml ABTS in 0.1 M NaH_2PO_4, pH 4 and 30% H_2O_2 was added. After an incubation time of 45 min at RT, the optical density was determined at a wave length of λ= 405 by an ELISA reader.

3.2.8.2 Charaterization and Quantification of VLP or VSV

To analyze molecules displayed by retrovirus-like particles, 96 well Nunc Maxisorb ELISA plates were coated with purified VLP which were prediluted 1:10 in 0.1 M $NaHCO_3$, pH 9.6 and subsequently serially three fold diluted (10xlog3). For detection of VSV-G molecules on purified VSV, 96 well Nunc Maxisorb ELISA plates were coated with 1:1000 prediluted virus in a serially three fold dilution. Upon blocking with 100 µl 5% BSA in PBS 0.1% Tween, 50 µl/well of the primary antibody (Table 16) diluted in PBS, 0.1% Tween, 1% BSA was added for 2 h at RT. Upon thorough washing, bound antibody was decorated using appropriate HRP-conjugated secondary antibodies (80 µl/well) diluted in 1% BSA, PBS, 0.1% Tween 20. After 1 h incubation at RT plates were washed and bound HRP-coupled antibodies were measured as described in Chapter 3.2.8.1.

Table 16 Antibodies for VLP-ELISA

Antigen	Primary antibody	Secondary antibody
VSV-G	mAb VI24 (1:200)	anti-IgG_{2a}-HRP (1:1000)
PrP	6H4 (1:500)	polyclonal rabbit anti-mouse IgM, G+A-HRP (1:1000)
P30	Polyclonal anti-p30 (1:1000)	polyclonal rabbit anti-goat-HRP (1:500)
P24	mAb 880-A (1:500)	donkey anti human IgG-HRP (1:1000)

3.2.8.3 Analysis of PrP-specific serum binding

384 well Nunc Maxisorb ELISA plates were coated with 5 µg/ml per well of $mPrP^{REC121-231}$ (purified in Chapter 3.2.3.4) diluted in PBS and blocked with 50 µl 5% bovine serum albumin (BSA). Serial PrP-specific serum dilutions in PBS, 0.1% Tween, 1% BSA were added. After 2 h incubation at RT, plates were thoroughly washed and 1:1000 diluted HRP-conjugated polyclonal rabbit anti-mouse Ig M, G+A antibody was added. After 1 h incubation at RT plates were washed and bound HRP-coupled antibodies were measured as described in Chapter 3.2.8.1.

3.2.9 Flow cytometric analysis

3.2.9.1 Flow cytometric determination of PrP^C-specific serum binding

For flow cytometric determination of PrP^C-specific serum antibody binding, 10 µl heparinized tg33 mouse blood (1:15 in FACS buffer) was applied on 96 well V-bottom cell culture plate and washed with 150 µl FACS buffer by centrifugation (300 x g, 4°C for 5 min). Serum of immunized mice (1 µl), preimmune serum (1 µl), isotype controls (1 µl) or the positive control 6H4 (1:200) were separately mixed with anti-CD3-PE (0.5 µl) and incubated with tg33 blood cells for 20 min at 4°C. After washing with 150 µl FACS buffer at 300 x g, 4°C for 5 min, blood cells were incubated additionally for 20 min at 4°C with 10 µl of donkey anti-mouse IgG-FITC (1:50) or goat anti-mouse IgM-FITC (1:50). After washing, pellets were resuspended in 200 µl red blood cell lysing buffer for 15 min at RT. Finally, cells were washed two times, and pellet was resuspended in 150 µl FACS buffer. Samples were measured on a FACScan machine by acquiring 10000 events in the lymphocyte gate. Data analysis was performed using the BD Cell quest software.

3.2.9.2 Detection of germinal center B cells by FACS analysis

Spleens were removed as described in Chapter 3.2.6.4 and single cell suspensions were prepared. After red blood cell lysis by treatment with 5 ml red

blood lysing buffer, splenocytes were centrifugated (300 x g, for 5 min at 4°C) and the pellet was resuspended in 3 ml FACS buffer. For staining procedures $1x10^6$ cells were added in a 96 well V-bottom cell culture plate and pelleted by an additional centrifugation step (300 x g, for 5 min at 4°C). Next, splenocytes were incubated with biotinylated peanut hemagglutinin (PNA) (1:2000) in FACS buffer at 4°C for 15 min. After extensive washing with 180 µl FACS buffer (300 x g for 5 min at 4°C), cells were stained with a mixture of streptavidin-PE (10 µl), B220-PECy5.5 antibody (1 µl), FITC-conjugated anti-CD21 (1 µl) and APC-conjugated anti-CD23 (1 µl) for 10 min at 4°C in a total volume of 25 µl FACS buffer. After two washing steps, cells were resuspended in 150 µl FACS buffer and samples were analyzed on a FACS BD LSR II using BD FACS Diva software.

3.2.9.3 Purification of PrP-specific memory B cells

Splenocytes from six immunized homozygous C57/BL6 *Prnp*$^{0/0}$ donor mice were prepared as described in Chapter 3.2.6.4 and subsequently pooled in 12 ml MACS buffer for sorting experiments. MACS buffer was used in all staining steps.

$1.2\ x10^8$ splenocytes were stained with CD19-PE (1:800), CD4-FITC (1:1000) and CD8-FITC (1:800) for 15 min at 4°C and centrifugated for 5 min 300 x g at 4°C. Pellet was resuspended in 10 ml MACS buffer before cell suspension was filtered through a 70 µm Filicon and titrated to $6x10^7$ cells/ml.

Cell sorting was performed by a BD MoFLo Cell Sorter. Preparation of splenocytes as well as cell sorting procedure was accomplished by the group of T.Winkler in Erlangen.

For adoptive transfer experiments *Prnp*$^{+/+}$ recipient mice were injected i.v. with $1x10^7$ CD19$^+$ B cells/mice.

3.2.9.4 Competition assay

Sera of immunized mice or mAb 6H4 were first titrated for 80% binding capacity. Thus, 10 µl blood of tg33 mice was incubated with 10 µl of different

serial log 5 dilutions of the 6H4 antibody. In case of serum antibodies, 10 µl of different serial log 3 dilutions were added together with 1 µl anti-CD3-PE for 20 min at 4°C. Staining was performed as described in detail in Chapter 3.2.9.1. For competition assay limiting antibody concentrations were incubated together with 200 ng $mPrP^{REC121-231}$ which was purified as described in Chapter 3.2.3.4. Different concentrations of VLP-PrP^{D111} (total volume of 30 µl) were used as competitors. Serum antibodies and competitors were incubated for 3 h at 4°C on a shaker. PrP^{C}-specific binding of mAb 6H4 or serum antibodies to native PrP^{C} was measured by FACS using 10 µl blood of tg33 mice overexpressing PrP^{C} on T cells (see Chapter 3.2.9.1).

3.2.9.5 Counting of absolute cell numbers by FACS

To directly count absolute numbers of lymphocytes, a quantitative method on the base of reference counting beads was performed. Counting beads, which contained about 1000 beads/µl, were pipetted into 96 well plates together with splenocytes ($1x10^6$ cells) in a ratio 1:1. The samples were stained as described in detail in Chapter 3.2.9.1. To count absolute numbers of peripheral blood lymphocytes by FACS, cell numbers were analyzed as described in the manufacturer´s instructions. In brief, the counting beads were gated simultaneously in the forward scatter (FSC)/side scatter (SSC) (Figure 5, left) as well as in the fluorescence channel 2/SSC (Figure 5, right).

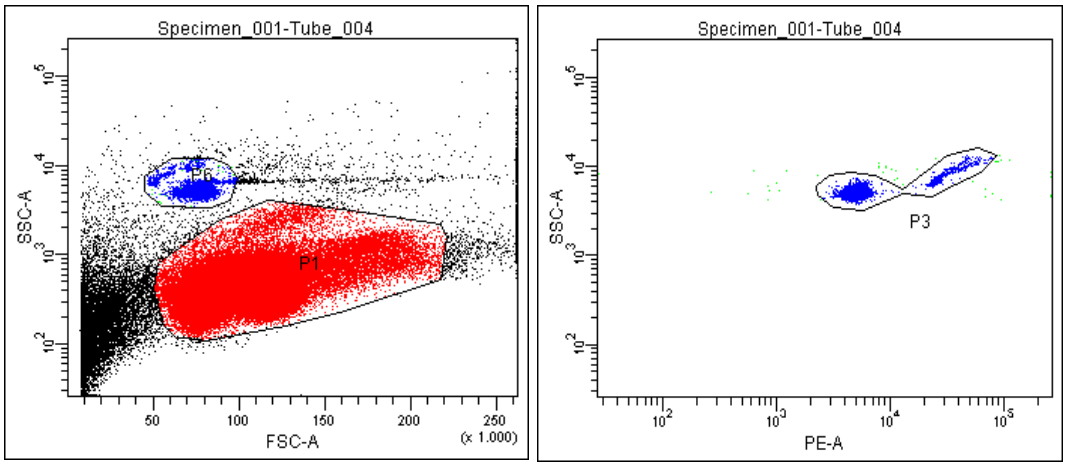

Figure 5 **Lymphocyte count by FACS.** Left plot shows the FSC/SSC plot with lymphocyte gate (P1) and beads gate (P6), right: fluorescence 2/SSC with combined beads gate (P3). Events were depicted in dot plots to adjust the detritus threshold. The samples were measured for 5000 beads.

4 Results

In this thesis the question was addressed whether in analogy to vaccination against “normal” pathogens, protective antibody responses can be induced against prions. In the first chapter of this thesis, virus-like particles (VLP) displaying the vesicular stomatitis virus (VSV) glycoprotein (VSV-G) were generated (VLP-VSV) to assess the immunogenicity of VLP. Furthermore, VLP were tested whether they are suitable for the induction of protective immunity against “normal” pathogens. Interestingly, the VLP-VSV mediated induction of VSV neutralizing IgG antibodies was type I IFN dependent. In the second chapter, different types of VLP displaying parts of the cellular prion protein on the surface were produced and tested for their capacity to induce PrP^{C}-specific antibody responses. Probably due to immunological tolerance, vaccination against prion diseases turned out to be rather difficult in wild-type mice. Therefore, a series of immunization strategies was studied to circumvent tolerance to PrP^{C}. VLP-induced anti-PrP^{C} antibodies were subsequently analyzed in *in vitro* and *in vivo* settings for their potential to inhibit PrP^{Sc} propagation. Furthermore, PrP^{C}-displaying VLP were tested in a competition assay to study the fine specificity of anti-PrP^{C} antibody responses.

4.1 Virus-like particles (VLP) can trigger VSV neutralizing antibody responses

Bacteria or viruses that infect a host are immediately recognized by the immune system to ensure surveillance of the infective agent and survival of the host. In contrast, infective prions share the identical amino acid sequence of endogenously expressed prion protein. Thus, upon scrapie infection, PrP^{Sc} is not attacked by immune defense mechanisms. The molecular structure of an antigen plays a major role for the induction of antibody responses. Soluble foreign proteins such as chicken gamma globulin (CGG) injected into mice provide very limited or no danger signals and therefore elict only very poor immune responses. In contrast, VSV shows a repetitive organization of the

immunogenic VSV-G protein on the surface that is one reason accounting for the strong immunogenicity of the virus. In addition, the viral genome is recognized by TLR7 [Lund et al., 2004; Kawai et al., 2006] and thus serves as a "danger" signal. Furthermore, virus replication can be sensed by the helicase RIG-I [Kato et al., 2005; Kawai et al., 2007]. For safety reasons, vaccines are based on antigens that are very immunogenic and replication deficient. In a first approach we addressed whether non-replicative virus-like particles expressing the major antigen of VSV on the surface are able to induce antibody responses that protect against VSV. If VLP-VSV turned out to be an efficient inducer of protective antibody responses against the virus they might be good vaccine candidates for PrP^C-specific immunization as well. Because VLP are able to present different kinds of antigens at the outer particle surface [Deml et al., 2005], PrP^C-displaying VLP can be readily generated.

4.1.1 Generation of virus-like particles displaying the VSV-G or EGF protein on the surface

First, we generated murine leukemia virus (MLV)-derived VLP that display the vesicular stomatitis virus glycoprotein VSV-G on the surface. To produce such VLP, a new subclone of the human kidney derived cell line HEK 293FT was chosen. HEK 293FT cells grow faster than the original clone and express the large T antigen (SV40), facilitating optimal viral production. HEK 293FT cells were cotransfected with the expression plasmid *pHIT60* coding for the MLV viral structure proteins *gag/pol* together with the VSV-G expression construct *pmDG*. 48 h after transfection, cell culture supernatant was harvested and particles were concentrated by low speed centrifugation (Figure 6).

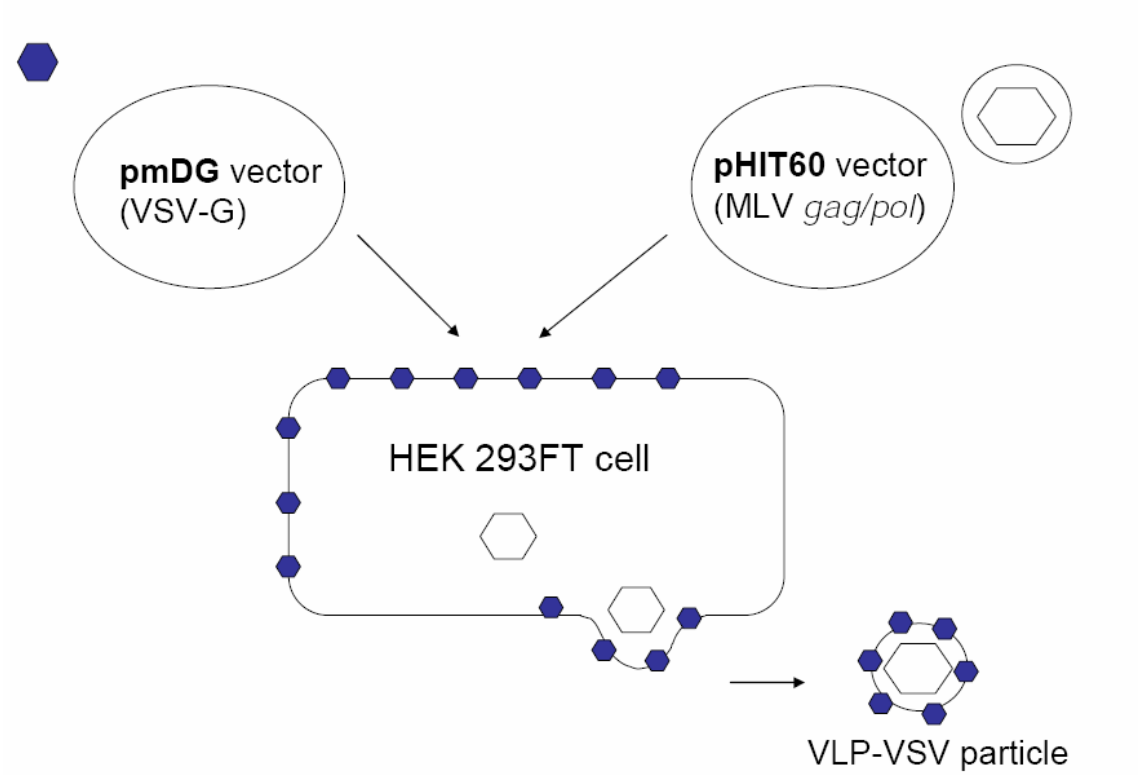

Figure 6 Production of virus-like particles (VLP) expressing the VSV-G protein. Plasmids coding for either the VSV-G sequence or the MLV structural proteins gag/pol were cotransfected into HEK 293FT producer cells. VLP incorporating VSV-G into the viral envelope (VLP-VSV) are subsequently released.

In addition to VLP-VSV expressing the VSV-G protein (Figure 7 A), VLP-EGF^{D} control particles were generated which display the human epidermal growth factor (EGF) on surface (Figure 7 B). In case of VLP-EGF^{D} the *pD-EGF* plasmid was used instead of the *pmDG* VSV-G expression plasmid. The EGF coding sequence was inserted in a commercially available display vector (*pDisplay (pD)*). The pDisplay system functions as a multi-fusion protein, in which the target sequence is N-terminally flanked by the murine immunglobulin κ chain signal peptide and C-terminally flanked by the transmembrane domain of the platelet derived growth factor receptor (PDGFR) anchoring the protein into the plasma membrane.

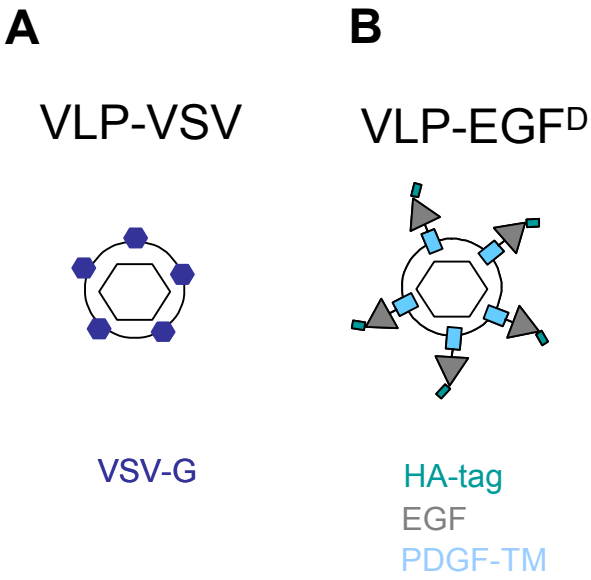

Figure 7 Schematic representation of virus-like particles displaying VSV (A) or EGF (B) on the surface.

The VSV or EGF protein encoded by the *pmDG* or *pD-EGF* plasmids is unspecifically incorporated into VLP derived from the murine leukemia virus (MLV). Generally, proteins that are presented on the cell surface in a high amount seem to be incorporated by viral particles in a passive process, while the budding from the cell surface resulted in the production of protein displaying virus-like particles. In this way, virus-like particles harboring the protein of interest in their membranes can be produced [Nikles et al., 2005].

In particle preparations it might be possible that besides virus-like particles which are regular, round-shaped and equal in size, vesicle-like structures that potentially bud from the cell surface are also present. The latter would also penetrate through the filter and would co-sediment with viral particles upon centrifugation of the sample, because of similar weight and density. Therefore, the structure of virus-like particles and the quality of each preparation was analyzed by electron microscopy method.

4.1.2 Characterization of VLP-VSV by electron microscopy

The expression of VSV-G protein on the surface of virus-like particles was analyzed by immunogold-labeling and subsequent visualization by electron microscopy (Figure 8). VSV-G was marked by a polyclonal rabbit serum specifically binding VSV-G which was detected by a gold-labeled anti-mouse antibody, as described in detail in Chapter 3.2.4.1.

Particle preparations showed mostly 50% of virus-like particles that exhibit the typical morphology of C-type retroviruses, which were determined as VLP-VSV. Furthermore, pleomorphic vesicle-like structures were detectable. Both types of particles were present in roughly similar amounts and were surrounded by numerous immunogold particles. VLP-VSV displayed the VSV-G protein on the surface in a highly organized fashion (Figure 8).

The specificity of the anti-VSV-G staining was confirmed by using VLP-EGF^{D} as a control. VLP-EGF^{D} was negative for anti-VSV-G staining (Figure 3). Because VSV shows high expression of VSV-G protein on the surface it was chosen as a positive control for VSV-G specific protein staining. Indeed, immunoelectron microscopic analysis revealed that VSV was significantly decorated by polyclonal rabbit serum specifically binding to VSV-G (Figure 8).

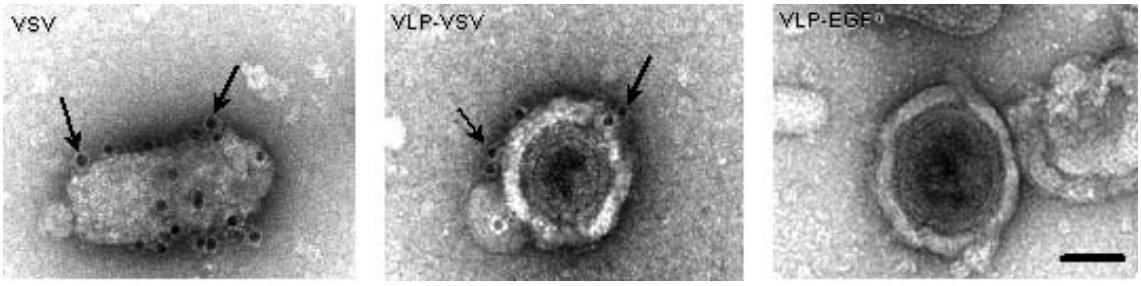

Figure 8 Analysis of VSV-G expression on the surface of VLP by immunoelectron microscopy. Samples of VSV, VLP-VSV and VLP-EGF^{D} were applied to glow-discharged-carbon coated Formvar grids. VSV-G was labelled by a polyclonal anti-VSV-G rabbit serum and a 10 nm diameter gold particle-labelled anti-rabbit-IgG (arrowheads). The bar is equivalent to 50 nm.

4.1.3 Characterization of VLP-VSV and live VSV by ELISA

VLP-VSV was further characterized for VSV-G expression by ELISA. VLP-VSV, VSV and VLP-EGF^{D} were coated in log 3 dilution steps on ELISA plates. After incubation with the VSV neutralizing mAb VI24, only VSV and VLP-VSV, but not VLP-EGF^{D}, showed binding of the anti-VSV-G antibody VI24. Staining with a VLP-specific anti-p30 serum was positive only for VLP-VSV and VLP-EGF^{D} but not for VSV (Figure 9). Thus, VLP-VSV displayed VSV-G in a way that neutralizing determinants, as recognized by VI24 in an ELISA assay, were expressed.

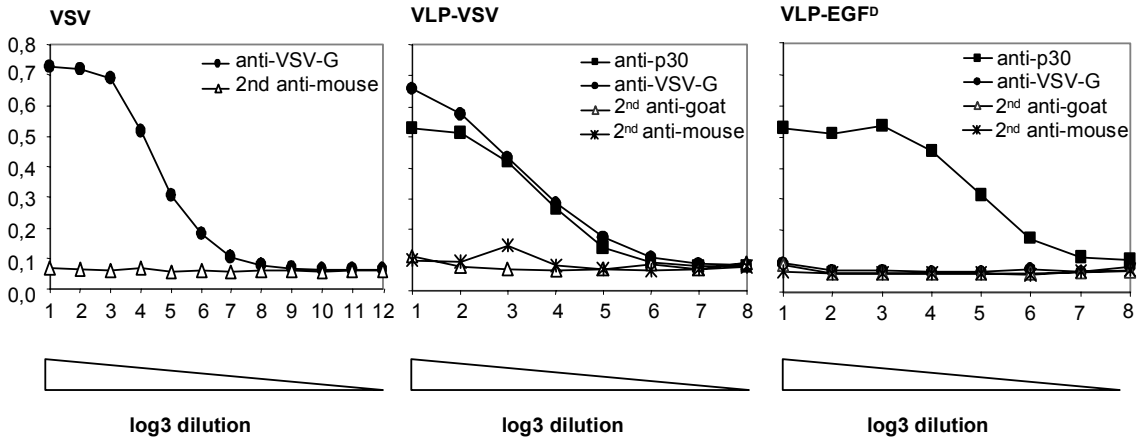

Figure 9 Analysis of VSV-G expression by ELISA. ELISA plates were coated in log 3 dilution steps with graded concentrations of VLP-EGF^{D}, VLP-VSV and VSV. After blocking of unspecific binding, plates were incubated with the VSV-G-specific mouse mAb VI24 (filled circles) or with MLV-specific goat anti-p30 polyclonal serum (filled squares). Bound antibodies were detected by an anti-goat IgG-HRP (open triangles) or anti-mouse IgG_{2a}-HRP (asterisks) antibody.

These results clearly demonstrated that VLP-VSV incorporated VSV-G and displayed the protein on the surface. Moreover, preparations concentrated by low-speed centrifugation of cell culture supernatants contained vesicles and vesicle-like structures, presenting VSV-G as well. The conservation of the immunogenic VSV-G epitopes was confirmed by ELISA which further served as equilibration method of individual VLP preparations.

4.1.4 Quantification and equilibration of VLP-VSV

The efficient production of MLV-derived VLP and the expression of VSV-G on the surface were successfully analyzed by electron microscopy and by ELISA. However, for mouse immunization experiments, it was necessary to determine the amount of relevant antigen injected. Standard methods for quantification of MLV-derived VLP are reverse transcriptase (RT) assays. Usually, the activity of RT in virus stocks is determined by RT assays. To estimate absolute particle numbers, RT units were measured from VLP preparations in a C-type RT activity assay (performed by the group of C. Buchholz). The amount of VLP-particle in the preparations tested, varied between 50 and 450 RT units/ml (data not shown). Assuming that 1 RT unit corresponded to $3x10^9$ VLP [Pyra et al., 1994] approximately 10^9 particles were used for typical immunization experiments. For further equilibration of different particle preparations, ELISA tests were performed. To this end, particles were analyzed by coating log 3 dilutions of concentrated stocks on ELISA plates. For quantification of VLP, anti-p30 serum was used in combination with a goat-specific secondary HRP-labelled antibody. In a next step, relative VLP concentrations were calculated comparing half-maximum values of each particle preparation (Figure 10).

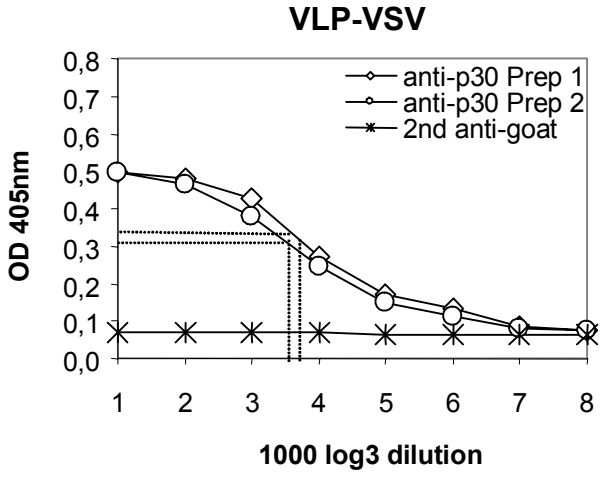

Figure 10 Equilibration of VLP-VSV by ELISA. ELISA plates were coated with two different VLP-VSV preparations (Prep 1 and Prep 2) in indicated dilutions. MLV-specific p30 proteins were detected by polyclonal anti-p30 antiserum (open symbols). A 2nd anti-goat antibody was used as a negative control (asterisks). Half-maximal dilution is indicated by dotted lines.

Throughout this study, the ELISA method was used in addition to the RT assay to standardize particle preparations for immunization purposes.
Taken together, virus-like particles displaying the VSV-G protein on the surface were successfully generated as characterized by electron microscopy and by ELISA. The next chapter addresses the question whether those particles were suitable for inducing VSV neutralizing antibody responses.

4.1.5 Analysis of VSV neutralizing antibody responses induced by VLP-VSV or VSV

As indicated by electron microscopic studies and ELISA experiments, VSV and VLP-VSV expressed determinants recognized by the VSV neutralizing mAb VI24. To study next, whether VSV and VLP-VSV also induced similar VSV neutralizing antibody responses, wild-type mice were i.v. injected with approximately 10^9 VLP-VSV or $2x10^6$ PFU VSV. Live VSV was chosen as a positive control because it induces high anti-VSV-G antibody responses in wild-type mice [Gobet et al., 1988]. Every 4 days serum samples of VLP-VSV and VSV infected mice were collected. Determination of VSV neutralizing serum titers revealed that within 4 days after injection of VLP-VSV, wild-type mice mounted VSV neutralizing IgM that switched to the IgG subclass by day 12 and remained elevated (Figure 11, left upper panel). Similarly, VSV injected mice mounted neutralizing IgM by day 4 that switched to IgG by day 8 and remained elevated (Figure 11, left lower panel).
In summary, VLP-VSV induced IgM responses were slightly enhanced when compared to those induced by VSV, whereas IgG responses were approximately 2-4 log 2 steps lower than those induced by VSV (Figure 11, left panel).

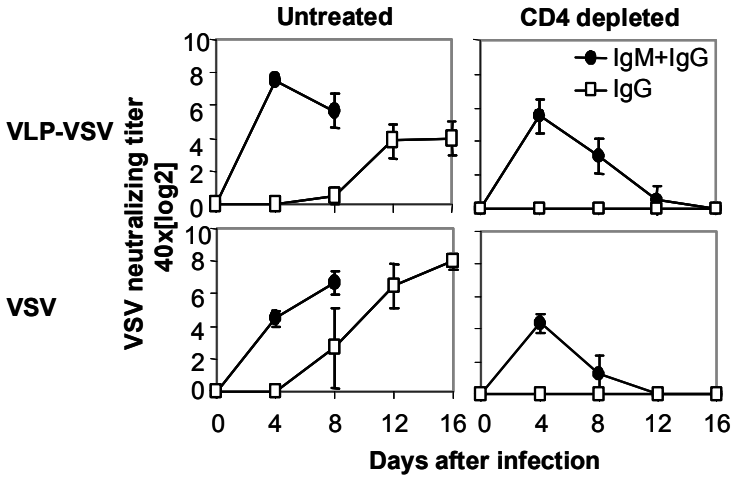

Figure 11 Similarly to VSV, VLP-VSV induces a T help-independent neutralizing IgM response that switches T help-dependently to IgG. For depletion of $CD4^+$ T cells, wild-type mice were treated intraperitoneally with the monoclonal antibody GK1.5 on day 3 and 1 before intravenous injection of VLP-VSV or $2x10^6$ PFU VSV. Serum samples were collected at the indicated time points and VSV neutralization assay was performed. Data shown are the mean of three mice per group ±SEM. One of two similar experiments is shown.

As described previously [Leist et al., 1987], upon VSV infection the IgG switch is T help-dependent. This was indicated by CD4-depleted mice that upon VSV infection mount VSV neutralizing IgM, but do not show a switch to IgG. To further analyze the T help-dependence of VLP-VSV induced antibody responses, untreated control mice and mice depleted of $CD4^+$ T cells were immunized with VSV or VLP-VSV and VSV neutralizing serum antibodies were determined. Similarly, VLP-VSV immunized mice devoid of $CD4^+$ T cells showed a neutralizing IgM response but no IgG switch (Figure 11, right upper panel). VSV- and VLP-VSV-induced IgM responses were slightly reduced in CD4-depleted mice when compared to untreated controls (Figure 11, right panel). Collectively, these results indicated that VSV and VLP-VSV induced T help-independent IgM responses that switched to IgG in a T help-dependent manner.

4.2 VLP induce antibody responses that are type I IFN dependent

Similarly to VSV, replication deficient VLP-VSV was able to induce strong VSV neutralizing IgM that switched to IgG. Therefore, VLP-VSV could be used as a tool for studying virus induced B cell responses. In the early phase of VSV infection, high amounts of type I IFN are secreted to assure the initial survival of VSV-infected mice. In previous studies it was shown that type I IFN stimulation can potently enhance humoral immunity towards the soluble protein chicken gamma globulin (CGG) via a direct effect on B cells [Le Bon et al., 2001; Le Bon et al., 2006]. The question whether virus-induced type I IFN does influence anti-viral B cell responses is controversially discussed because this question cannot be easily addressed. IFNAR-deficient mice that have been instrumental in studying type I IFN effects *in vivo* succumb to VSV infection within few days after injection of low doses of VSV. Thus, replication deficient VLP-VSV was used to analyze the role of endogenously produced type I IFN in virus neutralizing B cell responses.

4.2.1 Analysis of IFNAR dependence in the context of VLP-VSV induced antibody responses

Recent publications showed that virus-induced type I IFN may or may not have an impact on anti-viral antibody responses [van den Broek et al., 1995; Fink et al., 2006; Coro et al., 2006]. To assess the IFNAR dependence of VLP-VSV induced antibody responses, wild-type controls and mice that are deficient of the type I IFN receptor ($IFNAR^{-/-}$) were injected with VLP-VSV and serum samples were collected every 4 days.

VSV-specific Ig binding was assessed by ELISA. To this end, purified VSV was coated on ELISA plates and serially diluted serum samples were added to the plate. Specifically bound IgM or IgG was detected using a goat anti-mouse IgM or goat anti-mouse IgG antibody conjugated with HRP. Compared to wild-type controls, VLP-VSV injected $IFNAR^{-/-}$ mice showed slightly reduced VSV-specific IgM titers on day 4, whereas VSV-specific IgG titers on day 12 and 20 were

significantly reduced (Figure 12 A). Because virus neutralization per definition is more specific than ELISA binding and additionally reflects the biological functions of antibody responses, serum was further analyzed in a virus neutralizing assay. Similarly to VSV binding antibody responses, VSV neutralizing IgM responses were only slightly reduced in IFNAR$^{-/-}$ mice when compared to wild-type mice. In contrast, the switch to neutralizing IgG and the sustained IgG production at later time points was entirely missing in VLP-VSV treated IFNAR$^{-/-}$ mice (Figure 12 B).

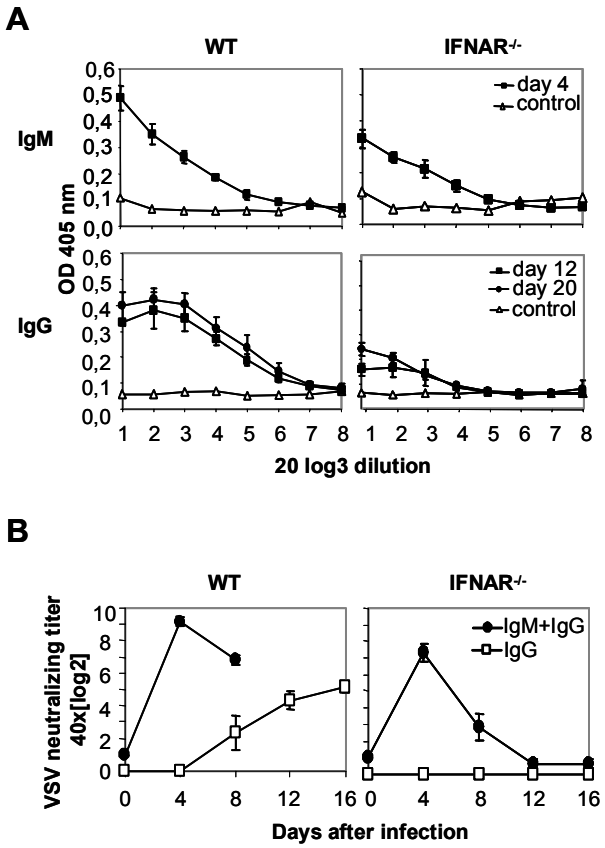

Figure 12 In the absence of a functional type I interferon system, VLP-VSV induces a VSV-specific IgM response but no switch to IgG. Wild-type and IFNAR$^{-/-}$ mice were immunized intravenously with VLP-VSV and serum samples were taken at indicated time points. **(A)** VSV-binding was analyzed by an ELISA method. Serum samples were taken on day 12 and 20 and tested in log3 serial dilutions (20-fold pre-diluted) for the presence of VSV-G-specific IgM or IgG. **(B)** VSV neutralizing antibodies were determined by a neutralization assay. On indicated days, blood was taken and the serum was analyzed for the presence of VSV neutralizing IgM+G (filled circles) or IgG (open squares) antibodies. Data shown are the mean of three mice per group ± SEM. One of two similar experiments is shown.

Thus, upon VLP-VSV immunization, the induction of neutralizing IgM was largely IFNAR-independent, whereas the T help-dependent switch to neutralizing IgG was strictly IFNAR-dependent.

4.2.2 Characterization of germinal center (GC) formation in IFNAR$^{-/-}$ mice upon VLP-VSV immunization

As germinal centers (GC) play a key role in subclass switch, GC formation was studied in wild-type controls and IFNAR$^{-/-}$ mice after VLP-VSV treatment. Histological analysis is a broadly used method for detection of germinal centers. Mice were injected with VSV or VLP-VSV, and 14 days later spleens were prepared for immunohistological analysis. GCs were identified by colocalization of peanut hemaglutinin (PNA) (Figure 13 A, upper panels) and M1 staining of follicular dendritic cells (FDC) on consecutive sections (Figure 13 A, lower panels). Spleens of untreated wild-type and IFNAR$^{-/-}$ mice basically did not show GCs, whereas after VLP-VSV or VSV immunization approximately 32 and 38 GCs per section were found in wild-type spleens, respectively (Figure 13 A+B). Upon VLP-VSV immunization, IFNAR$^{-/-}$ spleens showed approximately 18 GCs per section. Untreated animals were negative for PNA or FDC staining (Figure 13 B).

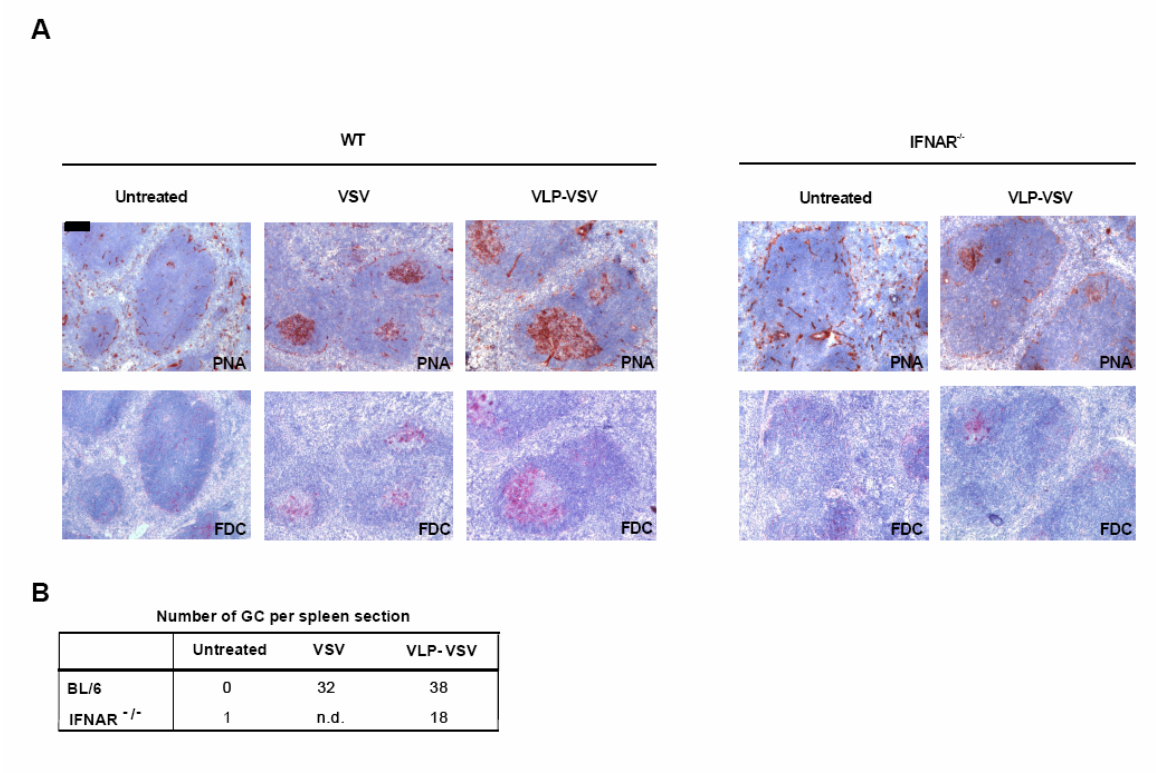

Figure 13 IFNAR$^{-/-}$ mice show a reduced germinal center formation after VLP-VSV immunization. (A) Histological analysis of germinal center formation after i.v. immunization with VLP-VSV. Representative sections of spleens from mice treated with or without VLP-VSV 14 days after immunization were analyzed. The stained markers are indicated in each panel: PNA, peanut hemaglutinin; FDC, follicular dendritic cells. Micrographs were taken at an original magnification of x 110, the bar is equivalent to 100 µm. **(B)** Number of GCs per spleen section. Spleens were analyzed for the presence of GCs. Sections from two to three different mice were analyzed.

Thus, VLP-VSV induced strong memory B cell responses with life-long elevated IgG titers in wild-type mice. Furthermore, a strong GC reaction was observed as reflected by PNA and FDC immunohistology stainings. The absence of anti-VSV IgG titers in IFNAR$^{-/-}$ mice was determined by a VSV neutralizing assay and correlated with a reduced GC reaction.

The presence of GC B cells was further evaluated by flow cytometric analysis. Therefore, we developed a method to stain VSV-specific B cells. 14 days after VLP-VSV or PBS treatment, splenocytes of IFNAR$^{-/-}$ mice and WT controls were stained with anti-B220, anti-CD21, anti-CD23 and PNA (Figure 14). PNA

decorates GC B cells whereas CD21 and CD23 were selected to distinguish marginal and follicular GC B cells from other B cell subsets. FACS analysis revealed that PBS-treated wild-type mice showed approximately 0.9% $B220^{+}PNA^{hi}$ GC B cells, whereas 14 days after VLP-VSV treatment 2.7% $B220^{+}PNA^{hi}$ GC B cells were detected. $B220^{+}PNA^{hi}$ GC B cells were primarily found amongst $CD21^{int}CD23^{hi}$ and $CD21^{lo}CD23^{lo}$ B cells that are referred to as follicular B cells and transitional B cells, respectively. In contrast, $B220^{+}PNA^{hi}$ GC B cells were only rarely found amongst $CD21^{hi}CD23^{lo}$ marginal zone B cells (Figure 14). In untreated $IFNAR^{-/-}$ mice, 0.9% $B220^{+}PNA^{hi}$ GC B cells were detected, whereas 14 days after VLP-VSV injection 1.4% $B220^{+}PNA^{hi}$ GC B cells were found. Also in $IFNAR^{-/-}$ mice the majority of $B220^{+}PNA^{hi}$ GC B cells were located amongst $CD21^{int}CD23^{hi}$ and $CD21^{lo}CD23^{lo}$ B cells (Figure 14). Overall, the distribution of marginal zone B cells and follicular B cells of approximately 5-7% and 80-85%, respectively, did not change significantly in wild-type and $IFNAR^{-/-}$ mice upon VLP-VSV treatment, whereas $CD21^{lo}CD23^{lo}$ B cells showed a slight increase in immunized mice.

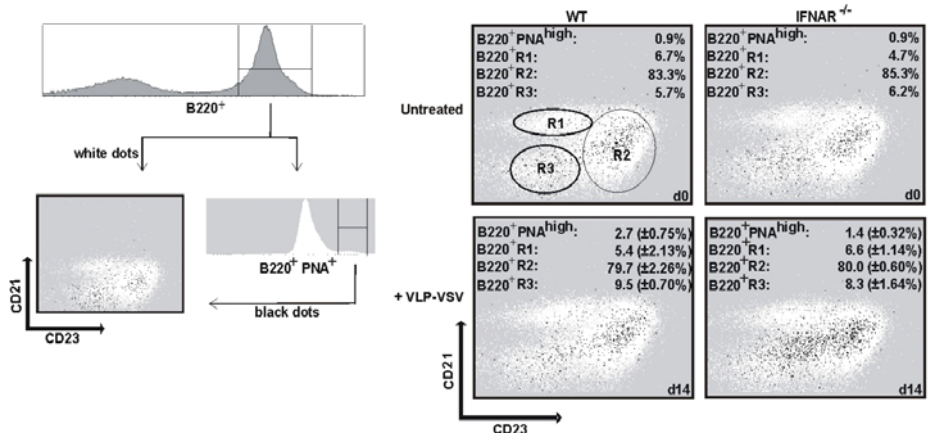

Figure 14 Expression of $B220^{+}PNA^{hi}$ GC B cells after VLP-VSV immunization in wild-type (WT) and $IFNAR^{-/-}$ mice by FACS analysis. Cells were stained with anti-B220-PE Cy5.5, anti-CD21-FITC, anti-CD23-APC antibodies and PNA-streptavidine-PE. In FACS analysis, $B220^{+}$ B cells (white dots) were examined for the expression of CD21 and CD23 to identify $CD21^{+}CD23^{lo}$ marginal zone B cells (R1), $CD21^{int}CD23^{hi}$ follicular B cells (R2) and $CD21^{lo}CD23^{lo}$ transitional B cells (R3). Furthermore, $B220^{+}$ B cells were analyzed for PNA binding. In the CD21/CD23 diagram, $B220^{+}PNA^{hi}$ cells are shown as black dots. Representative data are shown of splenocytes from naïve mice (d0) or VLP-VSV immunized mice (d14).

In conclusion, both immunohistological and FACS analysis revealed that VLP-VSV treatment induced a GC reaction that was moderately reduced in IFNAR$^{-/-}$ mice when compared to wild-type controls.

4.2.3 Neutralizing antibody responses in VLP-VSV primed and VSV-boosted IFNAR$^{-/-}$ mice.

To address whether in complete absence of a functional type I IFN system the subclass switch of neutralizing antibody responses could be induced at all, wild-type controls and IFNAR$^{-/-}$ mice were primed with VLP-VSV and challenged with VSV. After VLP-VSV priming and VSV challenge of wild-type mice, VSV neutralizing IgM was induced by day 4 and significant IgG titers were detected after 8 days (Figure 15, protocol A and B). When IFNAR$^{-/-}$ mice were challenged 2 days after VLP-VSV treatment, no VSV neutralizing antibodies were induced and mice succumbed to infection by day 4 (Figure 15, Protocol A). In contrast, mice that were VSV challenged 4 days after VLP-VSV priming survived for a total of 10 days before first signs of disease became apparent and the experiment had to be discontinued. Under such conditions, day 10 sera showed neutralizing IgG in all animals tested (Figure 15, Protocol B). Thus, compared to IFNAR$^{-/-}$ mice, wild-type controls showed an earlier switch to the IgG subclass by day 6 instead of day 10. Nevertheless, IFNAR$^{-/-}$ mice were able to mount neutralizing IgG responses, if stimulated appropriately.

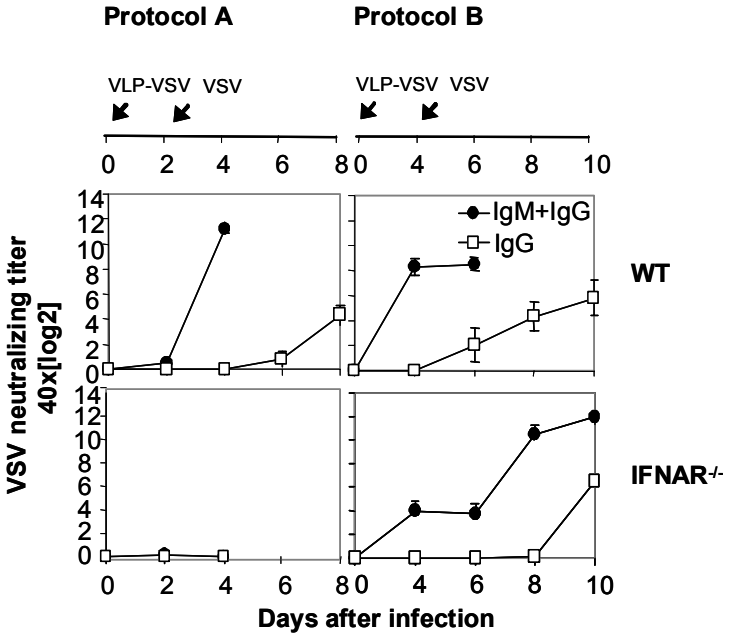

Figure 15 VLP-VSV primed IFNAR$^{-/-}$ mice mount neutralizing IgG antibodies after VSV challenge. WT and IFNAR$^{-/-}$ mice were first injected intravenously with 10^9 VLP-VSV particles. Two (**Protocol A**) or 4 days (**Protocol B**) later mice were challenged with $2x10^6$ PFU of live VSV. Serum samples were collected at the indicated time points and VSV neutralizing IgM+G (filled circles) or IgG (open squares) antibodies were determined by a neutralization assay. Data shown are the mean of three mice per group ± SEM. One of two similar experiments is shown.

4.2.4 Analysis of direct IFNAR-triggering of lymphocytes in VLP-VSV infected mice.

As the VLP-VSV induced IgG switch was T help-dependent, it was analyzed whether direct IFNAR triggering of T cells and/or B cells played a critical role. To this end, conditional mice with a T cell (IFNAR-T), a B cell (IFNAR-B) or a combined B and T cell-specific (IFNAR-BT) IFNAR ablation were injected with 10^9 VLP-VSV. Immunized mice showed high anti-VSV-G IgM titers at day 4. Interestingly, all analyzed cell type-specific IFNAR deficient mouse lines showed an IgG switch, although IgG responses in IFNAR-BT mice were reduced when compared to IFNAR-B, IFNAR-T and wild-type controls (Figure 16).

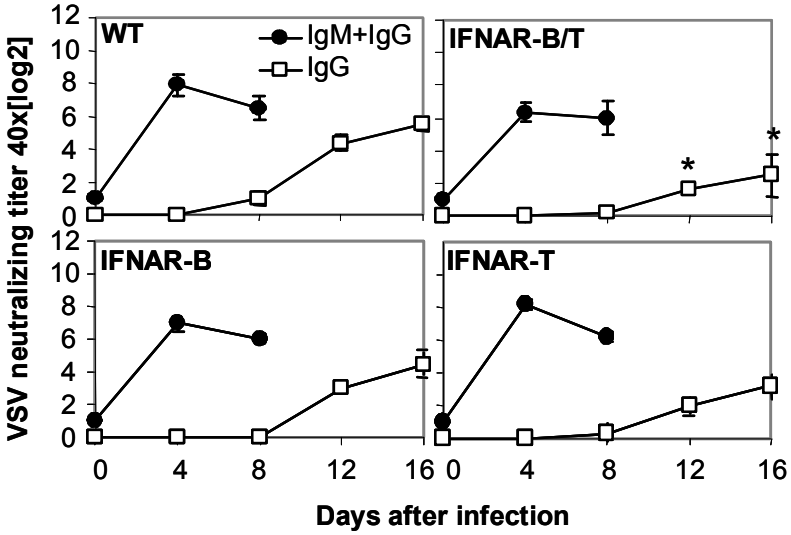

Figure 16 Direct IFNAR triggering on lymphocytes has no impact on the VLP-VSV induced IgG subclass switch. Mice with a cell-type specific type I IFN receptor ablation in B and T lymphocytes (CD19-Cre$^{+/-}$CD4-Cre$^{+/-}$IFNAR$^{flox/flox}$; IFNAR-BT), or only in B cells (CD19-Cre$^{+/-}$IFNAR$^{flox/flox}$; IFNAR-B), or only in T cells (CD4-Cre$^{+/-}$IFNAR$^{flox/flox}$; IFNAR-T) were immunized intravenously with VLP-VSV. VSV neutralizing IgM+G (filled circles) or IgG (open squares) antibodies were determined at the indicated time points in a neutralization assay. The slopes of the IgG curves of IFNAR-B and wild-type mice are statistically significantly higher than those of IFNAR-B/T and IFNAR-T mice (p=0.0003). Moreover, the absolute neutralization titers on day 12 and 16 of IFNAR-B/T mice are significantly reduced when compared with the other groups (* p=0.0046). Data shown are the mean of three mice per group ± SEM.

Thus, direct IFNAR triggering of B cells or T cells was not critically required to promote the VLP-VSV induced IgG switch. Nevertheless, reduced IgG levels observed in IFNAR-BT mice suggested that IFNAR triggering of both lymphocyte subsets further improved the IgG switch.

4.2.5 Analysis of VSV induced neutralizing antibody responses in mice with a lymphocyte-specific IFNAR deletion.

To study whether upon VSV infection direct IFNAR triggering of B and/or T cells played a role, conditional knockout mice with a lymphocyte-specific IFNAR ablation were VSV infected and blood samples were collected at the indicated time points. Interestingly, IFNAR-BT as well as IFNAR-B or IFNAR-T mice

mounted neutralizing IgM and IgG antibody responses that were very similar to those of VSV infected wild-type mice (Figure 17).

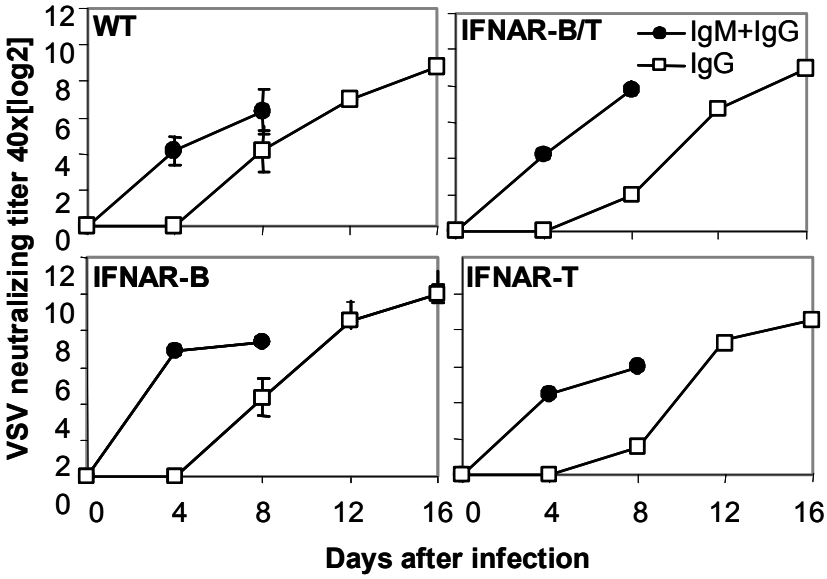

Figure 17 Mice with a lymphocyte-specific IFNAR ablation mount normal neutralizing antibody responses after VSV infection. Wild-type, IFNAR-B/T, IFNAR-B and IFNAR-T mice were injected intravenously with $2x10^6$ PFU of VSV and VSV neutralizing IgM+G (filled circles) or IgG (open squares) serum titers were determined at the indicated time points in a neutralization assay. Data shown are the mean of three mice per group ± SEM.

In a next step, GC formation after VSV infection was analyzed in IFNAR-B versus wild-type mice by immunohistological analysis. To this end, spleen sections of untreated and VSV infected wild-type or IFNAR-B mice were prepared 14 days after VSV infection and stained with a PNA-, FDC- or a VSV-specific B cell antibody. Spleen sections of VSV-infected IFNAR-B mice revealed a normal GC formation (Figure 18). In addition, numbers of GCs per spleen section were similar in IFNAR-B mice and wild-type controls (approximately 41 and 32 GCs, respectively).

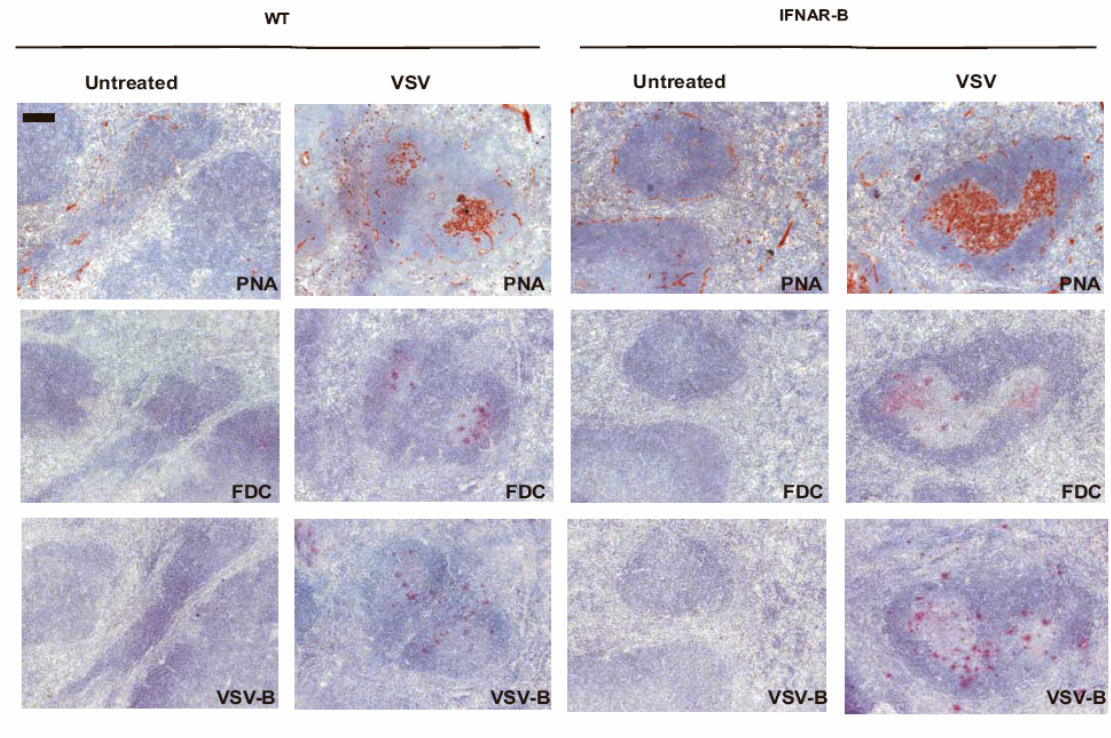

Figure 18 VSV infected mice with a B lymphocyte-specific IFNAR ablation show a normal GC formation. Histological analysis of germinal center formation after VSV infection. Representative sections of spleens from mice treated with or without VSV were analyzed 14 days after VSV infection. Stained markers are indicated in each panel: PNA, peanut hemaglutinin; FDC, follicular dendritic cells, VSV-B, VSV-specific B cells. Micrographs were taken at an original magnification of x 110, the bar is equivalent to 100 µm.

Furthermore, GC formation was analyzed in VSV infected IFNAR-B mice by FACS-analysis. Spleens of PBS treated or VSV infected wild-type and IFNAR-B mice were prepared at day 14 and stained for GC B cells with anti-B220, anti-CD21, anti-CD23 and PNA. FACS analysis showed a normal increase of 0.9% $B220^{+}PNA^{hi}$ GC B cells in untreated IFNAR-B mice to 1.7% $B220^{+}PNA^{hi}$ GC B cells in VSV-infected IFNAR-B mice (Figure 19).

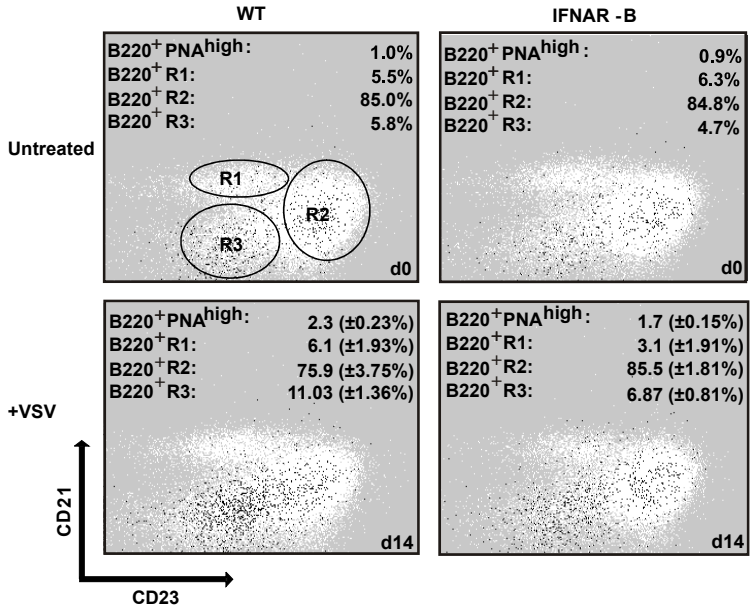

Figure 19 FACS analysis of PNA^{hi} B220^{+} GC B cells after VSV infection of wild-type (WT) and IFNAR$^{-/-}$ mice. Data shown are representative stainings of spleen cells from naïve mice (d0) or VSV infected mice (d14). Cells were stained with anti-B220-PE Cy5.5, anti-CD21-FITC, anti-CD23-APC antibodies and PNA-streptavidine-PE. PNA^{hi} GC B cells were analyzed amongst B220^{+} B lymphocytes (black dots). Data represent mean percentages ± SEM of three mice of one representative experiment out of three.

Thus, the data obtained so far indicated that after VSV infection direct type I IFN stimulation of lymphocytes is not critically required for the induction of neutralizing IgM responses and for the promotion of the T help-dependent IgG switch.

In a last approach IFNAR-B mice, IFNAR-B/T and IFNAR-T mice were analyzed for absolute counts and relative percentages of PNA^{hi} GC B cells (Figure 20). Similarly to the experiments described above, 14 days after VSV infection spleens were isolated and stained for B220^{+}PNA^{hi} GC B cells. For determination of absolute cell numbers, calibration beads were added to each sample which allowed acquisition of FACS data equivalent to a defined sample volume. As expected, wild-type and conditional knockout mice with a lymphocyte-specific IFNAR ablation showed an increase of B220^{+} PNA^{hi} GC B cells 14 days after VSV injection that was more pronounced in wild-type and IFNAR-B mice compared to IFNAR-B/T and IFNAR-T mice. Quantification of

absolute cell counts showed similar amounts of splenocytes in wild-type and conditional knockout animals before and after immunization (Figure 20). The VSV induced increase of GC B cells was statistically significant only in wild-type and IFNAR-B mice, whereas it was not in IFNAR-T and IFNAR-B/T mice. Thus, after VSV infection direct type I IFN stimulation of B cells is not critically required for the induction of neutralizing IgM responses.

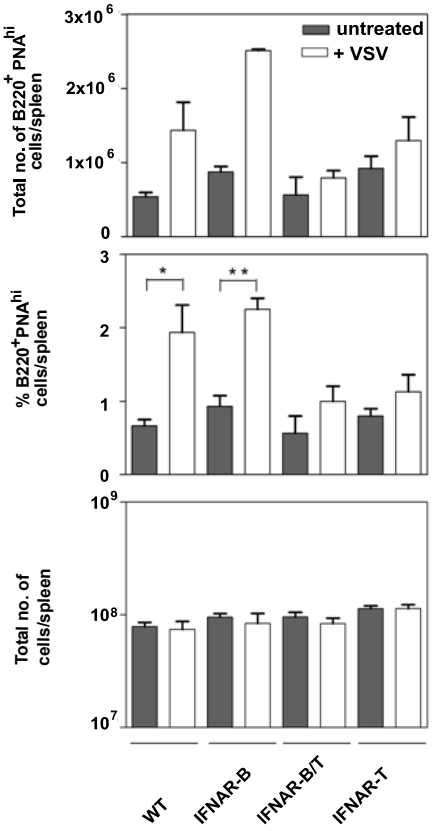

Figure 20 Total numbers of PNA^{hi} B220^{+} GC B cells were significantly increased in wild-type (WT) and IFNAR-B mice after VSV infection. Total spleen cells counts as well as absolute cell numbers and percentages of PNA^{hi} GC B cells per spleen were analyzed for wild-type, IFNAR-B, IFNAR-B/T and IFNAR-T mice before and after VSV injection (* $p<0.0304$ WT versus WT+VSV; ** $p<0,0091$ IFNAR-B versus IFNAR-B+VSV). Data represent mean percentages ± SEM of three mice.

In summary, VLP-VSV induced a T help-dependent IgG switch of VSV neutralizing antibodies which was critically dependent on IFNAR signaling. Although IFNAR triggering of lymphocytes is not a limiting step, it may gradually

enhance the IgG switch. In VSV infected mice, IFNAR triggering of B cells does neither critically affect germinal center formation nor the IgG switch of neutralizing antibody responses. Collectively these data illustrated that similar to live VSV, VLP-VSV showed a striking immunogenicity. As VLP-VSV turned out to be an extremely potent B cell antigen, VLP might also be suitable for inducing antibody responses against PrP^{C} displayed by VLP.

4.3 VLP represent potent B cell antigens in anti-PrP^{C} immunization approaches

Previous experiments showed that VLP, expressing the VSV-G protein in a highly organized fashion on their surface, were effective immunogens for inducing VSV neutralizing antibody responses. Besides many other features, VLP are non-replicative and thus present perfect B cell antigens for vaccination purposes. Many anti-PrP^{C} vaccination approaches failed to induce anti-PrP^{C} antibodies in wild-type mice because of immunological tolerance phenomena. Reasoning that on the surface of virus-like particles PrP^{C} could also be presented in an ideal way to serve as a B cell immunogen, such VLP were developed as a potent vaccine candidate against mouse scrapie. To this end, PrP-displaying virus-like particles were generated to study the cellular and molecular basis of tolerance to PrP^{C}. The retroviral display system was used to generate different VLP displaying amino acids 121 to 231 of PrP^{C} on the envelope of murine leukemia virus-like particles (termed VLP-PrP^{D111}). The C-terminal part of the PrP^{C} region is known to play a critical role in the conversion of PrP^{C} to PrP^{Sc}. After characterization of efficient PrP^{C}-display by ELISA and electron microscopy methods, VLP-PrP^{D111} was tested in a series of active immunization approaches. In a next step, the binding specificity of VLP-PrP^{D111}-induced serum antibodies was assessed by competition assays using VLP-PrP^{D111} as competitors. Finally, prion inoculation experiments were performed in VLP-PrP^{D111} vaccinated mice to test whether PrP^{C}-specific antibody responses were protective.

4.3.1 Generation of VLP-PrP^{D111}

Similarly to VLP-EGF^{D} described in Chapter 4.1.1 the pDisplay system was used to present the cellular isoform of the murine prion protein (mPrP) on the surface of virus-like particles derived from retroviruses.

The PrP expression plasmid that contains the murine mPrP DNA fragment coding for the C-terminal region aa 121-231 (mPrP111) was generated by Daphne Nikles and described in detail in [Nikles et al., 2005]. Cotransfection of a plasmid coding for the viral structural proteins *gag/pol* (*pHIT60*) and a plasmid coding for the transmembrane domain PrP-fusion-protein (*pDPrP111*) should allow the production of PrP^{D111} bearing VLP, which were termed VLP-PrP^{D111} (Figure 21).

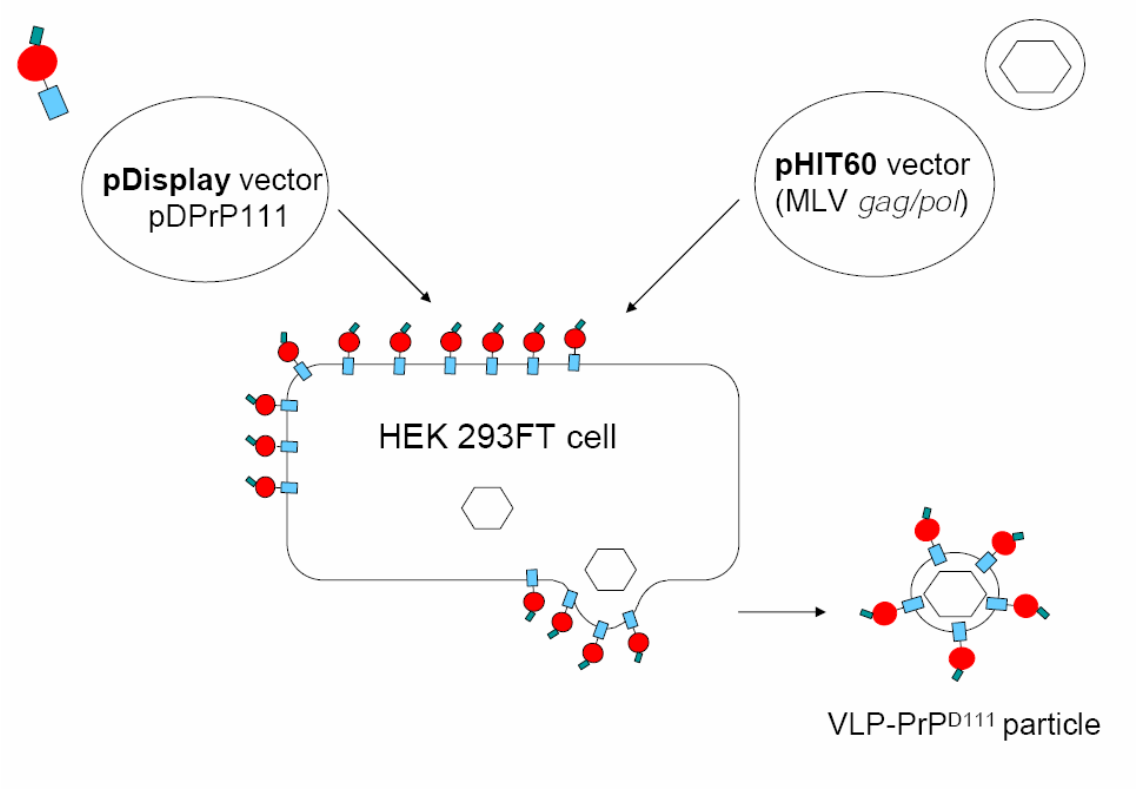

Figure 21 Production of VLP-PrP^{D111}. HEK 293FT cells were cotransfected with a pDisplay vector (*pDPrP111*) and the MLV *gag/pol* expression plasmid *pHIT60*. Transfectants produced MLV-derived VLP-PrP^{D111} that were harvested in the cell supernatant.

4.3.2 Characterization of VLP-PrP^{D111} by electron microscopy

Visualization of cell-surface located PrP^{D111} was achieved by electron microscopy with the anti-PrP monoclonal antibody 6H4. Secondary antibodies used for detection in electron microscopy were coupled to gold particles of 10 nm diameter. The specificity of the anti-PrP^{C} 6H4 staining was confirmed by using VLP-EGF^{D} particles as negative controls.

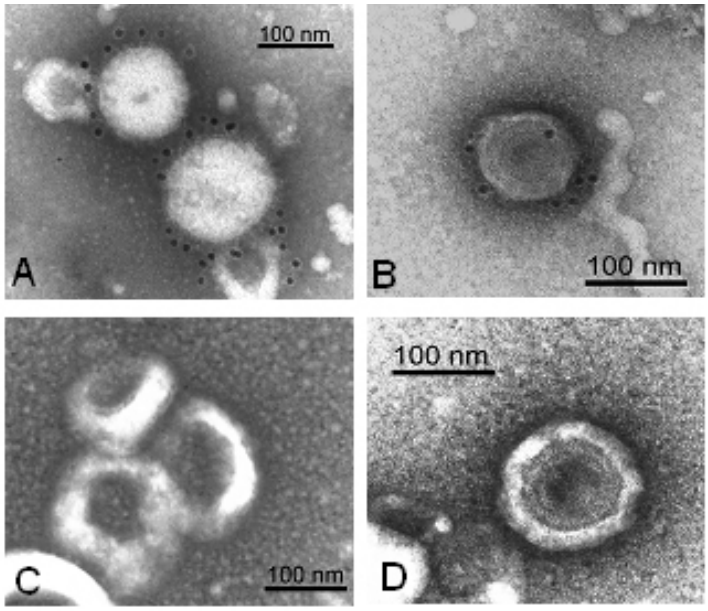

Figure 22 Electron microscopic pictures of VLP-PrP^{D111} and VLP-EGF^{D}. PrP^{C} (black dots) was labeled by anti-PrP 6H4 monoclonal antibody and a 10 nm gold particle labeled anti-mouse IgG **(A+B)**. VLP-EGF^{D}-retroparticles **(C+D)** were used as negative controls. VLP were stained either with methylwolframat (left panel) or uranylacetat (right panel). Bars represent 100 nm.

In low speed centrifugated cell culture supernatants, VLP-PrP^{D111} was present exhibiting the typical morphology of C-type retroviruses that were specifically surrounded by numerous immunogold particles (Figure 22 A+B). In contrast, VLP-EGF^{D} was completely negative for anti-PrP^{C} specific binding, showing that anti-PrP^{C} gold labelling was specific (Figure 22 B+D).

4.3.3 Quantification of VLP-PrP^{D111} by ELISA

In addition to electron microscopy, VLP-PrP^{D111} was characterized and equilibrated by ELISA (Figure 23). Therefore, VLP-PrP^{D111} was analyzed by coating log 3 dilutions of concentrated particle stocks on ELISA plates. PrP^{D111} was subsequently detected using the anti-PrP 6H4 antibody and an anti-mouse-IgG-HRP conjugated secondary antibody. To equilibrate particles in different preparations, anti-p30 serum was used in combination with a goat-specific secondary HRP-labelled antibody.

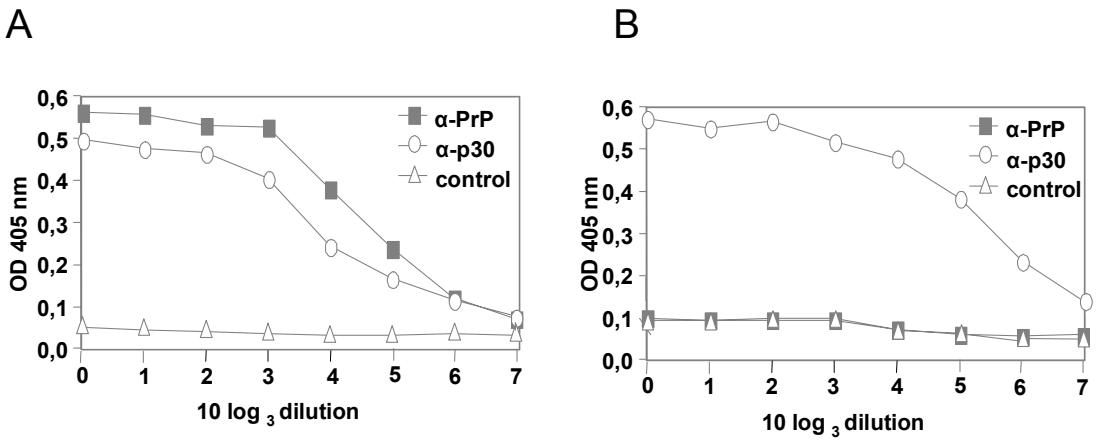

Figure 23 Analysis of VLP-PrP^{D111} (A) and VLP-EGF^{D} (B) by ELISA. ELISA plates were coated with concentrated stocks of particles at indicated dilutions. PrP^{D111} or viral expressed antigens were detected by the use of the anti-PrP mAb 6H4 (filled rectangles), polyclonal anti-p30 antiserum (open ovals), or mouse preimmune serum (open triangles). Data represent one out of two experiments with similar results.

VLP-PrP^{D111} showed strong binding of the PrP-specific 6H4 antibody (filled rectangles) and anti-p30 antibody (open ovals) (Figure 23 A). In contrast, no anti-PrP^{C} binding was observed for VLP-EGF^{D} (Figure 23 B). Taken together, these data clearly demonstrated that virus-like particles were successfully generated that efficiently displayed the cellular prion protein on their surface.

4.3.4 Expression and purification of recombinant mouse prion protein mPrP$^{REC121-231}$

For binding analysis of VLP-PrP^{D111}-induced serum antibodies and PrP^{C} competition experiments that are later described in chapter 4.3.6, a recombinant polypeptide comprising residues aa 121-231 of the mouse prion protein was expressed. To this end, the plasmid pRSET A mPrP(121-231) fused to an N-terminal histidine tag was transformed into E-coli. Bacteria were grown to an OD_{600} of 0.5 and then induced with 1 mM isopropyl-ß-D-galactopyranoside (IPTG). Cells were harvested 6 h after induction and checked for protein induction on SDS gel electrophoresis. The mPrP$^{REC121-231}$ protein (14,7 kDa) was induced after IPTG expression as shown in Figure 24. After sonification and centrifugation of the Guanidinium Hydrochloride (GdmCl) denaturated E.coli cell lysate, the soluble protein fraction was added to a nickel-nitrilotriacetic acid (NTA) agarose resin for purification. Finally, the mPrP$^{REC121-231}$ protein was eluated from the resin using immidazol and removal of the N-terminal histidine tail with thrombin resulted in a purified mPrP$^{REC121-231}$ protein (Figure 24).

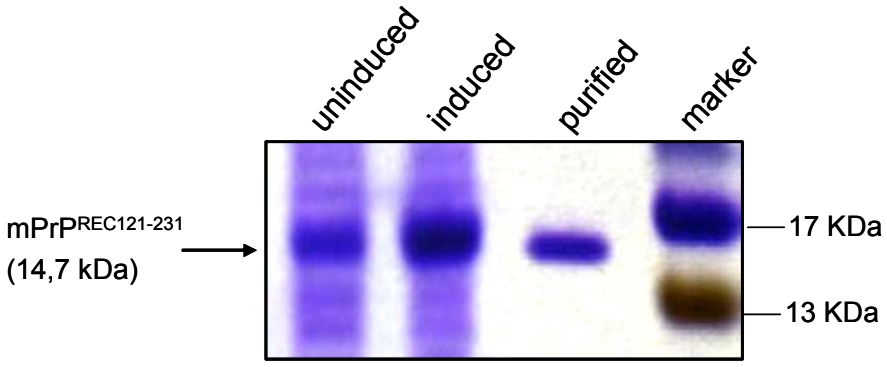

Figure 24 Purification of mPrP$^{REC121-231}$ protein. After induction with 1mM IPTG and expression in E.coli BL21(DE3), mPrP$^{REC121-231}$ was purified via an NTA agarose resin. The mPrP$^{REC121-231}$ was analyzed using a 10-20% Tricine gel (Comassie staining).

The bacterially expressed and purified mPrP$^{REC121-231}$ protein was used in experiments during this study.

4.3.5 Induction of anti-PrP^{C} response in mice immunized with VLP-PrP^{D111}

To verify the antigenicity of the VLP-PrP^{D111}, different types of mice were immunized. Firstly, *Prnp* knock-out mice (*Prnp*$^{0/0}$) were subjected to immunization experiments, in which the immune response was expected to be high because PrP^{C} is not expressed as a self-antigen in those animals. Since the main goal was to circumvent tolerance in animals expressing PrP^{C}, both *Prnp* heterozygous mice (*Prnp*$^{+/0}$) and wild-type mice (*Prnp*$^{+/+}$) expressing either one or two *Prnp* alleles were included in immunization studies. For this purpose, groups of three mice were intravenously (i.v.) immunized with approximately 10^{9} VLP-PrP^{D111} or VLP-EGF^{D} and serum was taken weekly (Figure 25).

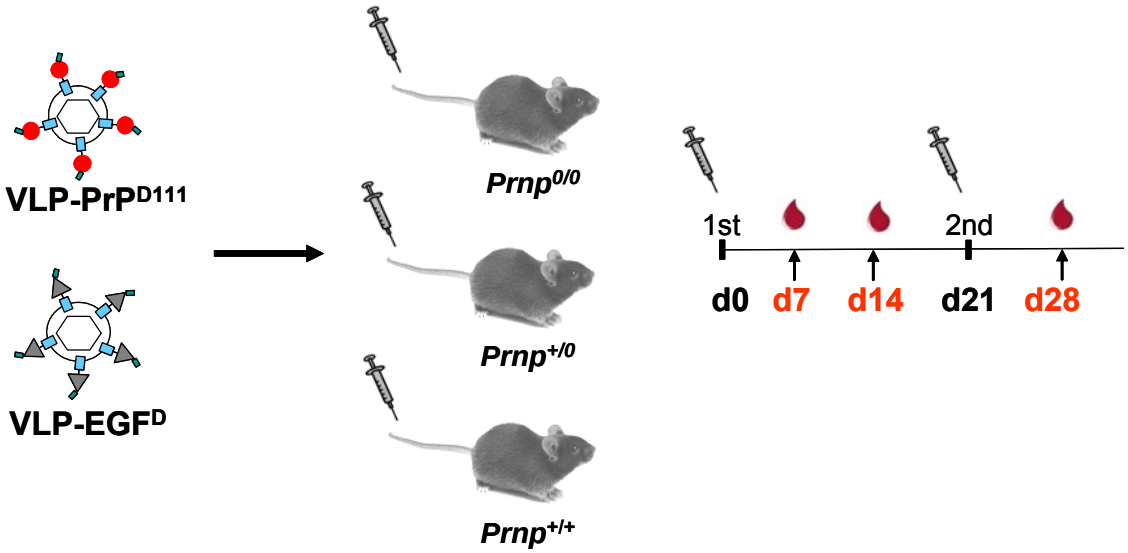

Figure 25 Schematic representation of VLP-PrP^{D111} immunization strategy. *Prnp*$^{0/0}$ *Prnp*$^{+/0}$ and *Prnp*$^{+/+}$ mice were immunized intravenously with PrP^{D111} or EGF-displaying VLP. Serum samples were taken weekly and analyzed for anti-PrP^{C}-specific antibodies.

In a first approach, serum samples of VLP-PrP^{D111}-immunized mice were analyzed for PrP^{C}-specific binding by ELISA. Therefore, ELISA plates were coated with recombinant mPrP$^{REC121-231}$ which was purified as described in Chapter 3.2.3.4. Prediluted serum was added in log 2 dilutions to the ELISA plate. Already seven days after immunization, *Prnp*$^{0/0}$ mice showed high titers of PrP-specific antibodies as indicated by an ELISA, detecting PrP^{C}-specific

immunoglobulin of the M, G, and A subclasses (Figure 26 A). Interestingly, despite the expression of one or two *Prnp* alleles, also *Prnp*$^{+/0}$ and *Prnp*$^{+/+}$ mice mounted PrP-specific antibody responses, albeit at substantially reduced levels when compared to *Prnp*$^{0/0}$ mice (Figure 26 B+C). Similarily, anti-PrP response curves were monitored with sera obtained 14 days after immunization (data not shown). PrP-specific antibody responses in *Prnp*$^{+/+}$ mice were slightly lower than in *Prnp*$^{+/0}$ mice which might be explained by a higher level of PrP-specific tolerance in *Prnp*$^{+/+}$ mice than in *Prnp*$^{+/0}$ mice.

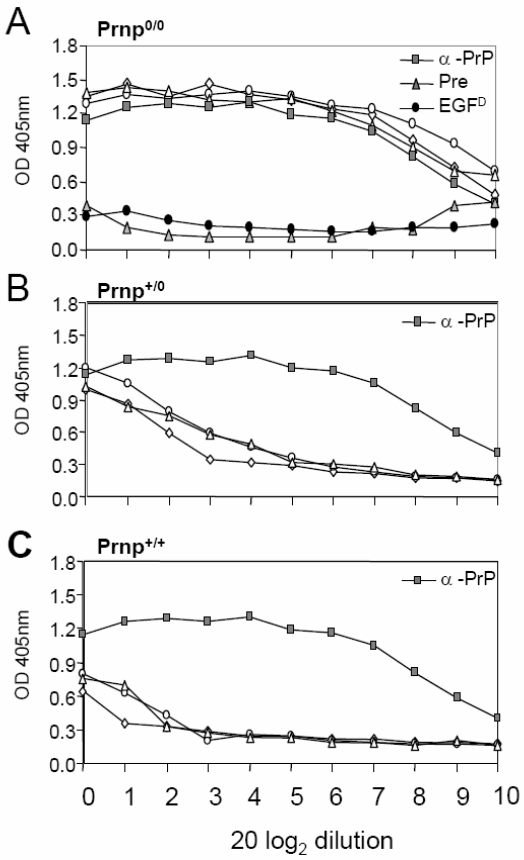

Figure 26 Sera of mice immunized with VLP-PrP^{D111} specifically bind recombinant mPrP$^{REC121-231}$ in ELISA. VLP-PrP^{D111}-retroparticles devoid of adjuvant were i.v. injected into three individual mice of the *Prnp*$^{0/0}$ **(A)**, *Prnp*$^{+/0}$ **(B)**, or *Prnp*$^{+/+}$ **(C)** genotypes, respectively (open symbols). Seven days after immunization, serum samples were taken and tested in log2 dilutions for the presence of PrP-specific immunoglobulin of the M, G, and A subclasses reactive against bacterially expressed mPrP$^{REC121-231}$. As controls, the anti-PrP monoclonal antibody 6H4 (filled rectangles), preimmune serum (filled triangles) or sera from mice injected with VLP-EGF^{D} (filled circles) were used. The experiments were repeated two times with similar results.

Next, studies were perfomed to analyze whether serum antibodies showing PrP-specific binding by ELISA would also bind the native form of PrP^C as expressed on the cell surface.

To this end, peripheral blood was taken from tg33 mice overexpressing PrP^C on T lymphocytes [Raeber et al., 1999]. CD3 positive T cells were tested for binding of serum IgM or IgG derived from immunized mice by FACS analysis (Figure 27).

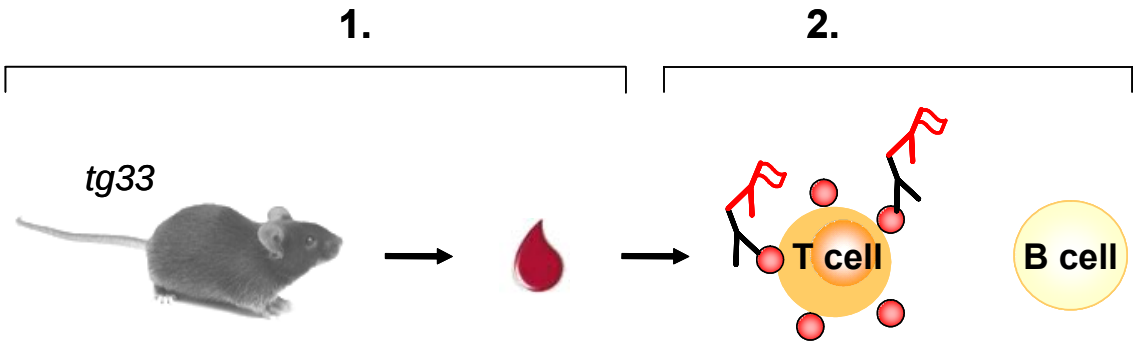

Figure 27 Schematic representation of tg33 FACS assay to detect cell surface PrP^C-specific binding of antibodies. Blood cells of tg33 mice overexpressing PrP^C on T cells **(1)** were incubated with sera of immunized mice and analyzed for Ig subtypes specifically binding PrP^C **(2)**.

At first, groups of three *Prnp*$^{0/0}$ mice were injected i.v. with VLP-PrP^{D111} or VLP-EGF^D and sera were analyzed for PrP^C-specific antibodies 14 days after immunization in the tg33 FACS assay (Figure 28). As controls, preimmune serum (green line) or the 6H4 antibody (red line) was used to determine the binding specificity of serum antibodies. VLP-EGF^D-immunized *Prnp*$^{0/0}$ mice (grey lines) do not show any PrP^C-specific binding. In contrast, *Prnp*$^{0/0}$ mice that were immunized with VLP-PrP^{D111} particles mounted high anti-PrP^C IgG titers and were comparable to 6H4 binding. Treatment with control particles expressing the EGF protein (VLP-EGF^D) instead of PrP^{D111} did not induce PrP^C-specific binding, neither *in Prnp*$^{0/0}$ nor in *Prnp*$^{+/+}$ mice. Thus, VLP-PrP^{D111} expressed PrP^C in a way that allowed efficient B cell activation.

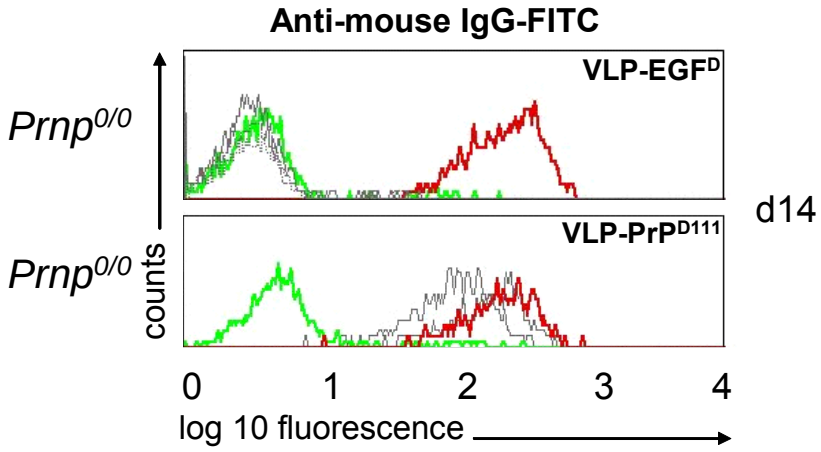

Figure 28 ***Prnp*$^{0/0}$ mice immunized with VLP-PrP^{D111} showed high anti-PrP^{C} specific IgG titers 14 days after immunization.** *Prnp*$^{0/0}$ mice were injected intravenously either with VLP-EGF^{D} or VLP-PrP^{D111}-retroparticles. Serum samples of three mice per group (grey lines) were analyzed for PrP^{C}-specific binding 14 days after immunization. As controls the 6H4 antibody (red line) or preimmune serum (green line) were used.

These data clearly indicated that VLP-PrP^{D111} induce native anti-PrP^{C} antibodies in *Prnp*$^{0/0}$ mice.

The anti-PrP^{C} specificity of the tg33 FACS method was additionally verified by using preimmune serum of *Prnp*$^{0/0}$ as well as serum of VLP-EGF^{D}-immunized *Prnp*$^{0/0}$ mice which do not bind PrP^{C} expressed on tg33 T cells. To further verify the specificity and reliability of the FACS method used for determination of PrP^{C}-reactive antibodies, a number of control experiments were performed as shown in Figure 29.

First, N2a neuroblastoma cells and tg33 derived T cells incubated with 6H4 antibody or various different PrP^{C}-reactive immune sera showed very similar staining, indicating that the tg33 based FACS method revealed binding of PrP^{C} as expressed on normal cells (data not shown). Secondly, a potential inter-individual heterogeneity with respect to spontaneous PrP^{C}-specific antibody titers was assessed. To this end, individual preimmune sera and pools of preimmune sera derived from wild-type *(Prnp*$^{+/+}$*)* and *Prnp*$^{0/0}$ mice were assayed for binding to tg33 cells in the tg33 based FACS assay. In no case significant PrP^{C} binding of preimmune serum was observed (Figure 29 A, lower panel). Furthermore, the very narrow scattering of the blots of staining with individual

preimmune sera demonstrated the reliability and reproducibility of the FACS method (Figure 29 A, lower panel).

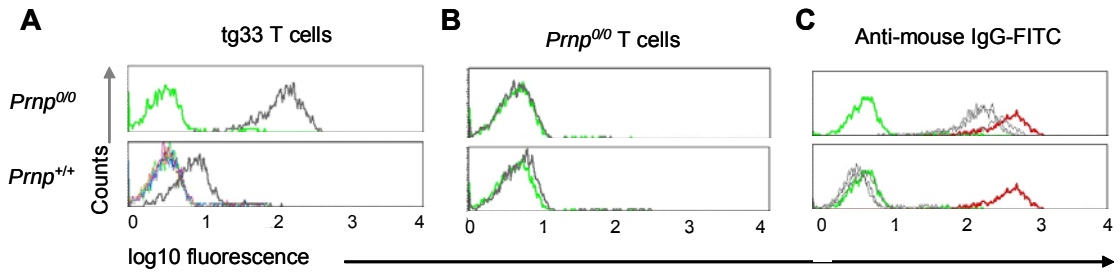

Figure 29 Different control experiments showed the specificity of the tg33 FACS assay for determination of PrP^C reactive antibodies. Sera from immunized *Prnp*$^{0/0}$ or *Prnp*$^{+/+}$ mice were tested for the reactivity of IgG subtypes with T cells from tg33 mice (**A**, upper panel, grey lines) or T cells from *Prnp*$^{0/0}$ mice (**B**, grey lines). Preimmune sera are shown in green. Preimmune sera from five individual *Prnp*$^{+/+}$ mice (**A**, lower panel, colored lines) or pooled preimmune sera from seven *Prnp*$^{0/0}$ mice (**A**, upper panel, green line) were tested for IgG reactivity against PrP^C as expressed on tg33 T cells. **(C)** *Prnp*$^{0/0}$ mice immunized with $mPrP^{REC121-231}$ in CFA and IFA mounted significant levels of anti-PrP^C antibodies, whereas *Prnp*$^{+/+}$ mice were unresponsive to immunizations. Bacterially expressed $mPrP^{REC121-231}$ emulsified in CFA and IFA was injected into mice of the *Prnp*$^{0/0}$ and *Prnp*$^{+/+}$ genotypes [Polymenidou et al., 2004]. At 28 days after immunization, serum samples were analyzed for their IgG reactivity against PrP^C expressed on tg33-derived T cells. Three individuals were analyzed per group (grey lines). Cells incubated with preimmune serum (green) or 6H4 (red) were used as controls. Histograms in all panels show PrP^C-specific binding gated on CD3-positive T cells.

To further verify the PrP^C-specificity of serum binding, *Prnp*$^{0/0}$ derived T cells were included in the FACS analysis as negative controls. Even if strong binding of tg33 derived T cells was observed, no IgG binding of *Prnp*$^{0/0}$ derived T cells was detected, neither with serum from *Prnp*$^{0/0}$ nor with serum from *Prnp*$^{+/+}$ mice (Figure 29 B). Finally, sera from *Prnp*$^{0/0}$ and *Prnp*$^{+/+}$ mice immunized with bacterially produced $mPrP^{REC121-231}$ were analyzed by the tg33 based FACS assay. In contrast to the sera obtained from immunizations with VLP-PrP^{D111}, no antibodies were detected in *Prnp*$^{+/+}$ mice that recognized the native cell surface exposed PrP^C (Figure 29 C lower panel). This failure of $mPrP^{REC121-231}$ to

circumvent tolerance in wild-type animals is in line with recently published data [Gilch et al., 2003; Polymenidou et al., 2004] .

After analyzing the specificity of the tg33 FACS assay, serum samples of VLP-PrP^{D111}-immunized *Prnp$^{0/0}$*, *Prnp$^{+/0}$* *and* *Prnp$^{+/+}$* mice which were previously tested for PrP^{C}-specific binding by ELISA (Figure 26), were next analyzed for native anti-PrP^{C} specific IgM or IgG binding in the tg33 cell based FACS assay (Figure 30).

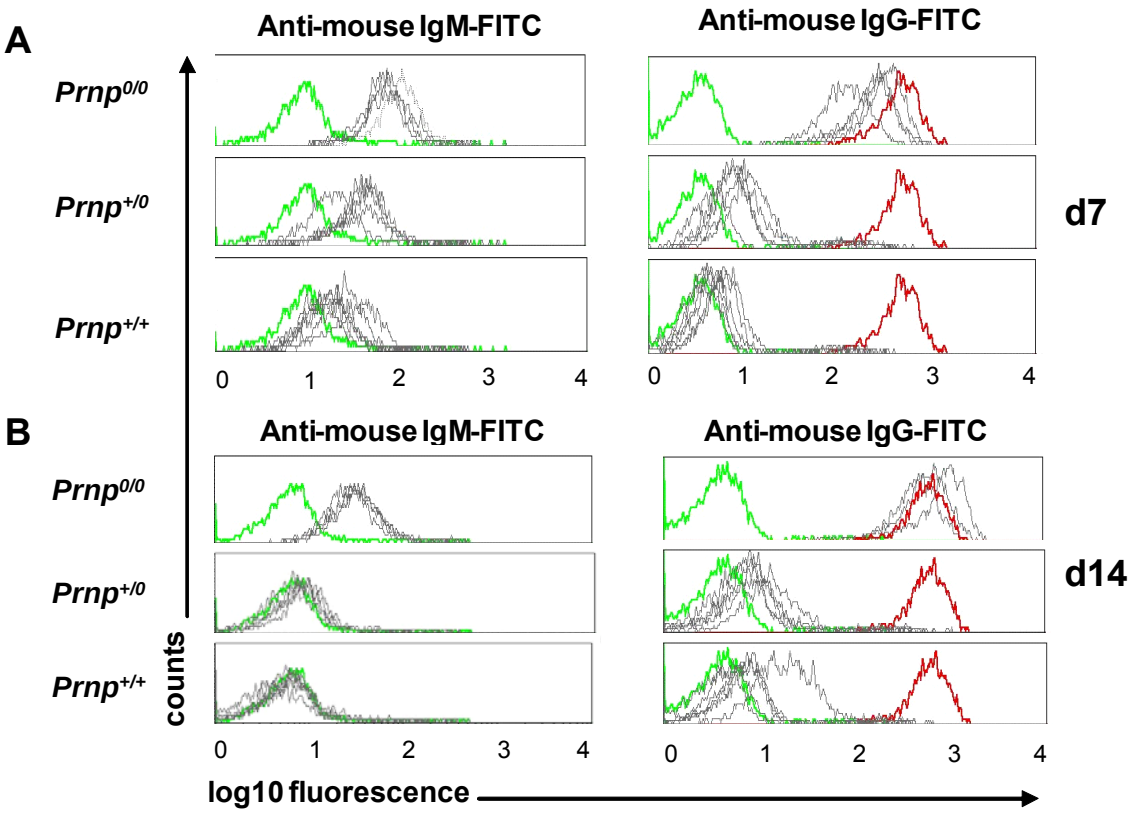

Figure 30 Sera of mice immunized with VLP-PrP^{D111} specifically bind the native form of PrP^{C} as expressed on the cell surface of tg33 derived T cells. Serum samples taken 7 **(A)** or 14 days **(B)** after i.v. injection of VLP-PrP^{D111} into *Prnp$^{0/0}$*, *Prnp$^{+/0}$* or *Prnp$^{+/+}$* mice were analyzed for their reactivity against PrP^{C} as expressed on T cells derived from PrP^{C} overexpressing tg33 transgenic mice. Five individuals were analyzed per group (grey lines). IgM (left panels) and IgG subtypes (right panels) were determined. The histograms show PrP^{C}-specific binding gated on CD3-positive T cells. Cells incubated with preimmune serum (green) or 6H4 (red) were used as controls.

Seven days after immunization of *Prnp*$^{0/0}$ mice, serum showed PrP^{C}-specific IgM binding that was slightly decreased by day 14. In contrast, strong PrP^{C}-specific IgG binding was detected on day 7, that was further increased by day 14, even beyond the binding strength of the positive control 6H4 (Figure 30 A+B). Reminiscent of the above ELISA results (Figure 26), 7 days after immunization of *Prnp*$^{+/0}$ mice, serum showed PrP^{C}-specific IgM binding that was slightly lower than that of *Prnp*$^{0/0}$ mice and slightly higher than that of *Prnp*$^{+/+}$ mice (Figure 30 A). However, no PrP^{C}-specific IgM binding was detectable 14 days after immunization, neither in serum of *Prnp*$^{+/0}$ nor *Prnp*$^{+/+}$ mice (Figure 30 B). Compared to *Prnp*$^{0/0}$ mice, PrP^{C}-specific IgG binding was substantially reduced in the serum of *Prnp*$^{+/0}$ and *Prnp*$^{+/+}$ mice, whereas serum of *Prnp*$^{+/0}$ mice showed slightly higher binding than that of *Prnp*$^{+/+}$ mice. Interestingly, some PrP^{C}-specific IgG was still detectable 14 days after immunization (Figure 30 B). VLP-PrP^{D111} boosting did not enhance or prolong the anti-PrP^{C} antibody response.

In conclusion, VLP-PrP^{D111} is a good B cell antigen as indicated by strong antibody responses induced in *Prnp*$^{0/0}$ mice. Furthermore, VLP-PrP^{D111} can induce low but significant native PrP^{C}-specific IgG antibodies in mice carrying one or two *Prnp* wild-type alleles, thus being superior to recombinant, bacterially expressed PrP.

In the end, those data showed that immunological tolerance towards the self-determinant PrP^{C} left some space for activation of potentially self-reactive PrP^{C}-specific B cells.

4.3.6 VLP-PrP^{D111} as a tool to map the fine specificity of antibodies binding to PrP^{C}

VLP-PrP^{D111}-retroparticles were determined as striking immunogens in anti-PrP^{C} immune responses. Furthermore, serum antibodies of VLP-PrP^{D111}-vaccinated mice detected the native form of PrP^{C}. Besides their properties in inducing anti-PrP^{C} specific antibodies, VLP-PrP^{D111} can be used for definition and characterization of antibody binding specificities. To this end, binding of the

PrP^C reactive mAb 6H4 and of polyclonal PrP^C-specific serum antibodies induced by VLP-PrP^{D111} was assessed by a competition analysis comparing bacterially expressed $mPrP^{REC121-231}$ and VLP-PrP^{D111} as competitors. For this approach, the tg33 cell based FACS assay was selected for determination of PrP^C-specifc binding qualities (Figure 31).

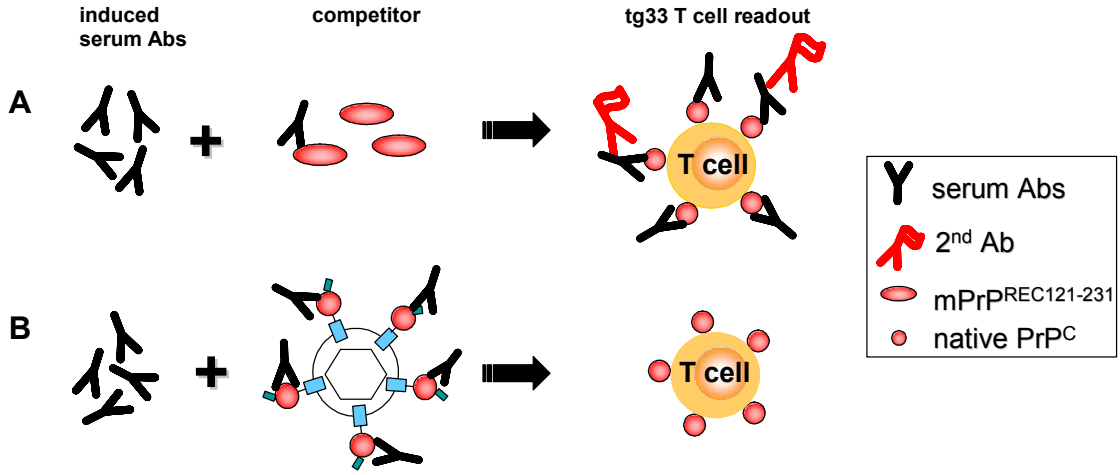

Figure 31 Schematic representation of tg33 FACS competition assay. Serum antibodies of VLP-PrP^{D111}-immunized mice or mAb 6H4 were first titrated for 80% binding capacity as shown in Figure 32. Limiting antibody concentrations were incubated together with $mPrP^{REC121-231}$ **(A)** or VLP-PrP^{D111} **(B)** as competitors for 3h at 4°C. PrP^C-specific binding of mAb 6H4 or anti-PrP^C specific serum antibodies to native PrP^C was measured in an FACS assay using blood of tg33 mice overexpressing PrP^C on T cells.

Before PrP^C-specific serum antibodies or 6H4 were tested for binding properties, limiting antibody concentrations that showed 80% binding capacity to tg33 blood cells have to be determined. At first, positive control 6H4 was added in different log 5 dilutions to tg33 blood cells and tested for binding capacitiy to native PrP^C in the tg33 FACS assay (Figure 31). 80% of 6H4 binding to native PrP^C was assessed when the antibody was diluted 1:5000. Serum of VLP-PrP^{D111}-immunized *Prnp*$^{0/0}$ mice was used for titration of anti-PrP^C serum antibodies. Therefore, serum was prediluted 1:10 and subsequently added to tg33 cells in different log 3 dilutions. Serum antibodies of VLP-PrP^{D111}-immunized *Prnp*$^{0/0}$ mice showed a limiting binding capacity of about 80% when

it was added in a 1:30 dilution (data not shown). Concentrations of titrated anti-PrP^C antibodies were used in the following FACS competition assays.

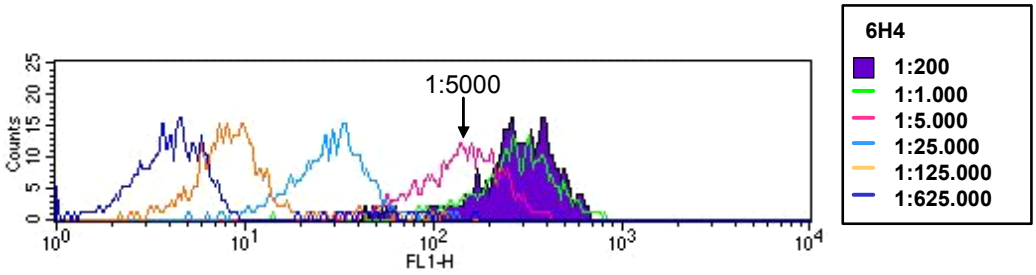

Figure 32 Titration of mAb 6H4 on tg33 cells. 6H4 was titrated in log 5 dilution and limiting antibody binding concentration was analyzed on blood cells of tg33 mice. 6H4 antibody showed 80% binding capacity to native PrP^C when added in a 1:5000 dilution.

In a first attempt binding of anti-PrP^C serum antibodies from VLP-PrP^{D111}-immunized *Prnp*$^{0/0}$ mice was analyzed by competition with bacterially expressed $mPrP^{REC121-231}$ protein. This approach might give a hint whether VLP-PrP^{D111}-induced serum antibodies bind linear epitopes of PrP. We therefore incubated d14 serum of VLP-PrP^{D111}-immunized *Prnp*$^{0/0}$ mice (Figure 33 A) or *Prnp*$^{0/0}$-preimmune serum (Figure 33 B) together with 200 ng of $mPrP^{REC121-231}$. After 3 h incubation at 4 °C, serum was analyzed in the tg33 FACS assay for capacity of binding to native PrP^C. As positive control the 6H4 antibody was included (Figure 33 C). Binding of the PrP^C-specific mAb 6H4 to native PrP^C was quantitatively competed by using bacterially expressed $mPrP^{REC121-231}$ as a competitor (Figure 33 C, green line). In contrast, PrP^C-specific serum antibodies that were induced in *Prnp*$^{0/0}$ mice upon VLP-PrP^{D111} immunization were only partially inhibited by $mPrP^{REC121-231}$ (Figure 33 A, green line). As expected, incubation of preimmune serum of *Prnp*$^{0/0}$ mice was negative for anti-PrP^C binding (Figure 33 B).

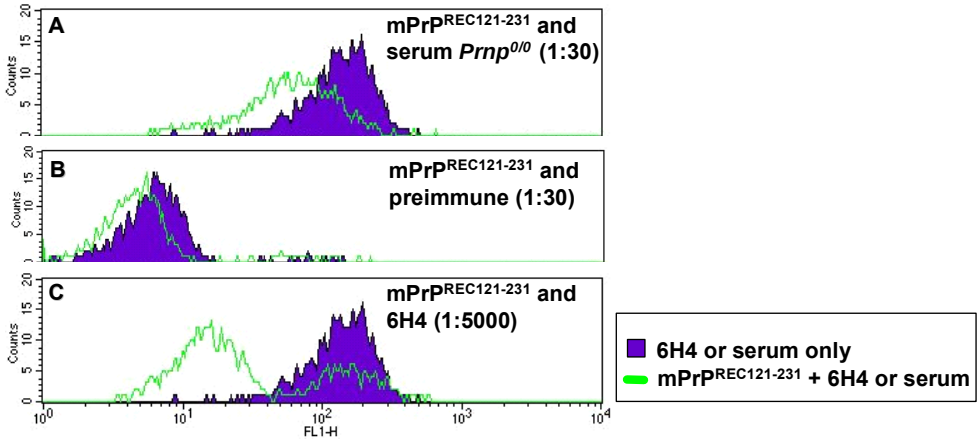

Figure 33 Binding of mAb 6H4 or anti-PrP^C serum antibodies to native PrP^C was only partially inhibited by mPrP$^{REC121-231}$ in the tg33 FACS competition assay. Bacterially expressed mPrP$^{REC121-231}$ (200 ng) was used for anti-PrP^C antibody competition. mPrP$^{REC121-231}$ was able to partially inhibit binding of anti-PrP^C specific serum antibodies of *Prnp$^{0/0}$* **(A)** or mAb 6H4 **(C)** to native PrP^C. As a negative control *Prnp$^{0/0}$* preimmune serum was used **(B)**.

Those findings suggested that PrP^C, as expressed on the surface of VLP-PrP^{D111}-retroparticles, shared many more antigenic determinants of native PrP^C than bacterially expressed PrP.

To determine whether VLP-PrP^{D111}-retroparticles that express the PrP^C protein in a native form on the VLP surface are able to compete binding of anti-PrP^C serum antibodies to native PrP^C, they were next tested as competitors. To this end, serum of VLP-PrP^{D111} immunized *Prnp$^{0/0}$* mice was simultanelously incubated with different concentrations of log 5 diluted VLP-PrP^{D111} (Figure 34 A). Additionally, serum of VLP-PrP^{D111}-immunized *Prnp$^{+/+}$* mice (1:10 diluted) was tested (Figure 34 B). For controls *Prnp$^{0/0}$* preimmune serum (Figure 34 C) and 6H4 (Figure 34 D) were used. As expected, the binding of 6H4 and *Prnp$^{0/0}$* serum antibodies to native PrP^C was quantitatively inhibited by VLP-PrP^{D111} up to a VLP dilution of 1:125 (Figure 34 A+D). When serum of *Prnp$^{+/+}$* mice was incubated with undiluted VLP-PrP^{D111}, binding to native PrP^C was completetly competed by VLP-PrP^{D111} (Figure 34 B, green line). *Prnp$^{0/0}$* preimmune serum did not interfere with VLP-PrP^{D111} and showed no anti-PrP^C binding (Figure 34 C).

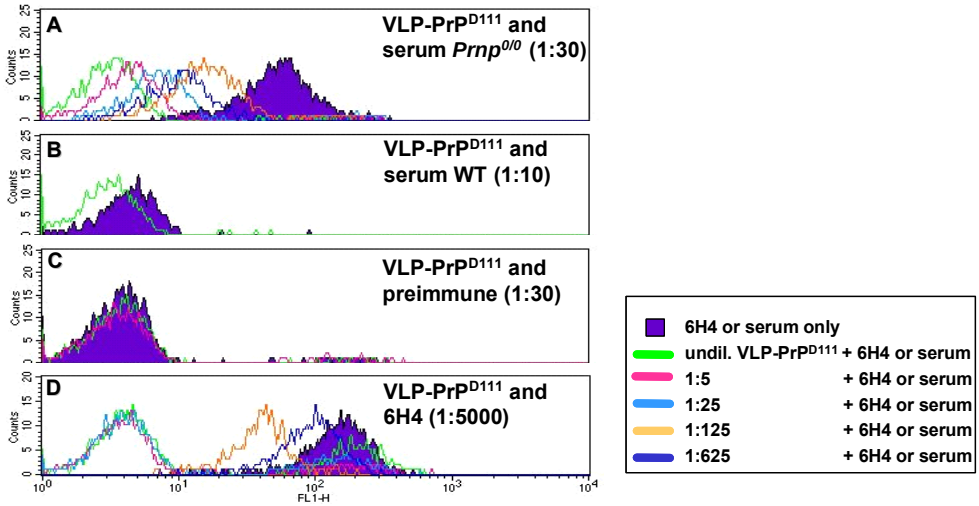

Figure 34 Binding of 6H4 or serum antibodies to native PrP^{C} was quantitatively inhibited by VLP-PrP^{D111}. VLP-PrP^{D111}-retroparticles were incubated in log 5 dilutions together with serum antibodies of immunized *Prnp$^{0/0}$* **(A)** or *Prnp$^{+/+}$* mice **(B)** or *Prnp$^{0/0}$* preimmune serum **(C)**. Binding of serum antibodies to native PrP^{C} was inhibited by VLP-PrP^{D111}. VLP-PrP^{D111} was able to inhibit binding of mAb 6H4 to native PrP^{C} completely **(D)**.

Those data clearly indicated that in VLP-PrP^{D111}-immunized mice native anti-PrP^{C} antibodies were induced. To prove the specificity of VLP-PrP^{D111} competition, VLP-EGF^{D} was included in this study. Therefore, VLP-EGF^{D} was incubated together with different dilutions of serum antibodies from VLP-PrP^{D111}-immunized *Prnp$^{0/0}$* mice or 6H4. No competition of anti-PrP^{C}-specific antibodies was observed by VLP-EGF^{D} (Figure 35).

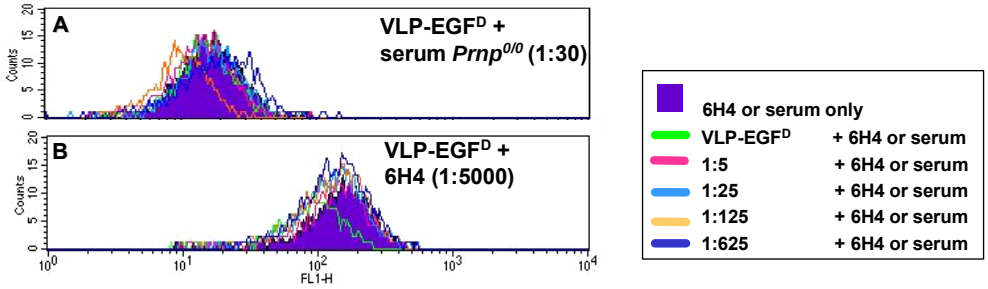

Figure 35 VLP-EGF^{D}-retroparticles were not able to compete PrP^{C}-specific binding of mAb 6H4 or serum antibodies to native PrP^{C}. VLP-EGF^{D} was incubated with PrP^{C}-specific serum of an immunized Prnp$^{0/0}$ mouse) **(A)** or mAb 6H4 **(B)** and tested in the tg33 FACS competition assay. Binding to native PrP^{C} was unaffected by VLP-EGF^{D}.

Taken together, data showed that VLP-PrP^{D111}-retroparticles are a good tool for mapping fine specificity of antibodies binding to the cellular form of the prion protein. Further insights of binding properties of anti-PrP^{C} specific antibodies could be analyzed by PrP^{C} deletion mutants that are displayed on VLP surface.

4.4 Circumventing tolerance to PrP^{C} in wild-type mice by different VLP immunization approaches

Above data indicated that breaking tolerance to the self-expressed protein PrP^{C} seems to be very difficult. VLP-PrP^{D111} induced high titers in *Prnp*-deficient mice and wild-type (*Prnp*$^{+/+}$) mice mounted native anti-PrP^{C} IgM antibodies. However, anti-PrP^{C} IgG titers in wild-type mice were rather low and declined early after immunization. Long term anti-PrP^{C} titers are necessary for protection against scrapie diseases. The major problem might be that the T cell-dependent switch from IgM to IgG isotype of PrP^{C}-specific antibodies was less pronounced. As a consequence, anti-PrP^{C} antibody titers were rather short-lived. Thus, it seemed that immunologic tolerance manifested on the T cell level can not easily be overcome. Some various experimental approaches were included in this study to overcome tolerance to PrP^{C} in wild-type mice which might resulted in long term anti-PrP^{C} antibodies.

4.4.1 Induction of anti-PrP^{C} antibody response by VLP-PrP^{D111} emulsified in different adjuvants

In several anti-PrP immunization approaches, PrP-antigens were combinded with different adjuvants to boost PrP-specific antibody responses [Hanan et al., 2001; Koller et al., 2002; Gilch et al., 2003; Polymenidou et al., 2004].

Thus, we assessed whether higher antibody titers against native PrP^{C} could be induced in wild-type mice when immunized with VLP-PrP^{D111} emulsified in various different adjuvants, such as TiterMax, aluminium hydroxide (Alum), Cytidyl-guanyl oligodeoxynucleotides (CpG1668) or Complete Freund´s adjuvant (CFA) (Figure 36).

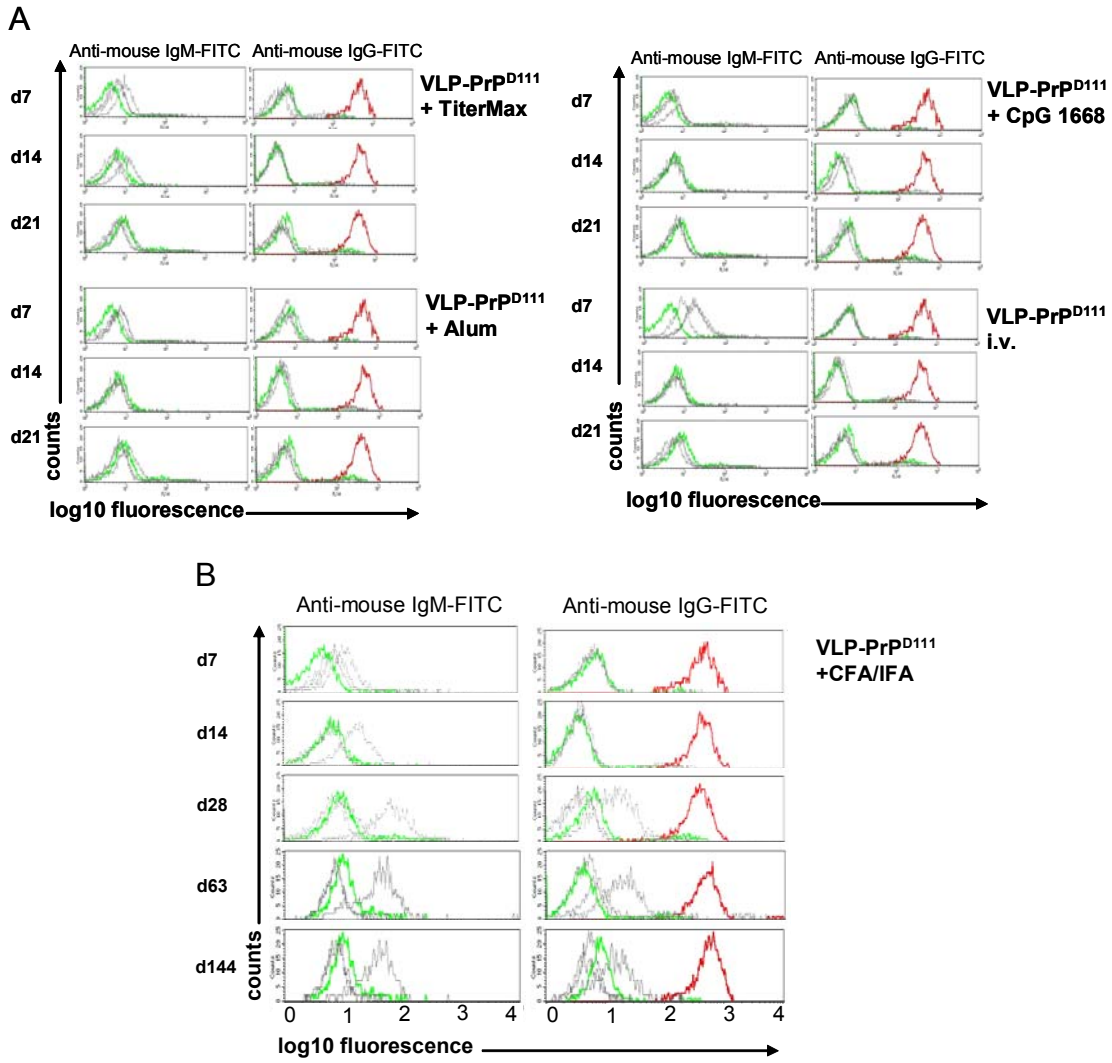

Figure 36 Induction of PrP^C-specific antibodies in *Prnp*$^{+/+}$ mice immunized with VLP-PrP^{D111} in combination with different adjuvants. *Prnp*$^{+/+}$ (three individuals per group, grey lines) were s.c. injected with VLP-PrP^{D111}emulsified in Titer Max, Alum, CpG1668 **(A)** or CFA/IFA **(B)**. As controls, mice were i.v. injected with VLP-PrP^{D111} devoid of adjuvant (**A**, right lower panel). PrP^C-specific binding of IgM (left panels) or IgG (right panel) was determined at the indicated days after immunization by FACS analysis using blood of tg33 transgenic mice overexpressing PrP^C specifically on T cells. 6H4 (red line) or preimmune serum (green line) were used as controls.

Upon subcutaneous (s.c.) immunization of *Prnp*$^{+/+}$ mice with VLP-PrP^{D111} emulsified in TiterMax, (Alum) and CpG1668, only low PrP^C-specific IgM titers were detectable at day 7 that rapidly declined at later time points. Under similar experimental conditions, CpG1668 did not show major adjuvant effects,

compared to *Prnp*$^{+/+}$ immunized i.v. with VLP-PrP^{D111} devoid of an adjuvant (Figure 36 A).

Additionally, we tested whether another commonly used adjuant CFA would have a boosting effect in anti-PrP^{C} specific antibody response. Therefore, *Prnp*$^{+/+}$ mice were primarily immunized with VLP-PrP^{D111} emulsified in CFA and boosted with antigen in incomplete Freund´s adjuvant (IFA) 2 weeks later (Figure 36 B). Seven days after primary immunization, *Prnp*$^{+/+}$ mice showed PrP^{C}-specific IgM titers that were generally lower than those of i.v. immunized mice (Figure 26 A right, lower panel). However, in single individuals this vaccination regimen resulted in increased native PrP^{C}-specific IgM titers (Figure 36 B, d7 and d14) that switched to the IgG serotype upon boosting (Figure 36 B, d28, d63, d144).

In summary, VLP-PrP^{D111} is a useful antigen for anti-PrP^{C} immunization strategies in *Prnp*$^{+/+}$ mice, irrespective of whether emulsified in adjuvant or not. Notably, co-existence of PrP^{C}-specific antibodies and of endogenous PrP^{C} in VLP-PrP^{D111}-immunized mice did not result in obvious signs of autoimmune side effects. If those induced antibodies have protective effects in prion pathogenesis remain to be elucidated.

4.4.2 Induction of anti-PrP^{C} antibody responses by PrP^{C}-displaying particles combined with different foreign T helper epitopes

To boost PrP^{C}-specific B cells and to overcome tolerance to PrP^{C} in wild-type mice some additional approaches were tried to trigger PrP^{C}-specific T cell help.

First, we analyzed whether a combination of PrP^{C} together with an additional foreign T-helper epitope presented on the same VLP, would enhance antibody responses in wild-type mice. Therefore, VLP were produced that displayed PrP^{D111} in combination with the VSV-G protein on the VLP surface (Figure 37 C). In a next approach, PrP^{C} expressing VLP based on the human immunodeficiency virus, denoted as HIV-PrP^{D111}, were tested for the induction of anti-PrP^{C} response (Figure 37 D). By definition, HIV-PrP^{D111} and VLP-PrP^{D111} shared PrP^{C} determinants but no other components. Such HIV-PrP^{D111} particles

may be useful to enhance immune responses against virus-derived display particles and to establish immunization protocols. Thus, priming/boosting schemes involving VLP-PrP^{D111} and HIV-PrP^{D111} could be analyzed.

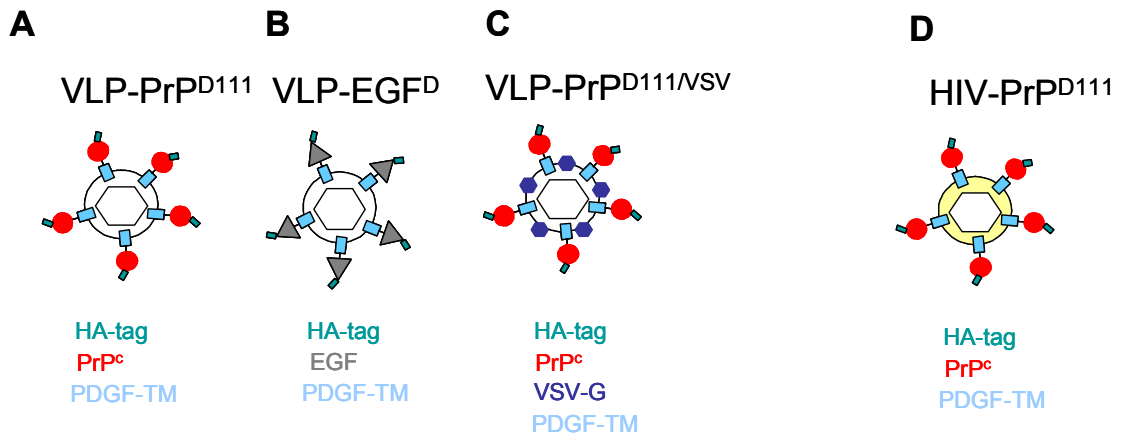

Figure 37 Overview of virus-like particles used in different anti-PrP^{C} immunization approaches. VLP that displayed proteins like PrP^{D111} **(A)** EGF^{D} **(B)** or VLP which displayed both PrP^{D111} and VSV-G protein on the surface **(C)** are derived from the murine leukaemia virus (white capsid). PrP-lentiparticles HIV-PrP^{D111} (yellow capsid) that displayed PrP^{D111} protein on the surface were produced using human immunodeficiency virus derived structural proteins encoded by *gag* and *pol* genes **(D)**.

4.4.2.1 Induction of PrP^{C}-specific antibody response by immunization with VLP-PrP$^{D111/VSV}$

In previous experiments (see chapter 4.1.1) it was shown that the VSV-G protein has been efficiently presented on VLP surface and was determined to be very immunogenic. Therefore, we generated MLV-derived particles that displayed both the PrP^{C} protein and the VSV-G protein on the same VLP surface. Efficient display of the VSV-G protein would act as a foreign T-helper epitope that potentially activates T cell help and might boost PrP^{C}-specific antibody response in wild-type mice.

4.4.2.2 Characterization of VLP-PrP$^{D111/VSV}$

VLP were produced as described in chapter 4.1.1. HEK 293FT cells were transfected with *pHIT60*, *pDPrPD111* and *pmDG* plasmid. *pHIT60* encodes for MLV structure proteins, *pDPrPD111* encodes for the PrP^{D111} protein and *pmDG* for the expression of the VSV-G protein.

48h after transfection particles were harvested from the supernatant and analyzed for protein expression by ELISA. VLP-PrP$^{D111/VSV}$ particles were coated on ELISA plates in different dilutions and PrP^{C} was detected using the 6H4 antibody. The efficient expression of the VSV-G protein was detected with the monoclonal anti-VSV-G (VI24) antibody (Figure 38).

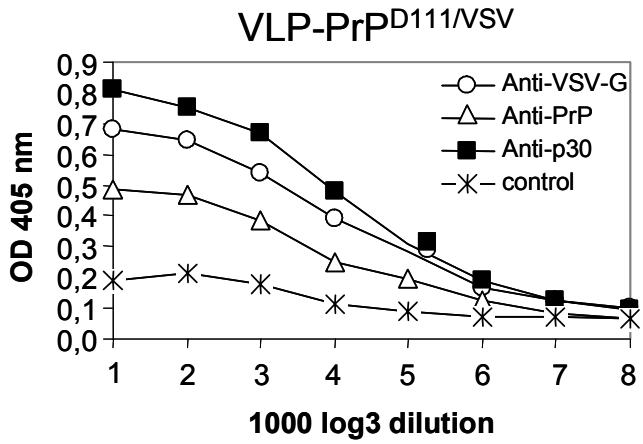

Figure 38 VLP-PrP$^{D111/VSV}$ expresses PrP^{C} and VSV-G protein simultaneously on the surface. Concentrated stocks of VLP-PrP$^{D111/VSV}$-retroparticles were coated in indicated dilutions on ELISA plates. PrP^{C} was detected by the 6H4 antibody (open triangles), MLV-derived protein p30 was analyzed with a polyclonal anti-p30 antiserum (filled squares). VI24 antibody detected the VSV-G protein (open circles). For control preimmune mouse serum was used (asterisks).

ELISA analysis showed that VLP-PrP$^{D111/VSV}$ was efficiently produced that expressed the VSV-G and PrP^{C} on VLP surface. Comparison of the VSV-G (open circles) and PrP^{C} (open triangles) ELISA curves implicated that the amount of expressed VSV-G protein was slightly higher than PrP^{C} expression (Figure 38). However, coexpression of PrP^{C} and VSV-G protein on the same VLP could not be determined by ELISA method.

The coexistenz of VSV-G and PrP^{C} on VLP-$PrP^{D111/VSV}$ was analyzed by electron microscopy. Two sizes of secondary gold-labled antibody (5 nm and 10 nm) were chosen for detection of expressed proteins. PrP^{C} was marked with the 6H4 antibody that subsequently was recognized by a secondary 5 nm diameter gold-labed antibody. In the same step VSV was marked by an anti-VI24 and a 10 nm-diameter gold-labeled anti-mouse IgG antibody (Figure 39).

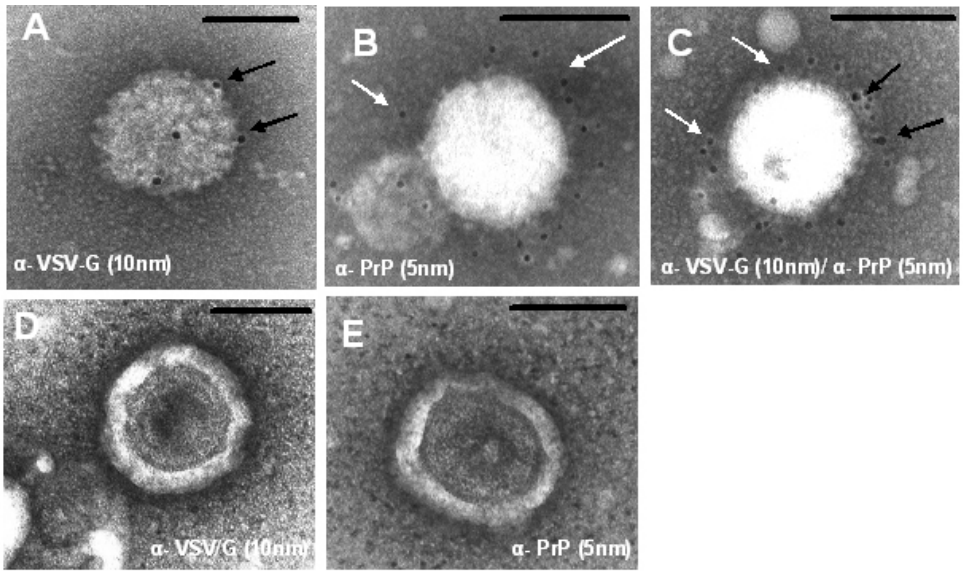

Figure 39 PrP^{C} and VSV-G was expressed simultaneously on VLP-$PrP^{D111/VSV}$-retroparticles. VSV-G protein (big dots, black arrowheads) was labeled by an anti-VSV-G VI24 antibody and a 10 nm gold-particle labeld anti-mouse IgG **(A, C)**. In addition, the PrP^{C} protein (small dots, white arrowheads) was marked by an anti-PrP 6H4 and an anti-mouse 5 nm gold-labled IgG antibody **(B, C)**. VLP-EGF^{D} **(D, E)** was used as a negative control. VLP-$PrP^{D111/VSV}$ was stained either with methylwolframat (upper panel) or uranylacetat (lower panel). Bars represent 100 nm.

Single stainings were performed using an anti-VSV-G/10nm IgG gold antibody or an anti-PrP^{C}/5nm gold-labled IgG antibody. The VSV-G protein (Figure 39 A) was displayed in a lower amount on VLP-$PrP^{D111/VSV}$ compared to PrP^{C} that showed specific and strong surroundings on the VLP surface (Figure 39 B). On each VLP, only 2 to 5 VSV-G proteins were detectable (Figure 39 A). This was also observed in double stainings (Figure 39 C). The specificity of anti-VI24 and anti-PrP^{C} staining was confirmed by using VLP-EGF^{D}-retroparticles as negative

controls (Figure 39 D+E). No antibody binding was observed in VLP-EGF^{D} particle preparations, verifying that anti-VSV and anti-PrP^{C} staining was specific.

Taken together, these data implicated that VLP-$PrP^{D111/VSV}$-retroparticles were successfully generated which displayed PrP^{C} and VSV-G simultaneously on one and the same VLP. Electron microscopic analysis revealed expression of more PrP^{C} than VSV-G proteins on the surface of VLP-$PrP^{D111/VSV}$. However, those data were contradictory to observations made by ELISA analysis (Figure 38).

4.4.2.3 Analysis of PrP^{C}-specific antibody responses induced by VLP-$PrP^{D111/VSV}$

To analyze the immunogenicity of VLP-$PrP^{D111/VSV}$, *Prnp*$^{0/0}$, *Prnp*$^{+/0}$ and *Prnp*$^{+/+}$ mice were i.v. immunized with VLP-$PrP^{D111/VSV}$ and analyzed for IgM or IgG PrP^{C}-specific binding in the tg33 FACS assay (Figure 40).

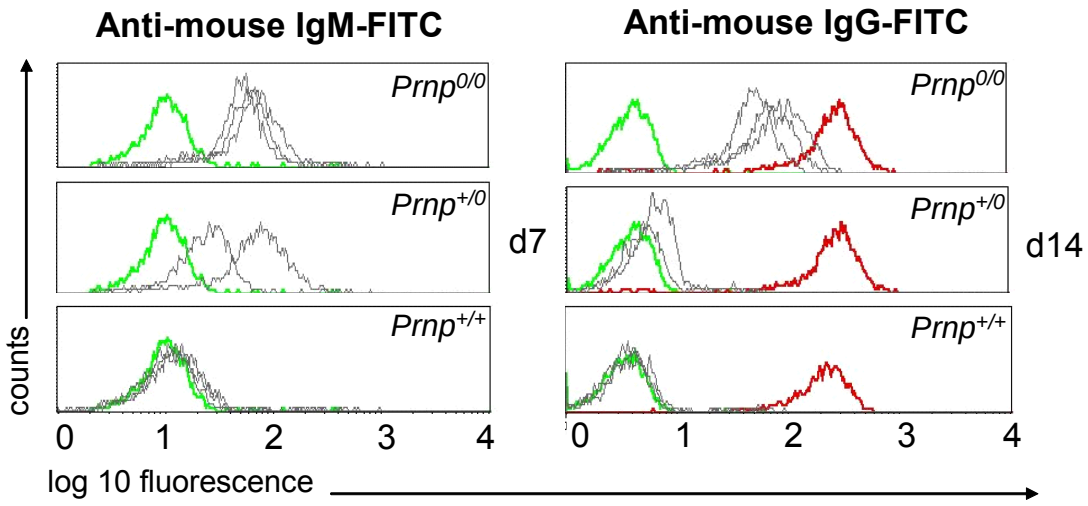

Figure 40 *Prnp*$^{0/0}$ and *Prnp*$^{+/0}$ mice mount anti-PrP^{C} IgM and IgG titers after immunization with VLP-$PrP^{D111/VSV}$, whereas *Prnp*$^{+/+}$ mice did not show any anti-PrP^{C} response. After i.v. immunization with VLP-$PrP^{D111/VSV}$ of *Prnp*$^{0/0}$, *Prnp*$^{+/0}$ and *Prnp*$^{+/+}$ mice, d7 and d14 sera were analyzed for their reactivity against native PrP^{C} in the tg33 FACS assay. Two to three individuals were analyzed per group (grey lines). IgM and IgG antibody titers were determined. Cells incubated with preimmune serum (green) were used as controls. 6H4 served as positive control.

As early as 7 days after priming with VLP-$PrP^{D111/VSV}$ high IgM PrP^{C}-specific antibody titers were induced in *Prnp*$^{0/0}$ mice that switched to the IgG subtype at day 14 (Figure 40). Compared to *Prnp*$^{0/0}$ *mice*, heterozygous *Prnp*$^{+/0}$ mice showed similar IgM PrP^{C}-specific antibody titers at day 7 but only weak anti-PrP^{C} specific IgG binding at day 14. Surprisingly, no anti-PrP^{C} IgM or IgG titers were observed in the *Prnp*$^{+/+}$ group at day 7 and day 14 after VLP-$PrP^{D111/VSV}$ immunization. This observation clearly showed that additionally expressed foreign T-helper epitopes like the VSV-G protein did not allow efficient B cell activation in *Prnp*$^{+/+}$ mice. Thus, VLP-$PrP^{D111/VSV}$-retroparticles seemed to be

good antigens for anti-PrP^{C} immunization in *Prnp$^{0/0}$* and *Prnp$^{+/0}$* mice. However, in *Prnp$^{+/+}$* mice they were not efficient for breaking tolerance to PrP^{C}.

4.4.3 VLP-PrP^{D111} priming and HIV-PrP^{D111} boosting strategies

Virus-like particle production, as described above for the C-type retrovirus candidate MLV, is also possible with lentiviral particles. Since vector systems based on the lentivirus HIV are available and the viral structural proteins coded by *gag* and *pol* are sufficient for particle budding, these viral particles can be produced in the same way as MLV derived VLP.

HIV-PrP^{D111}-retroparticles were produced by using *pCMV* plasmid that encodes for HIV-virus assembly together with the plasmid *pPrP111* which was formerly used for VLP-PrP^{D111} production. The transfection protocol was done according to Chapter 3.2.5.1.

PrP^{C} displayed on HIV-PrP^{D111} was verified by ELISA (Figure 41). HIV-derived capsid protein was detected by an anti-p24 antibody. PrP^{C} was stained with the 6H4 antibody.

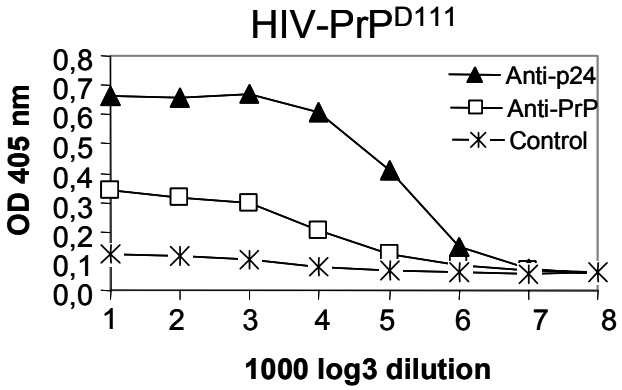

Figure 41 Analysis of HIV-PrP^{D111} by ELISA. Concentrated stocks of HIV-PrP^{D111}-retroparticles were coated on ELISA plates with indicated dilutions. Virally expressed antigens were detected by the use of polyclonal anti-p24 antiserum (filled rectangles). PrP^{C} was detected by the anti-PrP 6H4 antibody (open squares). For control mouse preimmune serum (asterisks) was used.

To determine the immunogenicity of HIV-PrP^{D111}, *Prnp$^{0/0}$*, heterozygous *Prnp$^{+/0}$* and *Prnp$^{+/+}$* mice were intravenously injected with 10^{9} HIV-PrP^{D111}. The serum

was analyzed 7 days after immunization for anti-PrP^{C} specific IgM binding in the tg33 FACS assay (Figure 42).

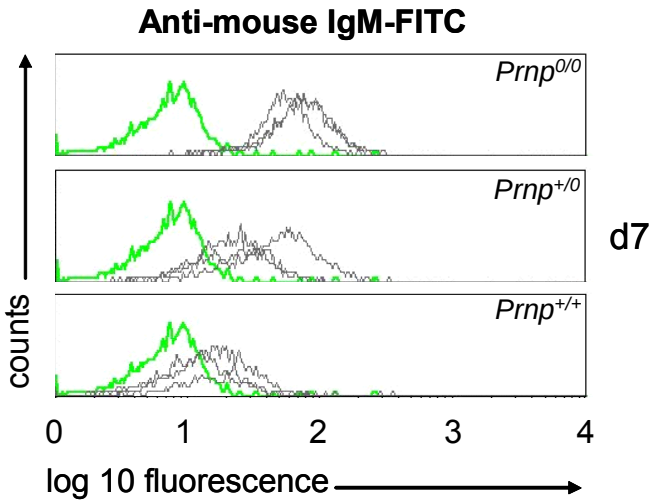

Figure 42 HIV-PrP^{D111} induces anti-PrP^{C} specific IgM antibodies in *Prnp*$^{+/+}$ mice. After i.v. injection of HIV-PrP^{D111} into *Prnp*$^{0/0}$, *Prnp*$^{+/0}$ or WT mice (*Prnp*$^{+/+}$), sera of immunized mice were analyzed for their reactivity against PrP^{C} as expressed on T cells derived from PrP^{C}-overexpressing tg33 transgenic mice. Three individuals were analyzed per group (grey lines). IgM antibody titers were determined. Cells incubated with preimmune serum (green lines) were used as controls.

Similarly to VLP-PrP^{D111}, HIV-PrP^{D111}-retroparticles were able to induce high IgM titers in *Prnp*$^{0/0}$ mice. In addition, *Prnp*$^{+/0}$ as well as *Prnp*$^{+/+}$ mice mounted anti-PrP^{C} IgM antibodies 7 days after immunization (Figure 42), indicating that HIV-PrP^{D111} also serves as a potent anti-PrP^{C} antigen. Furthermore, anti-PrP^{C} IgG titers were observed in all genotypes of *Prnp* mice 14 days after immunization (data not shown).

In a next approach priming/boosting protocols were performed, potentially enhancing immunization efficiencies. For this purpose, *Prnp*$^{0/0}$, *Prnp*$^{+/0}$ and *Prnp*$^{+/+}$ mice were primed with VLP-PrP^{D111} and boosted with HIV-PrP^{D111} vice versa. At different time points after immunization, serum was taken and analyzed for anti-PrP^{C} specific IgM or IgG titers. *Prnp*$^{0/0}$ and *Prnp*$^{+/0}$ mice showed high anti-PrP^{C} IgG titers that were more or less similar to those induced by single application of VLP-PrP^{D111} or HIV-PrP^{D111} (data not shown). This

indicated that priming/boosting protocols did not enhance antibody responses to PrP^{C}. Nevertheless, *Prnp*$^{+/+}$ mice were further analyzed in detail for anti-PrP^{C} IgG induction after priming/boosting immunizations (Figure 43).

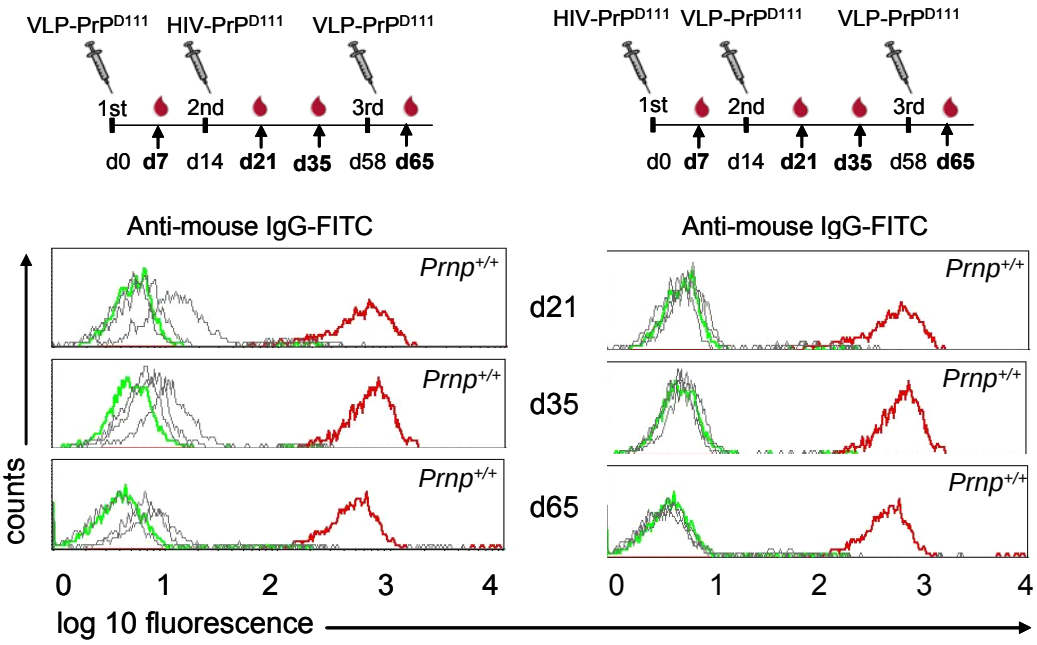

Figure 43 ***Prnp*$^{+/+}$ mice that were primed with VLP-PrP^{D111} and boosted with HIV-PrP^{D111} mounted anti-PrP^{C} IgG antibody titers.** After i.v. immunization with VLP-PrP^{D111} and boosting with HIV-PrP^{D111} vice versa, *Prnp*$^{+/+}$ sera were analyzed for their reactivity against native PrP^{C} at indicated time points by the tg33 cell based FACS assay. Three individuals were analyzed per group (grey lines). IgM antibody titers were determined. Cells incubated with preimmune serum (green) or 6H4 (red) were used as controls.

Prnp$^{+/+}$ mice that were primed with VLP-PrP^{D111} and boosted with HIV-PrP^{D111} mounted anti-PrP^{C} IgG titers at day 21 or 35 compared to HIV-PrP^{D111} primed or VLP-PrP^{D111} boosted animals (Figure 43). After analyzing the serum of *Prnp*$^{+/+}$ mice at day 65, IgG titers were still detectable but were not increased after a third boost with VLP-PrP^{D111}. Surprisingly, no anti-PrP^{C} IgG titers were found in HIV-PrP^{D111}/VLP-PrP^{D111}-immunized mice at any tested time points (Figure 43). These observations were also made in *Prnp*$^{+/0}$ mice that showed reduced IgG titers after immunization with HIV-PrP^{D111}/VLP-PrP^{D111} compared to the reversed VLP-PrP^{D111}/HIV-PrP^{D111} protocol (data not shown).

Thus, *Prnp*$^{+/+}$ mice primed with VLP-PrP^{D111} and boosted with HIV-PrP^{D111} showed PrP^{C}-specific IgG serum titers that were detectable up to 65 days after

a third VLP-PrP^{D111} boost. Those data implicated that the VLP-PrP^{D111}/HIV-PrP^{D111} immunization protocol was very effective and comparable to previous vaccination approaches. Unfortunately, induced anti-PrP^{C} IgG titers were still very low and did not increase during boosting protocols. Furthermore, a third VLP-PrP^{D111} boosting did not enhance or prolonged anti-PrP antibody response.

In conclusion, VLP seem to display PrP^{C} in a way that allowed efficient B cell activation. However, compared to *Prnp*$^{0/0}$ or *Prnp*$^{+/0}$ mice, *Prnp*$^{+/+}$ animals mounted reduced anti-PrP^{C} antibody levels in various anti-PrP immunizations. Data indicated that host tolerance to PrP^{C} still resides, at least in part of T helper cell tolerance. Further experiments would help clarifying, whether induced anti-PrP^{C} titers that were short-lived in *Prnp*$^{+/+}$ mice could potentially inhibit prion diseases.

4.5 PrP^{Sc} clearance by treatment with PrP^{C}-specific anti-sera

Above VLP-PrP^{D111} immunization experiments showed high induction of native anti-PrP^{C} antibodies in *Prnp*$^{0/0}$ mice. To test whether those VLP-PrP^{D111}-induced IgG antibody responses do inhibit prion replication, prion infected N2a #58-22L cells were treated with d14 serum of VLP-PrP^{D111}-immunized *Prnp*$^{0/0}$ mice and assayed for PrP^{Sc} formation. 6H4, *Prnp*$^{0/0}$-preimmune serum as well as serum of mice that were immunized with VLP-EGF^{D} were chosen as controls. Scrapie cells were exposed to 6H4 (10 µg) or to serum antibodies in dilutions from 1:50 to 1:100 and subsequently cultured for seven days without passaging. After cell lysis, antibody treated cells were analyzed for PrP^{Sc} load in western blot using mAb 6H4 for PrP detection (Figure 43). After PK treatment, PrP^{Sc} was barely detectable in case of 6H4 pretreatment (Figure 44, lane 5) or pretreatment with serum (1:50) of vaccinated *Prnp*$^{0/0}$ mice (Figure 44, lane 8). No toxic effects were observed. In contrast, anti-PrP^{C} serum of *Prnp*$^{0/0}$ mice showed only a slight PrP^{Sc}-inhibitory effect when added in a 1:100 dilution (Figure 44, lane 6). After treatment of cells with serum from immunized *Prnp*$^{+/+}$ mice no reduction in PrP^{Sc} levels was observed when serum was added at dilutions of 1:50 or 1:100

(Figure 44, lane 7 and 9). *Prnp*$^{0/0}$-preimmune serum (Figure 44, lane 3) or serum of VLP-EGF^{D}-immunized mice (Figure 44, lane 4) did not affect PrP^{Sc} levels. PrP^{Sc} infectivity and efficient PK digestion of N2a #58-22L cells was verified by application of untreated N2a #58-22L cells (Figure 44, lane 1 and 2).

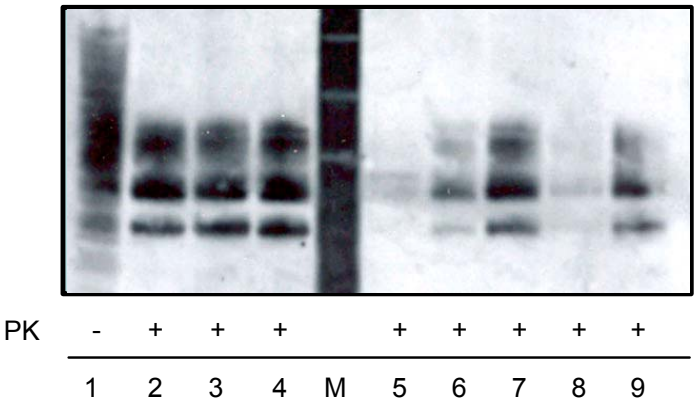

Figure 44 Levels of PrP^{Sc} in chronically infected N2a #58-22L cells after treatment with serum antibodies determined by western blot analysis. Cells were lysed and samples were incubated in the presence (+) or absence (-) of Proteinase K (20 µg/ml). N2a #58-22L cells that were left untreated (lane 1 and 2), treated with *Prnp*$^{0/0}$ preimmune serum (1:50) (lane 3) or with VLP-EGF^{D}-serum of *Prnp*$^{0/0}$ mice (1:50, lane 4) were used as controls. Cells treated with 6H4 antibody (lane 5) or with serum of *Prnp*$^{0/0}$ mice (lane 8,1:50) showed reduced scrapie levels after treatment. Serum of *Prnp*$^{0/0}$ mice (lane 6, 1:100) and *Prnp*$^{+/+}$ serum (lane 7, 1:100; lane 9, 1:50) did not show reduced srcapie levels.

In summary, serum antibodies of VLP-PrP^{D111}-immunized *Prnp*$^{0/0}$ mice, but not those of *Prnp*$^{+/+}$ mice diminished PrP^{Sc} levels *in vitro*. In further experiments, different concentrations of anti-PrP^{C} serum antibodies have to be titrated to determine optimal inhibitory conditions in conversion of PrP^{C} to PrP^{Sc}.

4.6 Assessment of *in vivo* protection against scrapie by VLP-PrP^{D111} immunization

Active immunization experiments described above showed, that native anti-PrP^{C} IgM and IgG antibodies were induced in VLP-PrP^{D111}-immunized *Prnp*$^{+/+}$ mice. However, anti-PrP^{C} antibody responses were rather short-lived. To

address whether already low levels of anti-PrP^C IgG have a protective effect in prion pathogenesis, *Prnp*$^{+/+}$ mice and *Prnp*$^{0/0}$ controls were tested in an *in vivo* protection assay. Therefore, groups of eight to ten *Prnp*$^{+/+}$ mice that were previously immunized with three different anti-PrP^C immunization protocols (Table 17) were challenged by i.p. injection of the mouse adapted prion strain RML 5.0. Afterwards, they were analyzed for the onset of scrapie symptoms (Figure 45 A).

Table 17 Anti-PrP^C immunization protocols

Group	Priming	1st Boost	2nd Boost	Synonym
I	VLP-PrP^{D111}	VLP-PrP^{D111}	HIV-PrP^{D111}	**MLV/MLV/ HIV**
II	VLP-PrP^{D111}	VLP-PrP^{D111}	-	**MLV/ MLV**
III	HIV-PrP^{D111}	-	-	**HIV**

The quality of the inoculum was approved by intracerebral (i.c.) inoculation of *Prnp*$^{+/+}$ mice that develop scrapie symptoms at day 190 when infected with an average dose of RML 5.0. Mock treated animals that received wild-type brain homogenates of uninfected mice were additionally included as well as *Prnp*$^{0/0}$ animals that are resistant to scrapie and fail to replicate the agent. Furthermore, a control group of non-immunized *Prnp*$^{+/+}$ mice were challenged with RML 5.0 inoculum.

To determine PrP^{Sc} infectivity in spleen and brain tissues from scrapie inoculated mice, several mice were sacrificed at different time points (Figure 45 B). Thus, spleens and brains from *Prnp*$^{+/+}$ mice were prepared on day 45, 60, 90, 150 post infection (d.p.i.) for transmission into tg20 indicator mice. Alternatively, prion titers in spleens and brains of infected mice could be analyzed by western blot.

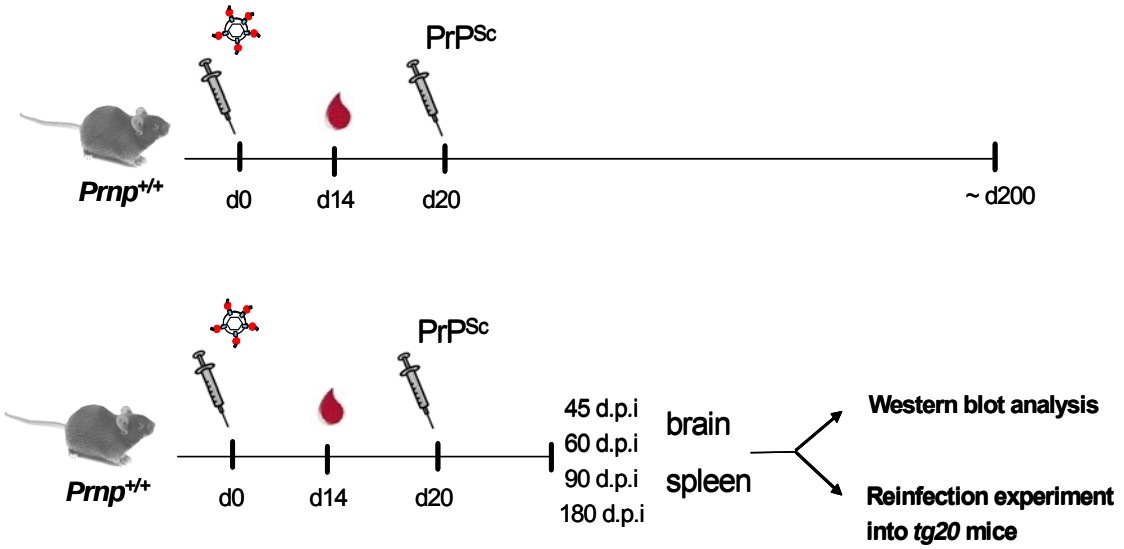

Figure 45 Schematic representation of *in vivo* protection assay. *Prnp*$^{+/+}$ mice were primarily immunized with VLP-PrP^{D111}. After determination of anti-PrP^{C} titers in the tg33 FACS assay, mice were infected i.p. with RML 5.0. At first, groups of mice were analyzed for scrapie symptoms until the onset of scrapie disease **(A)**. In a second approach spleen and brain tissues were isolated from PrP^{Sc} infected mice at different time points post infection. Homogenates of tissues were subsequently analyzed for PrP^{Sc} load in western blot. Alternatively, spleen homogenates were used for transmission experiments into tg20 mice **(B)**.

After inoculation of infectious agent, typical clinical signs of scrapie such as ataxia, hind leg paresis, plastic tail or waddling gait were daily analyzed at a time when usually first clinical symptoms appeared. The incubation time to terminal disease was measured. Despite the presence of substantial anti-PrP^{C} titers, immunized *Prnp*$^{+/+}$ mice did not exhibited a significant delay in the onset of prion disease (Table 18 and Figure 46). Most vaccinated animals succumbed to infection on day 230 p.i., whereas non-immunized *Prnp*$^{+/+}$ animals showed clinical signs of prion infection 225±5 d.p.i.. Moreover, no significant differences were observed between groups of mice that were immunized with different VLP-immunization protocols (Figure 46). Three of twenty-six vaccinated *Prnp*$^{+/+}$ mice survived prion inoculation but did not show increased anti-PrP^{C} titers. Mock treated *Prnp*$^{+/+}$ and *Prnp*$^{0/0}$ mice showed no clinical symptoms after i.p. challenge with scrapie (Figure 46).

Because in control groups one of eight non-immunized wild-type mice did not developed scrapie, it was difficult to comment on immunization efficiencies.

Table 18 Latency of scrapie in different immunized wild-type mice

	mouse line	treatment / immunization	mice succumbing to scrapie	terminal sick (days)	inocculation
Control	C57/BL6	No	3/3	191, 191, 191	100µl 10-4 RML 5.0 i.c
	C57/BL6	No	0/3	>275	100µl 10-4 Mock i.p
	Prnp$^{0/0}$	No	0/6	>275	100µl 10-4 RML 5.0 i.p
WT infected	C57/BL6	No	3/3	222, 227, 234	100µl 10-4 RML 5.0 i.p
	C57/BL6	No	1/1	249	100µl 10-4 RML 5.0 i.p
	C57/BL6	No	3/4	215*,221,234,>275	100µl 10-4 RML 5.0 i.p
WT immunized	C57/BL6	MLV/MLV/HIV	4/5	207,226,226,230, >275	100µl 10-4 RML 5.0 i.p
	C57/BL6	MLV/MLV/HIV	3/3	199**,221,229	100µl 10-4 RML 5.0 i.p
	C57/BL6	HIV	3/3	222,222,228	100µl 10-4 RML 5.0 i.p
	C57/BL6	HIV	5/5	222,229,230,233,>275	100µl 10-4 RML 5.0 i.p
	C57/BL6	MLV/MLV	5/5	207,226,233, 247,249	100µl 10-4 RML 5.0 i.p
	C57/BL6	MLV/MLV	4/5	227,229,233,251,>275	100µl 10-4 RML 5.0 i.p

killed *
died**

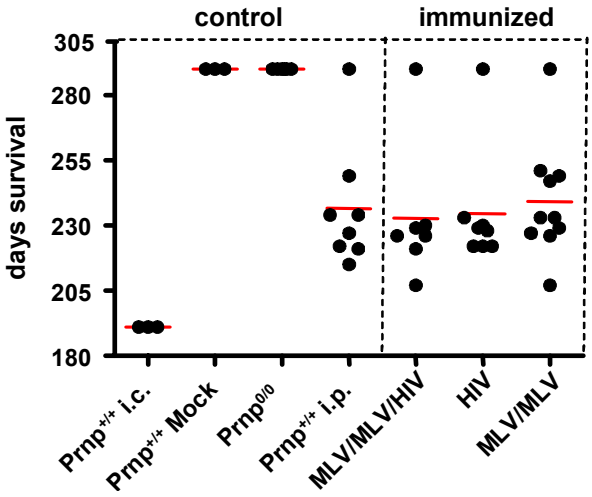

Figure 46 Different VLP-vaccination strategies did not increase survival times of *Prnp*$^{+/+}$ mice after scrapie inocculation. VLP-immunized *Prnp*$^{+/+}$ mice were analyzed for scrapie survival. Mock treated as well as i.p. or i.c. PrP^{Sc}-inoculated *Prnp*$^{+/+}$ mice were used as controls. Furthermore, a group of PrP^{Sc} infected *Prnp*$^{0/0}$ mice were included.

In order to determine prion infectivity over time in spleens of mice, we performed transmission assays into tg20 mice, which overexpressed mouse PrP^{C} and showed shortened incubation periods until obvious signs of prion disease became apparent. Therefore, four tg20 indicator mice per group were i.c. inoculated with 30 µl 1% spleen homogenates of VLP-immunized or control mice that were sacrificed at different time points before clinical symptoms became apparent (Table 19).

Table 19 Tg20 transmission assay with spleen homogenates of scrapie infected immunized *Prnp*$^{+/+}$ mice.

	mouse line	treatment immunization	days after inocculation	indicator mice succumbing to scrapie (tg20)	onset of disease (days)	inocculation
Control	C57/BL6	No	45	0/4	>142	30µl 1% slpeen homogenate
	C57/BL6	No	45	4/4	68*,70*, 70*, 90*	30µl 1% slpeen homogenate
	C57/BL6	No	60	4/4	64*, 64*, 64*, 66*	30µl 1% slpeen homogenate
	C57/BL6	No	60	0/4	>142	30µl 1% slpeen homogenate
	C57/BL6	No	98	2/2	70*, 73*	30µl 1% slpeen homogenate
	C57/BL6	No	98	2/2	71*, 205*	30µl 1% slpeen homogenate
	C57/BL6	No	98	3/3	73*, 73*, 90*	30µl 1% slpeen homogenate
	C57/BL6	No	98	5/5	66*, 66*, 66*, 68*, 68*	30µl 1% slpeen homogenate
	Prnp$^{0/0}$	No	45	0/4	>142	30µl 1% slpeen homogenate
	Prnp$^{0/0}$	No	60	0/4	>142	30µl 1% slpeen homogenate
	Prnp$^{0/0}$	No	60	0/4	>142	30µl 1% slpeen homogenate
	Prnp$^{0/0}$	No	60	0/4	>142	30µl 1% slpeen homogenate
WT immunized	C57/BL6	MLV/MLV/HIV	45	4/4	66*,66*,66*,68*	30µl 1% slpeen homogenate
	C57/BL6	MLV/MLV/HIV	45	0/4	>142	30µl 1% slpeen homogenate
	C57/BL6	MLV/MLV/HIV	60	2/2	71*,73*	30µl 1% slpeen homogenate
	C57/BL6	MLV/MLV/HIV	60	2/2	73*, 73*	30µl 1% slpeen homogenate
	C57/BL6	MLV/MLV/HIV	60	3/3	68*, 68*, 70*	30µl 1% slpeen homogenate
	C57/BL6	MLV/MLV/HIV	60	1/1	68*	30µl 1% slpeen homogenate
	C57/BL6	MLV/MLV/HIV	98	1/3	122* >142	30µl 1% slpeen homogenate
	C57/BL6	MLV/MLV/HIV	98	1/2	114*, >142	30µl 1% slpeen homogenate

killed*

Transmission of different spleen homogenates from non-immunized wild-type mice into tg20 indicator mice caused terminal disease after approximately 70 days. Unfortunately, two indicator mice did not succumb to scrapie after inoculation of spleen homogenates from non-immunized scrapie infected wild-type mice isolated at day 45 and 60. Those data might refer to inoculum application problems (Table 19). As controls, one group of tg20 mice were inoculated with spleen homogenates from *Prnp*$^{0/0}$ mice. Such mice did not show obvious scrapie symptoms.

Because MLV/MLV/HIV immunized *Prnp*$^{+/+}$ mice showed the highest level of anti-PrP^{C} titer in FACS assay, those mice were chosen for transmission. Therefore, spleens of MLV/MLV/HIV immunized mice were prepared on day 45, 60 or 98 dpi and homogenates were transmitted into groups of four tg20 mice. Similar incubation times were found after transmission, showing that infectivity in spleens was observed already after 45 days (Table 19). Tg20 mice

inoculated with PrP^{Sc} positive spleen homogenates isolated from MLV/MLV/HIV immunized wild-type mice developed typical scrapie symptoms within 70 d.p.i. (Table 19). However, a prolonged survival was observed in tg20 mice that were injected with spleen homogenates from 45 or 98 d.p.i..

Taken together these data implicated that in most cases VLP-immunizations did not prolong the onset of scrapie symptoms. Although antibodies against PrP^{C} were induced in wild-type mice, they did not significantly interfere with scrapie pathogenesis and were therefore not of therapeutic value.

4.7 Memory B cell based induction of PrP^{C}-specific immune response upon VLP-PrP^{D111} immunization

In VLP-PrP^{D111} vaccination approaches, the T cell-dependent switch from IgM to IgG isotype of PrP^{C}-specific antibodies was rather weak, probably due to tolerance of PrP-specific T helper cells. This further illustrated that tolerance manifested on the T cell level cannot easily be overcome by VLP-PrP^{D111} immunization. In a previous study it was shown that virus-specific “memory” B cells can be activated by viral particles to produce virus-specific IgG antibodies with neutralizing capacity in the absence of T helper cells [Hebeis et al., 2004]. In this study, activated “memory” B cells were adoptively transferred into RAG-$1^{-/-}$ mice that are deficient of B and T cells. Upon antigenic stimulation, rapid IgG production was induced. Reasoning that VLP-PrP^{D111} immunizations induced long lived anti-PrP^{C} specific IgG antibodies in *Prnp*$^{0/0}$ mice, it is a matter of question whether upon adoptive transfer of PrP-specifc “memory” B cells from *Prnp*$^{0/0}$ mice into wild-type mice, those memory B cells can be activated to produce PrP^{C}-specific IgG. If activation of “memory” B cells does not need T cell help, it should be possible to induce anti-PrP^{C} specific IgG antibody responses under such conditions. For adoptive transfer experiments donor and recipient cells have to share identical MHC genes. Therefore, SV129 x C57/BL6 *Prnp*$^{0/0}$ mice were backcrossed to the C57BL/6 background for 10 generations prior to the use in the context of adoptive transfer experiments. Homozygous C57BL/6 *Prnp*$^{0/0}$ offspring were first immunized with VLP-PrP^{D111}

and sorted *Prnp*$^{0/0}$ "memory" B cells were subsequently adoptively transferred into wild-type or *Prnp*$^{0/0}$ control animals. Because it has been previously reported that sublethal irradiation would improve the immunological susceptibility of adoptively transferred cells [Coligan et al., 1991], one group of *Prnp*$^{+/+}$ recipient mice was sublethally irradiated with 500 rad and subsequently adoptively transferred with PrP^{C}-specific memory B cells. For adoptive transfer, six weeks after the last immunization, CD19^{+} B cells were isolated from spleens of 7 VLP-PrP^{D111}-immunized *Prnp*$^{0/0}$ donor mice by two rounds of cell sorting (Sorting was performed with MoFlow in cooperation with T. Winkler, Erlangen). In general, a purity of >99.8% was achieved by this procedure. Individual *Prnp*$^{+/+}$ and *Prnp*$^{0/0}$ recipient mice were adoptively transferred with 1x10^{7} purified B cells. *Prnp*$^{0/0}$ recipients were included as controls to verify efficient transfer of B cell. Eight days after the B cell transfer, mice were challenged with VLP-PrP^{D111} and serum was analyzed for PrP^{C}-specific antibodies in the tg33 FACS assay at different time points post challenge. *Prnp*$^{+/+}$ and *Prnp*$^{0/0}$ recipient mice were subsequently inoculated with RML 5.0 (Figure 47).

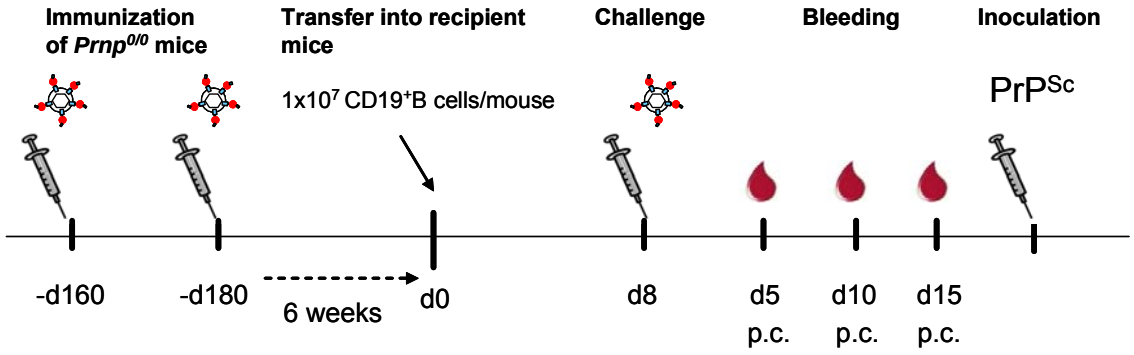

Figure 47 Overview of experimental the immunization protocol, adoptive transfer, and challenge with VLP-PrP^{D111}. *Prnp*$^{0/0}$ mice were immunized twice with VLP-PrP^{D111}. 180 days later, sorted B cells from the *Prnp*$^{0/0}$ spleens were adoptively transferred into *Prnp*$^{+/+}$ recipients.

Adoptively transferred *Prnp*$^{0/0}$ mice mounted high anti-PrP^{C} IgM responses 5 days after VLP-PrP^{D111} challenge (Figure 48 A). On day 15 high anti-PrP^{C} IgG titers were observed (Figure 48 B). Some individuals of *Prnp*$^{+/+}$ recipients

mounted increased anti-PrP^{C} IgM antibody responses 5 days after challenge. However, no anti-PrP^{C} IgG responses were found in *Prnp*$^{+/+}$ recipients (Figure 48 B) or in immunized mice that did not receive memory B cells (data not shown). Nevertheless, in some irradiated *Prnp*$^{+/+}$ recipients minor PrP^{C}-specific IgG titers were observed. *Prnp*$^{+/+}$ recipient mice that survived scrapie infection showed different IgM responses on day 5 (Figure 48 A, indicated in blue lines). Surprisingly, only one irradiated *Prnp*$^{+/+}$ mouse survived scrapie infection and showed anti-PrP IgG titer on day 15 (Figure 48 B).

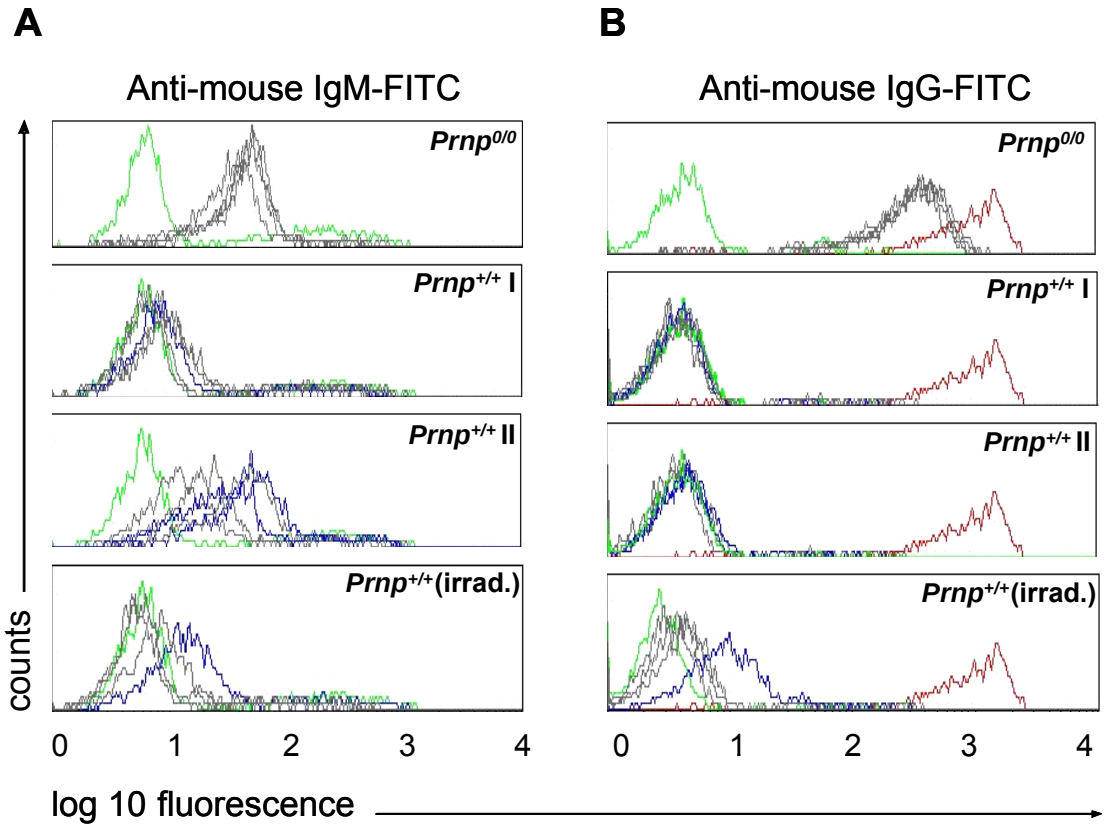

Figure 48 *Prnp*$^{0/0}$ and *Prnp*$^{+/+}$ recipients showed high native anti-PrP^{C} specific IgM antibodies already 5 days after VLP-PrP^{D111} challenge. Serum of adoptively transferred *Prnp*$^{0/0}$, *Prnp*$^{+/+}$ (a total of 10 mice was analyzed, 5 animals are shown in panel "group I" and 5 other animals shown in panel "group II") or *Prnp*$^{+/+}$ (irradiated) mice were analyzed for anti-PrP^{C} IgM titers on day 5 p.c. (A) or IgG titers on day 15 p.c. (B, grey lines). *Prnp*$^{+/+}$ mice that survived scrapie infection are indicated in blue lines. Cells incubated with preimmune serum (green) or 6H4 (red) were used as controls.

These experiments indicated, that PrP^C-specific memory B cells that were originally induced in a PrP deficient environment, were tolerized upon adoptive transfer into PrP competent mice. Thus, indeed peripheral mechanisms exist which reduce responsiveness of PrP-specific B cells in a PrP competent environment.

To check for protective effects that could have been mediated by memory B cells independently of PrP^C-specific antibody responses, adoptively transferred *Prnp*$^{+/+}$ and *Prnp*$^{0/0}$ recipient mice were inoculated i.p. with RML 5.0, and the time untill onset of terminal disease was monitored. Surprisingly, four of fifteen *Prnp*$^{+/+}$ animals carrying memory B cells did not develop scrapie and survived more than 290 days (Figures 49 and 50). By contrast, other *Prnp*$^{+/+}$ recipients in this group succumbed to scrapie within 230 days after RML 5.0 injection. Interestingly, in surviving *Prnp*$^{+/+}$ mice no significant anti-PrP^C IgG responses but increased levels of anti-PrP IgM antibodies were observed (Figure 48). *Prnp*$^{+/+}$ mice that were immunized with VLP-PrP^{D111} but were not transferred with PrP^C-specific “memory” B cells did not mount increased IgG titers and developed scrapie symptoms at times when non-immunized *Prnp*$^{+/+}$ controls usually develop disease (Figure 49). As expected, adoptively transferred *Prnp*$^{0/0}$ recipients or *Prnp*$^{0/0}$ control mice (without adoptively transferred B cells) that were infected with scrapie stayed healthy during the whole experiment.

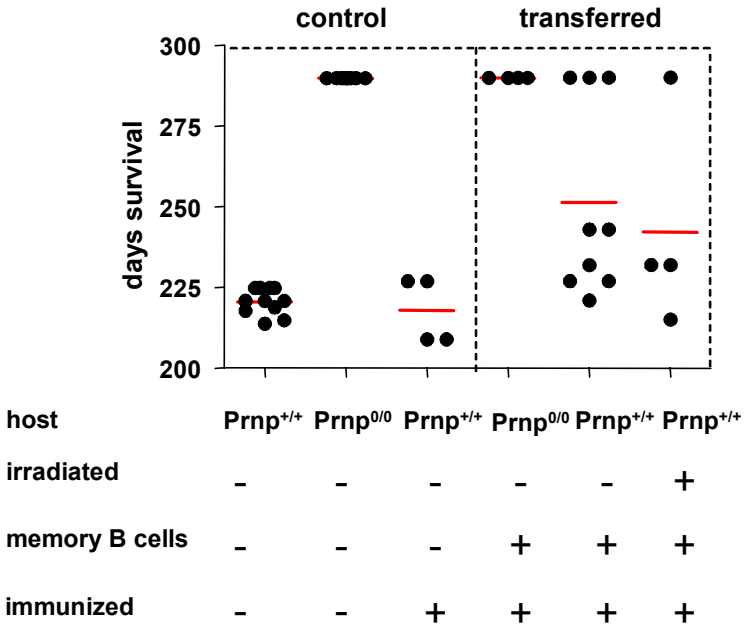

Figure 49 Adoptive transfer of "memory" B cells prolonged incubation times in *Prnp*$^{+/+}$ recipients after i.p. administration of scapie inocculum. *Prnp*$^{0/0}$ or *Prnp*$^{+/+}$ mice were infected with RML 5.0 after adoptive transfer of PrP^{C}-specific memory B cells and challenge with VLP-PrP^{D111}. Controls received no memory B cell preparations. Data represent incubation times of mice that succumb to terminal disease and had to be sacrified.

Four of fifteen *Prnp*$^{+/+}$ mice that received PrP^{C}-specific memory B cells from *Prnp*$^{0/0}$ mice did exhibit a significant delay in the onset of prion disease compared to mice that were just immunized with VLP-PrP^{D111} and did not receive PrP^{C}-specific memory B cells. Moreover, three of nine adoptively transferred *Prnp*$^{+/+}$ mice survived scrapie inoculation whereas *Prnp*$^{+/+}$ control animals developed typical scrapie symptoms and had to be sacrificed around day 225. Statistical analysis of survival curves yielded p=0.0177, indicating that the incubation times in both groups were significantly different (Figure 50).

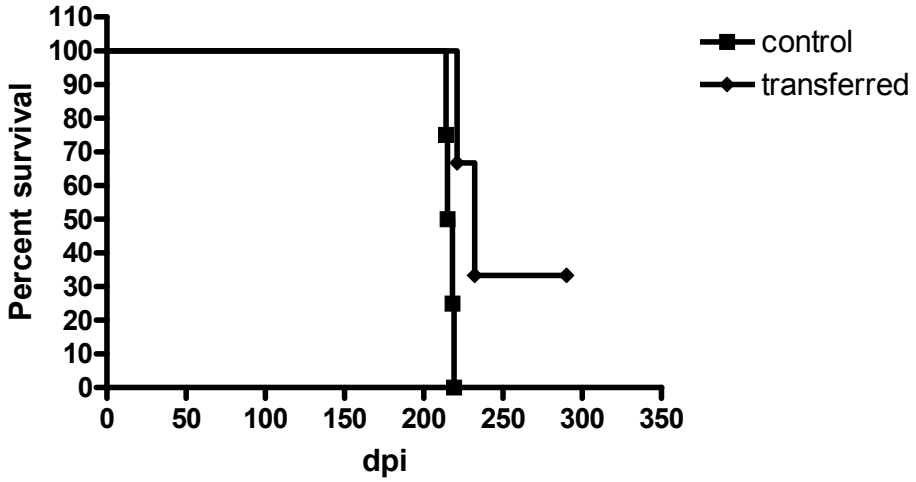

Figure 50 Survival plot visualizing incubation times until development of terminal disease of transferred *Prnp*$^{+/+}$ recipients in comparison to *Prnp*$^{+/+}$ controls after i.p. challenge with prions. Three of nine recipient mice did not develop scrapie symptoms until 290 d.p.i (p =0.017).

Those preliminary results suggested that adoptively transferred memory B cells are rendered less responsive in a PrP competent environment, despite the fact that B cells have originally been induced in PrP-deficient mice. Nevertheless, although PrP-deficient memory B cells showed a reduced PrP-responsiveness in PrP-competent recipients, they still supported PrP^{C}-specific immune responses and prevented prion infection in a certain proportion of *Prnp*$^{+/+}$ mice tested. PrP^{Sc} levels in spleen and brains from prion-infected mice have to be further investigated by western blot analysis and by histology.

5 Discussion

Prion diseases are fatal neurodegenerative diseases for which no therapeutic or prophylactic treatment is available, yet. A number of possible therapeutic agents such as Congo red (CR), anthrocyclines or quinacrine have been tested for their potency to interfere with PrP^{Sc} propagation. However, those reagents have limitations in terms of toxicity and ability to cross the blood-brain barrier [Rudyk et al., 2000; Head et al., 2000]. Besides compound treatment, passive immunizations against prion diseases using anti-PrP^{C} specific antibodies or active vaccination trials would be feasible approaches to prevent prion infection. TSE-infected animals do not mount measurable immune responses against infectious prion protein. Nevertheless, the immune system does play a role in TSE pathogenesis, i.e. for the transport of prions from the periphery to the CNS. This step is dependent on the lymphoreticular system [Aucouturier et al., 2001]. According to Klein et al. mature B cells, germinal centers and follicular dendritic cellular networks are required for the development of clinical scrapie after peripheral injection of pathogenic doses of PrP^{Sc} [Klein et al., 1997]. Thus, the immune system appears to assist rather than to impair the propagation of prions and their access to the CNS.

Passive immunization studies with PrP^{C}-specific antibodies that recognize the C-terminal part of the prion protein have been shown to be effective in blocking prion replication *in vitro* and *in vivo* or prolonging the incubation period of scrapie [Peretz et al., 2001; Sigurdsson et al., 2002; Sigurdsson et al., 2003; White et al., 2003]. However, a major obstacle of passive immunization strategies is the stable maintenance of protective antibody levels. In very elaborate studies passive immunization with anti-PrP^{C} monoclonal antibodies could delay scrapie [Sigurdsson et al., 2003; White et al., 2003], but active vaccination might be a straightforward approach for prophylaxis and treatment of prion diseases. Unfortunately, induction of PrP^{C}-specific antibody responses is hampered by tolerance phenomena to PrP^{C} which is an endogenous ubiquitously expressed self-protein [Bueler et al., 1993]. Experiments with transgenic mice expressing PrP^{C}-specific antibodies suggested that B cell

tolerance is not complete and that potentially auto-reactive PrP^C-specific B cells do develop *in vivo* [Heppner et al., 2001].

In this thesis it was studied whether it was possible to induce antibody responses against PrP^C in wild-type (*Prnp*$^{+/+}$) mice and whether such responses have protective effects. To address this issue, in a first step the immunogenicity of a replication deficient expression system was assessed. To this end, VLP expressing VSV-G on the surface was generated and analyzed for immunogenicity. Then, PrP^C-displaying VLP were generated and tested in different immunization approaches for the induction of anti-PrP^C specific immune responses. Finally, the protective capacity of PrP^C-specific immune respones was assessed.

5.1 VLP are highly immunogenic antigens

In order to study the immunogenicity of retrovirus-like particles, VLP expressing the VSV-G protein (VLP-VSV) and control VLP expressing the EGF protein (VLP-EGF^D) were generated. Based on their ability to accommodate foreign transmembrane proteins in their envelope membrane, retroviral particles were selected as display vehicles. An important prerequisite for good display of antigenic determinants on VLP is the efficient cell surface expression to increase the likelihood of incorporation of antigenic determinants as foreign transmembrane proteins at sites of viral budding. VLP contain many copies of antigens in a structured order, thereby mimicking viral surface structures. Since VLP-VSV was generated in the absence of Env, only cellular proteins and VSV-G constituted the surface components and unwanted regulatory proteins or infectious genetic material of the retrovirus were absent.

In a first step, VLP-VSV was characterized by ELISA and electron microscopy for efficient display of VSV-G. As a positive control, the replication competent and highly immunogenic VSV was used. ELISA and electron microscopic data showed that the VSV-G protein was efficiently displayed on VLP-VSV-retroparticles. Furthermore, VLP-VSV and VSV similarly expressed VSV neutralizing determinants. This was indicated by the observation that upon

pseudotyping of retroviral and lentiviral vectors, VSV-G forms a fully functional trimeric complex that mediates cell entry and membrane fusion [Cronin et al., 2005]. One difference of VLP-VSV compared to VSV is the amount of VSV-G expressed per particle, which is likely to be higher in VSV. Furthermore, bullet shaped VSV displays strictly ordered glycoprotein in a paracrystalline manner, whereas on spherically shaped VLP VSV-G is probably less ordered. Nevertheless, these differences are not expected to significantly affect the expression of VSV neutralizing epitopes as also supported by electron microscopic studies in which a polyclonal anti-VSV-G serum decorated VSV and VLP-VSV but not VLP-EGF^{D} (Figure 8 A).

In a next step, antibody responses induced by VLP-VSV or VSV were analyzed for their virus neutralizing activity using one and the same live VSV Indiana isolate in all neutralization tests. Indeed, reminiscent of live VSV, VLP-VSV turned out to be highly immunogenic and induced VSV neutralizing T independent IgM responses that switched to the IgG subclass in a T help-dependent manner. Thus, VSV and VLP-VSV can be classified as TI antigens. Nevertheless, as the switch to IgG responses towards VSV-G required T cell help [Leist et al., 1987; Bachmann et al., 1995], in case of VSV the discrimination between TI-1 or TI-2 antigens is not trivial and caused diverse discussions in the literature. Usually, the independence of T cell help is determined by using CD4-depleted X chromosome-linked immunodeficient (XID) mice which carry a missense mutation in the gene encoding for the intracellular Burton´s tyrosine kinase (Btk) that participates in BCR signal transduction. XID B cells exhibit an activation defect, which facilitated the identification of any residual requirements for T cell help during IgM responses [Boswell et al., 1980]. TI-1 antigens are completely independent of T cell help and can thus be elicted in XID mice, wheres TI-2 antigens require residual help from T cells or maybe even NK cells [Snapper et al., 1993; Mond et al., 1995]. Similarly to VSV, VLP-VSV leads to optimal BCR-crosslinking that provides strong activation for the induction of IgM responses in the absence of T cell help. Thus, VLP-VSV should be classified as a TI-1 antigen.

In conclusion, although VLP-VSV and VSV are considerably divergent reagents, the overall quality of antibody responses induced by these reagents are comparable in many regards. Furthermore, unlike UV-inactivated VSV that induces IgM, but no IgG responses at a broad range of doses, VLP-VSV was very immunogenic and turned out to be a good tool for studying virus-induced antibody responses.

5.2 VLP immune responses are critically dependent on IFNAR triggering

Antiviral host defenses are mediated by the rapid induction of type I IFN and proinflammatory cytokines, which plays a role in subsequent activation of the adaptive immune response [Le Bon et al., 2001]. Several vaccination studies performed by Proietti et al., Le Bon et al. and others indicated earlier that type I IFN stimulation may potently enhance antibody responses [Proietti et al., 2002; Le Bon et al., 2006]. Therefore, VLP-VSV was used as a tool to address the question whether virus-induced type I IFN responses had an impact on the induction of neutralizing antibody responses. This question is of particular interest, because virus particles often display highly ordered antigens that induce T help-independent IgM responses, whereas the switch to the IgG subclass is T help-dependent. In contrast, soluble antigens such as chicken gamma globulin (CGG) induce IgM and IgG responses in a T help-dependent manner [Le Bon et al., 2001]. Usually a time gap of several days exists between the induction of IFN-α/β responses and the appearance of neutralizing serum antibodies. Therefore, it is important to understand whether early IFN-α/β affects only early events such as the induction of IgM responses in primary foci and by local B cells. Alternatively, IFN-α/β could also have an impact on later immune reactions such as the IgG switch of protective neutralizing antibody responses. IFN-α/β receptor deficient ($IFNAR^{-/-}$) mice have been instrumental in studying IFN-α/β effects *in vivo*. Unfortunately, they are extremely sensitive to lethal VSV infection [Muller et al., 1994]. Thus, VLP-VSV that are entirely replication deficient, and thus non-infective, were used as an alternative to VSV

to analyze virus-induced immune responses in IFNAR$^{-/-}$ mice. VLP-VSV immunization data demonstrated that VSV neutralizing antibody responses showed a T help-dependent IgG switch that was critically dependent on IFNAR signaling. Furthermore, the lack of subclass switch in IFNAR$^{-/-}$ mice was associated with a reduced germinal center reaction, which was confirmed by immuno histochemistry and by FACS analysis.

The IFNAR dependence of VLP-VSV induced IgG switch raised the question of how type I IFN promotes the subclass switch. Many possible mechanisms were described including involvement of type I IFN in recruitment of lymphocytes into B and T cell zones [Kamphuis et al., 2006] and improvement of B cell-priming and the GC formation through upregulation of the costimulatory molecules on DCs, B and T lymphocytes [Klaus et al., 1994; McAdam et al., 2000; Walker et al., 2000]. Type I IFN stimulation enhances B cell survival *in vitro* [Jego et al., 2003] and could hence rescue B cells from apoptosis *in vivo*, an effect which was recently identified in CD8$^+$ T cells as a crucial mechanism to promote the generation of cytotoxic T lymphocytes [Kolumam et al., 2005]. Finally, virus infection may activate pDCs to secrete IFN-α/β which supports generation of non-Ig-secreting plasma blasts and IL-6 to promote differentiation into Ig-secreting plasma cells [Jego et al., 2003].

5.3 IFNAR signaling on the level of B cells does not contribute to the IgG switch

VLP-VSV-induced antibody responses showed a T help-dependent switch of neutralizing IgM to IgG that was critically dependent on IFNAR triggering. Interestingly under these conditions, IFNAR signaling on the level of B or T cells did not critically contribute to the IgG switch. The observation that mice with a combined B and T cell-specific IFNAR ablation showed moderately reduced neutralizing antibody responses upon VLP-VSV immunization suggested that IFNAR signaling on lymphocytes may synergize to further improve the IgG switch.

Conditional IFNAR mice with a B cell, a T cell or a combined B and T cell-specific IFNAR ablation infected with VSV mounted normal neutralizing IgM and IgG responses. Furthermore, IFNAR-B mice showed a normal GC reaction after virus infection. These observations are in contrast to a recent study by Fink et al. who observed reduced IgM responses in VSV infected mice [Fink et al., 2006]. In this study mice were used, that carried $3x10^6$ adoptively transferred VSV-specific B cells that were IFNAR proficient or deficient. It was shown that upon *in vitro* incubation of IFNAR-deficient splenocytes with VSV, any cell type including specific and non-specific B cells, macrophages, pDCs and DCs were readily infected. In contrast, IFNAR-competent splenocytes showed a strikingly reduced infection with basically only VSV-specific B cells and to a lesser extent unspecific B cells being infected. Thus, it is likely that in this system the $3x10^6$ adoptively transferred IFNAR-deficient B cells bound a good proportion of the $2x10^6$ PFU injected VSV that then resulted in infection of the B cells and subsequent cell lysis. In conclusion, it is possible that in mice carrying adoptively transferred IFNAR deficient B cells, VSV-induced antibody responses were reduced due to experimental conditions that favoured VSV infection of VSV-specific and IFNAR-deficient B cells.

In the mouse model used in this thesis, IFNAR-B mice showed a polyclonal B cell repertoire. Thus, in IFNAR-B mice effects as discussed above are unlikely to take place. Assuming the presence of more than 10^9 B cells in a mouse, basically all of which are IFNAR deficient [Kamphuis et al., 2006; Le Bon et al., 2006], less than 0.1% of the B cells can theoretically get infected upon injection of $2x10^6$ PFU VSV. Because in the absence of IFNAR, VSV-specific B cells do not seem to become preferentially infected [Fink et al., 2006], this would result in the infection and destruction of less than 0.1% of the VSV-specific B cell repertoire. Thus, the observations described here probably reflect the *in vivo* conditions more appropriately than adoptive transfer experiments.

Many controversial effects of IFNAR signaling on B cell responses were reported. One study by Coro et al. showed that influenza virus infection induced early local antibody responses that were dependent on B cell-specific IFNAR signaling [Coro et al., 2006]. In this study, a low pathogenic influenza virus

strain was used which was similarly well cleared in IFNAR$^{-/-}$ and wild-type mice and thus allowed a comparative analysis of influenza virus-specific B cell responses in both mouse strains.

In another model, LCMV infection induced similar immunoglobulin responses against the nuclear protein (NP) in IFNAR$^{-/-}$ and wild-type mice [van den Broek et al., 1995]. Although type I IFN responses are induced by LCMV [Malmgaard et al., 2002], these results suggested that in the case of LCMV-induced antibody responses IFNAR triggering did not play a role.

Upon *in vitro* B cell receptor (BCR) crosslinking, type I IFN was shown to increase the sensitivity of naïve B cells to produce IgM [Braun et al., 2002]. This suggested a lowered threshold for the induction of T help-independent IgM responses. Upon VLP-VSV immunization, IFNAR$^{-/-}$ mice raised slightly reduced IgM responses when compared to wild-type mice. Nevertheless, IFNAR-B mice did not show such a difference. Thus, in the case of the highly repetitive T cell-independent VSV-G surface antigen, optimal conditions for BCR cross-linking are provided [Bachmann et al., 1995; Bachmann et al., 1997] that cannot be further enhanced by type I IFN stimulation. This is in contrast to the T cell-dependent antigen CGG as discussed previously [Le Bon et al., 2006]. Thus, antibody responses that differ with respect to their IFNAR-dependence are induced depending on the nature of the administered antigen. Low immunogenic antigens such as CGG induce significantly improved antibody responses if co-administered with type I IFN. Under such conditions type I IFN has a direct impact on APCs, T cells and B cells. In contrast, VLP-VSV that is more immunogenic but replication deficient induced an IFNAR dependent IgG switch. Under such conditions, lymphocyte-specific IFNAR triggering played a very minor role. Local infection with low pathogenic influenza virus required IFNAR triggering of B cells. In this model it is possible, that IFN-γ and IFN-α/β crosstalk played a role [Takaoka et al., 2000]. Finally, replication competent LCMV or VSV induced antibody responses that were largely independent of B cell-specific IFNAR triggering. Hence, an overall strong immune activation could compensate for the lack of type I IFN stimulation. Indeed, considering that many viruses have developed means to interfere with the induction of type I IFN

[Ploegh, 1998; Foy et al., 2003; Stojdl et al., 2003; Abate et al., 2004; Dauber et al., 2004; DiPerna et al., 2004] it seems likely that some kind of functional redundancy has evolved to guarantee the efficient induction of protective anti-viral antibody responses.

Toll-like-receptors (TLR) play an important role in antiviral responses by recognizing viral components. It has been shown recently that VSV can trigger IFN-α production *in vivo* through TLR7 triggering [Lund et al., 2004]. Moreover, VSV mediated B cell activation was dependent on TLR-7 expression. However, it was unclear whether the B cell activation was mediated directly by TLR7 or IFN-α. Fink et al. reported that TLR7 expression on VSV-specific B cells supported B cell expansion and IgM production independently of IFN-α.

A requirement of TLR signaling in B cells for optimal T cell-dependent antibody responses was furthermore reported by the group of Medzhitov [Pasare et al., 2005]. In contrast, another study by the Nemazee group showed that the induction of antibody responses was possible even in the complete absence of TLR signaling. In this report mice lacking TLR signaling were able to respond to T cell-dependent antigens if the antigen was administered in an adjuvant. This suggested that TLR signaling was dispensible for vaccine-induced antibody responses [Gavin et al., 2006]. Thus, so far it cannot be ultimately stated whether TLR7 signaling of B cells played a role in the induction of VSV-specific antibody responses. Kato et al. observed that a cytoplasmic protein, retinoic-acid inducible gene-I (RIG-I), but not the TLR system, plays an essential role in antiviral responses in various cells, except for pDCs [Kato et al., 2005]. This observation indicates that type I IFN can be triggered by RNA viruses either via RIG-I or the TLR system, depending on the infected cell type.

In conclusion, VLP-VSV data showed that although IFNAR triggering of lymphocytes is not a limiting step, it may gradually enhance the IgG switch. In VSV infected mice, IFNAR triggering of B cells does neither critically affect germinal center formation nor the IgG switch of neutralizing antibody responses [Bach et al., 2007].

To study the mechanism of VLP-VSV mediated IFN-α induction, MyD88$^{-/-}$/TRIF$^{-/-}$ mice that are completely deficient of TLR signaling, were immunized with VLP-VSV and analyzed for VSV-neutralizing antibody responses. Upon VLP-VSV immunization, MyD88$^{-/-}$/TRIF$^{-/-}$ mice showed a T help-independent IgM whereas the switch to IgG was absent. Thus, TLR signaling seemed to have an influence on the subclass switch to VSV-neutralizing IgG. Currently, adoptive transfer experiments of MyD88$^{-/-}$ or TRIF$^{-/-}$ B cells into JHT mice which lack B cells are perfomed to analyze the role of TLR signaling in B lymphocytes. Furthermore, the question will be addressed whether IFN treatment of MyD88$^{-/-}$/TRIF$^{-/-}$ mice can restore the IgG switch after VLP-VSV immunization.

5.4 VLP induce high anti-PrP^{C} immune responses in *Prnp*$^{0/0}$ mice and represent a tool to study fine specificity of anti-PrP^{C} antibody responses

Because previous data showed that VLP are highly immunogenic, the retrovirus-like system was utilized to display the C-terminal part of the PrP domain (PrP111) via a PDGFR-derived transmembrane domain on the surface of VLP. Antibodies directed against this C-terminal region have previously been shown to interfere with prion propagation [Enari et al., 2001; Peretz et al., 2001; White et al., 2003; Beringue et al., 2004; Perrier et al., 2004; Miyamoto et al., 2005]. Electron microscopy and ELISA showed efficient display of PrP111 on VLP. In contrast, attempts to display the complete PrP molecule (PrP209) on VLP failed, probably because the rather flexible and disordered N-terminal domain of PrP impedes proper folding of the PrP209 molecule, while the globularly structured PrP111 and EGF molecules are well suited for expression in the retroviral membrane [Nikles et al., 2005].

Compared to the VSV-G protein displayed on VLP-VSV, PrP111 was better expressed on the VLP-PrP^{D111} surface. This variation in protein expression might result from the properties of both proteins. VSV-G has a larger globular structure than PrP^{C} and occupied more space on the VLP surface.

Next, VLP-PrP^{D111} was tested to determine whether such particles induce immune responses against PrP^{C}. Anti-PrP^{C} antibody responses were assessed by ELISA using bacterially expressed mPrP$^{REC121-231}$ coated to plastic and by FACS analysis using transgenic T cells overexpressing PrP^{C} on the cell surface. Data showed that a single i.v. immunization with VLP-PrP^{D111} was sufficient to induce native PrP^{C} binding of IgM and IgG antibodies in *Prnp$^{0/0}$* mice. Remarkably, the IgG serum antibodies showed at least as strong PrP^{C} binding as the monoclonal anti-PrP IgG antibody 6H4.

The magnitude of PrP^{C}-specific IgM responses upon i.v. VLP-PrP^{D111} immunization was inversely correlated with the number of *Prnp* alleles expressed, i.e. highest PrP^{C}-specific IgM was induced in *Prnp$^{0/0}$* mice, whereas intermediate and lower levels were detected in *Prnp$^{+/0}$ and Prnp$^{+/+}$* mice, respectively. Nevertheless, it is remarkable, that overall similar IgM levels were induced in mice of all three genotypes, especially at early time points.

Most immunization strategies described in the literature induced anti-PrP antibodies that bind recombinant PrP or peptides in an ELISA assay or western blot assay, but were never directed against the native form of PrP^{C} [Hanan et al., 2001; Hanan et al., 2001; Souan et al., 2001; Koller et al., 2002; Arbel et al., 2003; Gilch et al., 2003; Schwarz et al., 2003; Sigurdsson et al., 2003; Rosset et al., 2004].

Furthermore, it was shown that antibodies which exclusively bind recombinant PrP are not sufficient to confer prionostatic effects in wild-type mice following peripheral prion challenge [Heppner et al., 2004; Polymenidou et al., 2004]. However, a correlation between recognition of native anti-PrP^{C} and the effect on prion replication has been proposed [Heppner et al., 2004]. In a recent report, immunization with bacterially expressed recombinant full-length PrP emulsified in CFA resulted in the induction of antibodies directed against native PrP^{C}, only if mice aberrantly expressing transgenic PrP under the control of an oligodendrocyte and Schwann cell specific promoter were used, whereas wild-type controls and all other PrP transgenic mice tested showed at best serum binding to PrP^{REC} coated to plastic [Polymenidou et al., 2004]. Thus, upon

expressing PrP in most tissues except oligodendrocytes and Schwann cells, tolerance mechanisms were still operative.
Thus, in conclusion it was remarkable that native anti-PrP^{C} specific IgM and IgG titers were induced in *Prnp*$^{+/+}$ mice upon VLP-PrP^{D111} immunization. Moreover, no evidence for autoimmune reactions was observed in PrP-competent mice.

Based on the observation that VLP-PrP^{D111} was highly immunogenic, such particles were evaluated to characterize binding properties of PrP^{C}-specific antibodies induced by VLP-PrP^{D111}. Data showed that serum of VLP-PrP^{D111}-immunized *Prnp*$^{0/0}$ as well as *Prnp*$^{+/+}$ mice was quantitatively competed by VLP-PrP^{D111}, whereas the linear epitope of $mPrP^{REC121-231}$ was only partially able to compete anti-PrP^{C} antibodies. This observation further supported the concept that antibodies induced by VLP-PrP^{D111} bound the native form of PrP^{C}.
Because the retroviral-display system allows the display of various different deletion mutants of PrP on the VLP surface, this system can further be utilized for the analysis of the fine specificity of anti-PrP antibody responses. For example, polyclonal antibodies can be tested for preferential binding of either the C-terminal portion or the octarepeat region of PrP. This is of importance, because it was known that the C-terminal region was crucial for PrP^{Sc} inhibition, whereas the octarepeat sequence was not essential for PrP^{Sc} formation. Unfortunately, attempts to generate VLP displaying various different deletion mutants of PrP failed. Incorporated PrP mutant proteins were not detectable by electron microscopy and by ELISA (data not shown). This failure might be explained by inefficient display or wrong folding of PrP^{C} molecules on the VLP surface.

5.5 Wild-type mice immunized with VLP-PrP^{D111} mount PrP^{C}-specific antibody responses that recognize the native form of PrP^{C}

Because PrP^{C}-specific antibodies can block PrP^{Sc} formation, various attempts have been undertaken to induce PrP^{C}-specific antibody responses in wild-type

mice. Former studies showed that the application of an immunogen emulsified in an adjuvant induced a strong immune response [Freund , 1956; Warren et al., 1986]. Immune responses against Hepatitis B were enhanced when the antigen was coadministered together with CpG-ODN or IFA [McCluskie et al., 1998; Weeratna et al., 2001]. Thus, in a first attempt to further enhance PrP^{C}-specific antibody responses, wild-type mice were immunized with VLP-PrP^{D111} emulsified in various different adjuvants. VLP-PrP^{D111} immunization of wild-type mice showed early induction of native anti-PrP^{C} IgM antibodies. Remarkably, one out of three immunized mice mounted an IgG titer that was stable for up to 144 days after immunization. However, those anti-PrP^{C} titers declined when tested at later time points. The application of other adjuvants such as Titer Max, CpG1668 or Alum showed no effect. Overall, various different vaccination approaches based on numerous adjuvants revealed no significantly enhanced antibody responses against endogenous PrP^{C}.

Some disadvantages of adjuvant application were reported in several former vaccination studies. For instance, CFA application induced strong immunization effect but also resulted in destruction of tissues [Broderson, 1989]. Furthermore, one exciting study reported that high doses application of CpG-ODN protected mice from scrapie [Sethi et al., 2002]. In this study CpG applications resulted in destruction of the FDC network [Heikenwalder et al., 2004]. Thus, considering the deleterious effects of those compounds, it would be more appropriate to vaccinate in the absence of adjuvants.

Obviously, VLP-PrP^{D111} immunization data showed that immunologic host tolerance seems to be predominantly manifested on the T cell level. Thus, the magnitude of PrP^{C}-specific IgM responses is only gradually influenced by the expression level of the PrP^{C} self-determinant [Adelstein et al., 1991; Hartley et al., 1991; Tiegs et al., 1993]. Accordingly, the switch from the IgM to the IgG isotype of PrP^{C}-specific antibodies is less pronounced in wild-type animals when compared to *Prnp*$^{0/0}$ mice. However, T helper determinants accounting for the IgG switch in wild-type animals are probably provided by MLV related antigens.

To test whether the addition of foreign T helper epitopes would boost PrP^C-specific immune responses, VLP were generated that equally expressed PrP^C and VSV-G proteins on one and the same VLP particle. Electron microscopy and ELISA analysis suggested that both proteins were indeed co-expressed on the VLP surface. However, those particles did not induce significantly higher IgG antibodies in wild-type mice when compared with conventional VLP-PrP^{D111}. This result might indicate that in particle preparations only a minor portion of VLP coexpressed PrP and VSV-G.

In a last step, priming and boosting strategies with two different types of VLP were performed to test whether immune reactions against PrP^C can be enhanced. Similarly to the MLV display approach, HIV-PrP^{D111}-displaying virus-like particles were produced. HIV-PrP^{D111} turned out to be very immunogenic in inducing anti-PrP^C specific antibodies in *Prnp*$^{0/0}$ mice. Thus, they were tested for the induction of anti-PrP^C immune responses in wild-type mice. Immunization data revealed that VLP-PrP^{D111} and HIV-PrP^{D111} induced comparable anti-PrP^C antibody responses.

However, priming boosting approaches did not enhance anti-PrP^C IgG antibodies in wild-type mice, showing that even in the presence of diverse T helper epitopes, it was difficult to induce protective long-term anti-PrP^C IgG antibodies.

Taken together, the phenomenon of PrP^C-specific tolerance is a major hurdle that cannot easily be overcome. Nevertheless, virus-like particles seemed to be capable of inducing MLV-specific T cell help accounting for PrP^C-specific IgG production with low affinity in approximately 20% of the immunized wild-type animals in most of the tested vaccination protocols. Noteworthy, VLP-PrP^{D111} induced PrP^C-specific antibodies that are directed against the native form of PrP^C. In most vaccination studies published so far, PrP^C-specific antibody responses were rather weak and were never directed against the native form of PrP^C. Modest prionostatic effects observed in these settings are questionable, as control studies demonstrated prion inhibition after injection of certain adjuvants devoid of antigen.

In conclusion, it is remarkable that host tolerance left enough room for the induction of potentially autoreactive PrP^{C}-specific IgM antibody responses. VLP-PrP^{D111} are promising vaccine candidates, however, they were primarily able to induce rather short lived PrP^{C}-specific IgM responses due to limited T cell help.

5.6 VLP-PrP^{D111}-induced anti-PrP^{C} antibody responses inhibit prion replication in vitro but do not show in vivo protective effects

Next it was addressed whether VLP-PrP^{D111}-induced PrP^{C}-specific antibody responses are able to interfere with PrP^{Sc} propagation. To this end, serum of VLP-PrP^{D111} immunized *Prnp*$^{0/0}$ and wild-type mice were analyzed for PrP^{Sc} clearance in a cell culture system persistently infected with prions. Notably, PrP^{C}-specific serum of *Prnp*$^{0/0}$ mice was able to reduce PrP^{Sc} levels. Those data were in line with the findings of several other groups that showed a reduction of PrP^{Sc} after treatment with PrP^{C}-specific antibodies [Enari et al., 2001; Beringue et al., 2004; Miyamoto et al., 2005]. PrP^{C}-autoantibodies induced in wild-type mice by VLP-PrP^{D111} immunization did not show an inhibitory effect. This observation was in contrast to a recently published study which showed a reduction of PrP^{Sc} levels in cell culture after treatment with PrP^{C}-specific autoantibodies induced upon immunization with a PrP dimer [Gilch et al., 2003].

The failure of antibody mediated prion inactivation may result from weak binding of VLP-PrP^{D111}-induced antibodies to PrP^{C}. It would be important to test whether higher concentrations of PrP^{C}-specific antibodies are able to reduce PrP^{Sc} levels. How can PrP^{C}-specific antibodies interfere with neoformation of PrP^{Sc}? Recently, several discussed mechanisms of prion neutralization have been summarized (as reviewed in [Buchholz et al., 2006]). Examples of PrP^{Sc} neutralization include antibody binding to a region within the helix 1 of PrP^{C} that inhibits the interaction between PrP^{C} and PrP^{Sc} [Enari et al., 2001; Peretz et al., 2001; White et al., 2003; Beringue et al., 2004; Perrier et al., 2004; Miyamoto et al., 2005]. Alternatively, specific binding of the misfolded PrP^{Sc} could be

effective [Paramithiotis et al., 2003]. Furthermore, antibody binding to endogenously expressed PrP^{C} on the cell membrane was proposed as a mechanism that limits the availability of PrP^{C} as a substrate for conversion into PrP^{Sc} [Perrier et al., 2004].

Additionally, two independent studies identified mAbs that inhibited PrP^{Sc} formation via binding sequences in the octapeptide repeat region [Kim et al., 2004; Perrier et al., 2004]. Finally, PrP^{C}-specific monovalent Fab antibody fragments [Peretz et al., 2001] or single-chain Fv fragments derived from the scrapie neutralizing mAb 6H4 [Donofrio et al., 2005] were reported to inhibit PrP^{Sc} formation which excluded Fc mediated effects to play a crucial role in prion neutralization.

Upon VLP-PrP^{D111} immunization, wild-type mice mounted anti-PrP^{C} IgG antibody responses. Because a correlation between recognition of native cell surface PrP^{C} and inhibition of prion replication has been proposed [Heppner et al., 2004] it was a matter of question whether induced antibody levels sufficed to prevent prion disease *in vivo*.

Therefore, wild-type mice were immunized with different immunization protocols and subsequently inoculated with the mouse adapted scrapie isolate RML 5.0. Two weeks after immunization, wild-type mice were screened for PrP^{C}-specific IgM and IgG serum antibodies. All immunized mice showed high PrP^{C}-specific IgM titers. However, only weak IgG titers were observed in few wild-type individuals. RML 5.0 challenge of wild-type mice revealed that irrespective of which immunization protocol was used, no significantly delayed prion pathogenesis was observed. Remarkably, one RML 5.0 infected mouse in each VLP-immunization group survived scrapie infection. However, the prolonged survival of individual mice did not correlate with increased IgG antibody titers. Thus, it is difficult to speculate which mechanism was responsible for PrP^{Sc} inhibition. Unfortunately, one *Prnp*$^{+/+}$ mice in the control group did also survive scrapie infection, indicating that the survival of VLP-immunized mice was rather associated with inoculum application problems than with immunological effects induced upon VLP-immunization.

The tg20 transmission assay further indicated that in the above discussed experiment inoculation problems played a role: Individual tg20 indicator mice which received spleen homogenates from a VLP-immunized mouse survived reinfection. However, also two tg20 control groups that were inoculated with spleen homogenates from non-immunized mice showed no clinical symptoms.

Thus, although in some wild-type mice PrP^{C}-specific IgG antibody responses were induced, they did not mediate protection. Reasons for that might be low levels and short half-lifes of the PrP-specfic IgG responses. When PrP-specific IgG levels in wild-type mice declined before the infectious material was cleared, animals succumb of scrapie disease.
Future experiments will reveal whether individual $Prnp^{+/+}$ mice showed differences in the PrP^{Sc} load. Therefore, levels of PrP^{Sc} deposition in spleen and brain homogenates from VLP-immunized $Prnp^{+/+}$ mice will be quantified by western blot.

5.7 New strategies to overcome PrP^{C}-specific tolerance

As PrP^{C}-specific tolerance hampered efficacious anti-PrP^{C} vaccination, two additional strategies are being evaluated, i.e. adoptive transfer of PrP^{C}-specific “memory cells” and VLP-PrP^{D111} immunization of Treg deficient mice.
In the literature it was described that virus-specific “memory” B cells can be activated by viral particles to produce virus-specific neutralizing IgG antibodies in the absence of T helper cells [Hebeis et al., 2004]. Thus, in the last part of this thesis it was studied whether sorted PrP^{C}-specific “memory” B cells that were originally induced in *Prnp*$^{0/0}$ mice, can be adoptively transferred into wild-type recipient mice to induce PrP^{C}-specific IgG antibody responses upon VLP-PrP^{D111} treatment. If indeed in the absence of T help PrP^{C}-specific “memory” B cells can be activated in wild-type recipients upon VLP-PrP^{D111} challenge, it should be possible to induce significant PrP^{C}-specific IgG antibody responses.
Indeed, naïve *Prnp*$^{0/0}$ recipients mounted anti-PrP IgM antibodies already 5 days post VLP-PrP^{D111} challenge. Furthermore, high levels of PrP^{C}-specific IgG

antibodies were detected in the serum of *Prnp*$^{0/0}$ mice at day 15 post challenge. Despite *Prnp*$^{+/+}$ recipients showed rather high levels of IgM titers 5 d.p.i., none of them mounted IgG antibodies at day 15. As an exception, wild-type mice which were irradiated before adoptive transfer of PrP^{C}-specific memory B cells mounted very low IgG titers. Sublethal irradiation of mice leads to an increased susceptibility to "memory" B cells and probably PrP^{C}-specific IgG levels were detectable after VLP-PrP^{D111} immunization.

Surprisingly, scrapie inoculation experiments using the group of non-irradiated mice revealed that although no PrP^{C}-specific IgG titers were observed, several wild-type mice that received memory B cells (3 of 9 animals) were protected against prion infection.

Overall, PrP^{Sc} protected mice showed higher IgM anti-PrP^{C} specific antibodies than all other recipients in the group. Thus, it is conceivable that efficient induction of native anti-PrP^{C} antibodies can protect against prion disease.

One can speculate that already IgM antibodies that were induced after adoptive transfer in individual *Prnp*$^{+/+}$ recipients interfered with PrP^{Sc}. Prevention of scrapie pathogenesis was also observed by Heppner et al. who showed that transgenic mice expressing IgM antibodies mounted reduced infectivity in spleen and brain after intraperitoneal challenge [Heppner et al., 2001]. The mechanism of PrP^{Sc} interference may rely to IgM antibodies that hinder interaction of prions with PrP^{C} or capturing the incoming PrP^{Sc} inoculum.

Additional adoptive transfer experiments are planned to quantitate the level of PrP^{Sc} deposition in spleen and brain of *Prnp*$^{+/+}$ recipient mice. Furthermore, various inoculation setups can clarify whether high IgM levels suffice to clear PrP^{Sc} infection. For this purpose, the inoculum is applied few days directly after VLP-PrP^{D111}challenge. In another approach, the survival of transferred "memory" B cells in *Prnp*$^{+/+}$ recipient mice will be monitored by FACS-analysis using an antibody recognizing an allotype-specific Ly-5 marker that is only expressed on the transferred B cells. For such experiments congenic C57BL/6 mice expressing the Ly5.1 marker will be used to distinguish between host and transferred "memory" B cells the latter of which express Ly5.2.

Finally, a second strategy is being tested that is based on deletion of Treg cells. Treg cells have been described to play an important role in modulating host responses against tumors and in inhibiting the development of autoimmunity [Sakaguchi, 2005; Coombes et al., 2005]. Currently it is tested whether in the absence of Treg cells specific anti-PrP^{C} immune responses can be induced upon VLP-PrP^{D111} immunization. In this context, a transgenic mouse model is used in which Foxp3 positive Treg cells can be selectively depleted upon Diphtheria toxin (DT) treatment [Lahl et al., 2007].

In conclusion, VLP-PrP^{D111} turned out to be a versatile tool to elucidate basic mechanisms of PrP^{C}-specific tolerance. In addition, findings were obtained with VLP-PrP^{D111} that are encouraging to pursue the development of a prion vaccine. Also in terms of Alzheimer's diseases (AD), VLP might be potent vaccine candidates. Early trials of VLP-Aß immunization studies in transgenic AD model mice showed an induction of Aß-specific antibody responses (data not shown). Furthermore, VLP-Aß immunization resulted in a reduced amyloid plaque load in the brain of vaccinated mice (data not shown).
In contrast to all other PrP vaccination approaches that have been tested until now, VLP-PrP^{D111} is able to induce native PrP^{C}-specific antibody responses. Recently, one publication showed that immunization of rabbits with papillomavirus-like particles displaying the murine/rat PrP^{C} protein on the surface (PrP-VLPs), resulted in the induction of native anti-PrP^{C} antibodies that inhibited PrP^{Sc} *de novo* synthesis in prion infected cells [Handisurya et al., 2007]. However, whether papillomavirus-like particles induced PrP^{C}-specific antibodies are also effective *in vivo* remains to be elucidated.
A recently described Salmonella typhimurium derived vaccine is currently regarded as the most promising candidate for anti-PrP vaccination. A study in which mucosal vaccination with recombinant S. typhimurium encoding PrP was carried out, showed increased survival times of orally exposed mice, indicating that the route of vaccination and infection might play a critical role [Goni et al., 2005]. Notably, about 30% of the vaccinated animals were free of symptoms at 500 days post vaccination.

Arguing that BSE can be a thread for humans, and that BSE-specific immunity could serve as a first-line defense on mucosal epithelia, an interesting approach was followed in which mice were orally immunized against bovine PrP. These experiments illustrated possible directions of future vaccine development.

Due to “spontaneous misfolding” of the endogenous PrP^C protein in cattle, BSE still constitutes a threat for humans. The generation of PrP^C-deficient cattle is a promising attempt to prevent BSE distribution due to “spontaneously mutated prions” [Richt et al., 2007]. Also in terms of “vaccine production” the issue of scrapie safety is critical, because vaccines may be contaminated by animal materials (e.g. contaminated FCS in cell culture) that contain misfolded prions and other transmissible agents. Thus, a therapeutic and prophylactic anti-PrP^C vaccine would be desirable to diminish the risk of TSE infectivity.

Recent developments in the prion field may well influence new vaccination strategies against other self-antigens, e.g. for the treatment of cancer or Alzheimer’s disease. However, for prion diseases, the option of triggering a selective immune response against the pathogenic form of PrP should be kept in mind as well. Although currently out of reach, such a vaccine would resemble the successful strategy behind the marketed vaccines against other pathogens that resulted in complete or partial eradication of many widespread infectious diseases of bacterial or viral origin.

6 Summary

Transmissible spongiform encephalopathies (TSEs) or prion diseases are a group of infectious neurodegenerative diseases that are associated with misfolding of the cellular form of the cellular prion protein (PrP^{C}) into a disease associated conformer (PrP^{Sc}). No therapy for prion diseases is available at present. So far, anti-PrP^{C} vaccination is hampered by immunological tolerance of the mammalian immune system to endogenous PrP^{C}. The aim of this thesis was to set up a new vaccination strategy based on virus-like particles (VLP) to induce anti-PrP^{C} antibody responses in PrP^{C}-competent mice.

In a first step it was assessed whether VLP have the capacity to induce antibody responses that are protective against conventional pathogens. For this purpose, VLP displaying the vesicular stomatitis virus-gylcoprotein (VLP-VSV) were generated and tested for their immunogenicity. Similarly to live vesicular stomatitis virus (VSV), replication deficient VLP-VSV induced T help-independent VSV neutralizing IgM responses that switched to the IgG subclass in a T help-dependent manner. Furthermore, type I IFN receptor (IFNAR) triggering only marginally affected VLP-VSV induced neutralizing IgM responses, whereas it was critically required to promote the IgG switch. The analysis of conditional knockout mice with a lymphocyte-specific IFNAR deletion revealed that IFNAR triggering of lymphocytes did not play a crucial role, neither upon VLP-VSV nor VSV immunization. Collectively, these data verified the high immunogenicity of VLP.

Therefore, in a next step VLP were generated displaying the C-terminal half of PrP (residues 121-231aa) fused to the platelet derived growth factor receptor (PDGFR) transmembrane region (VLP-PrP^{D111}) for anti-PrP^{C} immunization. On the surface of such retroparticles, PrP^{C} was expressed at high levels as determined by electron microscopy. VLP-PrP^{D111} immunization of *Prnp*-deficient ($Prnp^{0/0}$) mice resulted in antibody response specifically binding the cellular form of PrP^{C}. Upon intravenous injection of wild-type mice, high PrP^{C}-specific IgM responses were induced, whereas the T cell-dependent switch from the IgM to the IgG subclass was less pronounced. As a consequence, anti-PrP^{C}

titers were rather short-lived. The impaired subclass switch was probably related with host T cell tolerance to endogenous PrP^{C}. Attempts to increase anti-PrP^{C} IgG responses in wild-type mice via administration of VLP-PrP^{D111} emulsified in various different adjuvants failed. Nevertheless, in single individuals low IgG antibodies were induced after immunization of VLP-PrP^{D111} emulsified in CFA. To circumvent T cell tolerance in wild-type mice, a multitude of different immunization strategies was tested, including priming and boosting protocols with different types of VLP or VLP expressing PrP^{C} together with foreign T helper epitopes. Overall, those efforts did not improve anti-PrP^{C} IgG responses in wild-type mice. Interestingly, anti-PrP^{C} antibodies induced in *Prnp*$^{0/0}$ mice reduced PrP^{Sc} levels in prion infected cell cultures, whereas serum of vaccinated wild-type mice did not. To assess the protective capacity of VLP-PrP^{D111} induced immune responses, vaccinated wild-type mice were infected with scrapie (RML 5.0). Unfortunately, vaccinated mice did not show a significant delay in the onset of scrapie. In a last part of the thesis it was studied whether in the absence of T cell help activated “memory” B cells were able to produce anti-PrP^{C} specific antibodies. To address this question, PrP^{C}-specific memory B cells were sorted from vaccinated *Prnp*$^{0/0}$ mice and adoptively transferred into wild-type recipient mice. Upon VLP-PrP^{D111} challenge, no PrP^{C}-specific IgG titers were induced in the recipients. Nevertheless, several VLP-PrP^{D111} challenged recipient mice were protected against scrapie infection.

In conclusion, VLP were characterized as highly immunogenic vaccines that were used to elucidate various questions concerning adaptive immune response and basic mechanisms of PrP^{C}-specific tolerance vs. immunity. Remarkably, VLP-PrP^{D111} was able to induce native PrP^{C}-specific antibodies in wild-type mice but major difficulties associated with PrP^{C}-specific tolerance made efficacious scrapie vaccination impossible. New vaccination approaches are being tested to overcome these limitations.

7 German Summary

Prionkrankheiten sind tödlich verlaufende neurodegenerative Erkrankungen des zentralen Nervensystems. Der Erreger ist das infektiöse pathologisch gefaltete Prionen Protein PrP^{Sc}, welches durch Umfaltung des zellulären ubiquitär exprimierten Prionen Proteins PrP^{C} entsteht. Bis heute existieren keine erfolgreichen Therapiemöglichkeiten für Prionkrankheiten. Aus unterschiedlichen Zellkulturstudien ist jedoch bekannt, dass Antikörper, die gegen das zelluläre PrP^{C} gerichtet sind, eine PrP^{Sc} Ausbreitung verhindern können. Weiterhin zeigen Infektionsstudien in Mäusen, in denen passive Immunisierungen mit PrP^{C}-spezifischen Antikörpern vorgenommen wurden, eine Verlängerung der Inkubationszeit bis zum Ausbruch der Erkrankung.

In dieser Arbeit sollte untersucht werden, ob es möglich ist, durch eine aktive Immunisierung mit Virus-ähnlichen Partikeln (VLP) anti-PrP^{C} spezifische Antikörperantworten zu induzieren, die gegen Prionkrankheiten Schutz vermitteln können. Dazu wurde zuerst die Immunogenität von VLP bestimmt, um anschließend PrP^{C} exprimierende VLP als Antigene für PrP-Immunisierungen zu entwickeln.

Im ersten Teil dieser Arbeit wurden replikationsdefiziente VLP, die als fremdes Protein das Vesikuläre Stomatitis Virus Glykoprotein auf der Oberfläche exprimieren, hergestellt (VLP-VSV). VLP-VSV immunisierte Mäuse zeigten analog zu VSV infizierten Tieren T-Zell Hilfe unabhängige neutralisierende IgM Antikörperantworten und einen T-Zell Hilfe abhängigen Subklassenwechsel nach IgG. Interessanterweise ist nach VLP-VSV Immunisierung die frühe Induktion von neutralisierenden IgM Antikörpern unabhängig vom Typ I Interferon Rezeptor (IFNAR) Signalweg. Dagegen wird für den Subklassenwechsel nach IgG der IFNAR-Signalweg benötigt. Mäuse mit einer lymphozytenspezifischen IFNAR-Deletion zeigten nach VLP-VSV oder VSV Infektion IgM und IgG Antikörperantworten gegen VSV. Diese Beobachtungen zeigten, dass der Signalweg über den IFNAR auf Lymphozyten keine entscheidende Rolle bei der Induktion von VSV-neutralisierenden IgG Antikörpern spielte. Zusammenfassend ergab sich aus den Daten, dass VLP-

VSV Retropartikel starke Immunogene sind, geeignet um schützende Immunantworten gegen ein Modellvirus zu induzieren.

Im zweiten Teil der Arbeit wurden PrP^{C} exprimierende VLP hergestellt. Da der C-terminale Teil des Prionenproteins eine wichtige Rolle bei der Umfaltung von PrP^{C} nach PrP^{Sc} spielt, wurde die distale Domäne (Aminosäure 121-231) auf der Oberfläche von VLP exprimiert (VLP-PrP^{D111}). Die erfolgreiche Inkorporation von PrP111 auf VLP konnte mittels Elektronenmikroskopie gezeigt werden. Im nächsten Schritt wurden PrP-defiziente (*Prnp*$^{0/0}$) Mäuse mit VLP-PrP^{D111} immunisiert und auf PrP^{C}-spezifischen Antikörperantworten untersucht. Tatsächlich induzierte die Immunisierung mit VLP-PrP^{D111} starke Antikörperantworten mit hohen IgG Serum-Titern, die spezifisch die native Form des Prionen Proteins erkannten. Nach VLP-PrP^{D111} Immunisierung von Wildtyp Mäusen wurde eine Induktion von frühen IgM Antikörperantworten beobachtet, der Subklassenwechsel nach IgG erfolgte jedoch nur sehr schwach. Die induzierten IgG Antikörper zeigten eine geringe Affinität zu PrP und waren nicht lange im Serum nachweisbar. Eine mögliche Ursache hierfür ist die PrP^{C}-spezifische T-Zell Toleranz. Die Zugabe von unterschiedlichen Adjuvanzien zu VLP-PrP^{D111} verbesserte die IgG Antwort nicht. Als Ausnahme konnte in einzelnen Wildtyp Mäusen nach Immunisierung mit VLP-PrP^{D111} in „complete Freund´s Adjvant“ (CFA) IgG Antikörper detektiert werden, die bis zu 144 Tage nach der Immunisierung im Serum wiederzufinden waren. Zu einem späteren Zeitpunkt waren diese PrP^{C}-spezifischen Antikörper jedoch nicht mehr detektierbar.

Um die T-Zell Toleranz zu umgehen, wurden im nächsten Schritt unterschiedliche Retropartikel in verschiedenen Immunisierungsstrategien getestet. Im Einzelnen wurden verschiedene Typen von PrP-exprimierende HIV oder MLV Retropartikel in Primär- und Sekundärimmunisierungen eingesetzt oder VLP hergestellt, die zusätzlich zum Prion-Protein das VSV-G Protein als fremdes T-Helfer Epitop auf der Oberfläche exprimierten. Mit Hilfe dieser Immunisierungsansätze konnten jedoch keine verstärkten IgG Antikörperantworten in Wildtyp Mäusen erzielt werden.

In Zellkultur konnten die in *Prnp*$^{0/0}$ Mäusen induzierten PrP^{C}-spezifischen Antikörper den PrP^{Sc}-Gehalt in Prion-infizierten Zellen reduzieren. Die Seren der VLP-PrP^{D111} immunisierten Wildtyp Mäuse zeigten jedoch keinen Schutzeffekt. Im Weiteren wurde getestet, ob VLP-PrP^{D111} immunisierte Wildtyp Mäuse nach Inokulation eines Maus-adaptierten Scrapiestammes (RML 5.0) geschützt sind. Die VLP-PrP^{D111} immunisierten Mäuse erkrankten jedoch im gleichen Zeitraum wie nicht immunisierte Kontrolltiere.

Der letzte Teil dieser Arbeit beschäftigte sich mit der Frage, ob nach adoptivem Transfer von *Prnp*$^{0/0}$ B-Gedächtniszellen in Wildtyp Rezipienten eine Steigerung der PrP^{C}-spezifischen Immunantwort in Abwesenheit von T-Zellhilfe erzielt werden kann. Dazu wurden aus VLP-PrP^{D111} immunisierten *Prnp*$^{0/0}$ Mäusen B-Zellen isoliert und adoptiv in Wildtyp Rezipienten transferiert. Nach VLP-PrP^{D111}-Immunisierung der Wildtyp Rezipienten konnten keine erhöhten IgG Antikörper Titer beobachtet werden. Trotzdem waren einzelne Wildtyp Mäuse nach PrP^{Sc} Inokulation gegen Scrapie geschützt.

Zusammenfassend wurde in dieser Arbeit gezeigt, dass VLP-PrP^{D111} sehr gute Antigene sind, die durchaus eine Umgehung der PrP-spezifischen Toleranz erlauben. Im Vergleich zu anderen bisher beschriebenen PrP-spezifischen Antikörperantworten, die nach Immunisierung vorzugsweise lineare Epitope erkennen, induzierten VLP-PrP^{D111} Autoantikörperantworten, die gegen das native PrP^{C} Protein gerichtet sind. Schwierigkeiten bezüglich aktiver PrP-Immunisierungen liegen jedoch in der verbleibenden T-Zell Toleranz gegenüber PrP^{C}.

8 Appendix

8.1 Plasmid maps

8.1.1 pDPrP111

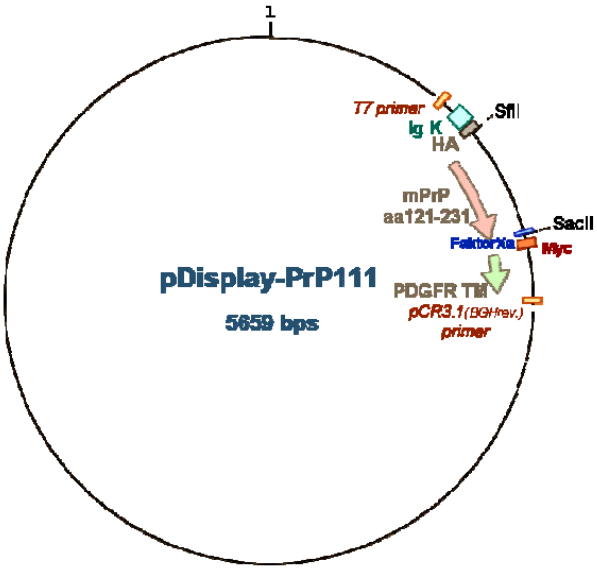

translated sequence

HA-Tag SfiI PrP-110

```
 800  tatccatatg atgttccaga ttatgctggg gcccagccgg ccaaagtggg gggccttggt ggctacatgc
        y  p  y   d  v  p   d  y  a  g   a  q  p   a  k  v   g  g  l  g   g  y  m

 870  tggggagcgc catgagcagg cccatgatcc attttggcaa cgactgggag gaccgctact accgtgaaaa
        l  g  s   a  m  s   r  p  m  i   h  f  g   n  d  w   e  d  r  y   y  r  e

 940  catgtaccgc taccctaacc aagtgtacta caggccagtg gatcagtaca gcaaccagaa caacttcgtg
        n  m  y   r  y  p   n  q  v  y   y  r  p   v  d  q   y  s  n  q   n  n  f  v

1010  cacgactgcg tcaatatcac catcaagcag cacacggtca ccaccaccac caaggggggag aacttcaccg
        h  d  c   v  n  i   t  i  k  q   h  t  v   t  t  t   t  k  g  e   n  f  t

1080  agaccgatgt gaagatgatg gagcgcgtgg tggagcagat gtgcgtcacc cagtaccaga aggagtccca
        e  t  d   v  k  m   m  e  r  v   v  e  q   m  c  v   t  q  y  q   k  e  s

                  Faktor Xa          SacII              myc epitop
1150  ggcctattac gacgggagaa gatccagcat cgagggaagg ccgcggctgc aggtcgacga acaaaaactc
        q  a  y   y  d  g   r  r  s  s   i  e  g   r  p  r   l  q  v  d   e  q  k  l

                  PDGFR-TM
1220  atctcagaag aggatctgaa tgctgtgggc caggacacgc aggaggtcat cgtggtgcca cactccttgc
        i  s  e   e  d  l   n  a  v  g   q  d  t   q  e  v   i  v  v  p   h  s  l

1290  cctttaaggt ggtggtgatc tcagccatcc tggccctggt ggtgctcacc atcatctccc ttatcatcct
        p  f  k   v  v  v   i  s  a  i   l  a  l   v  v  l   t  i  i  s   l  i  i

1360  catcatgctt tggcagaaga agccacgtta g
        l  i  m   l  w  q   k  k  p  r   -
```

8.1.2 pD-EGF and pmDG

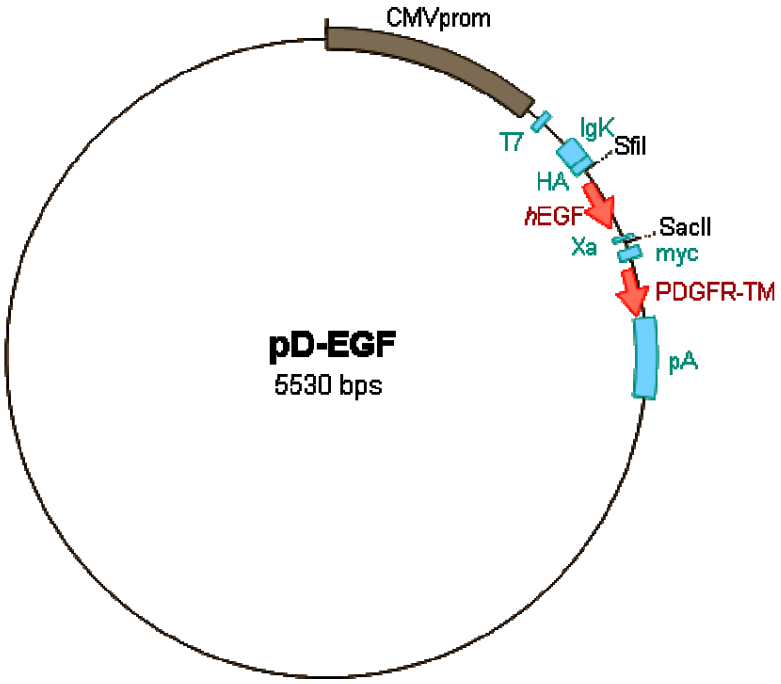

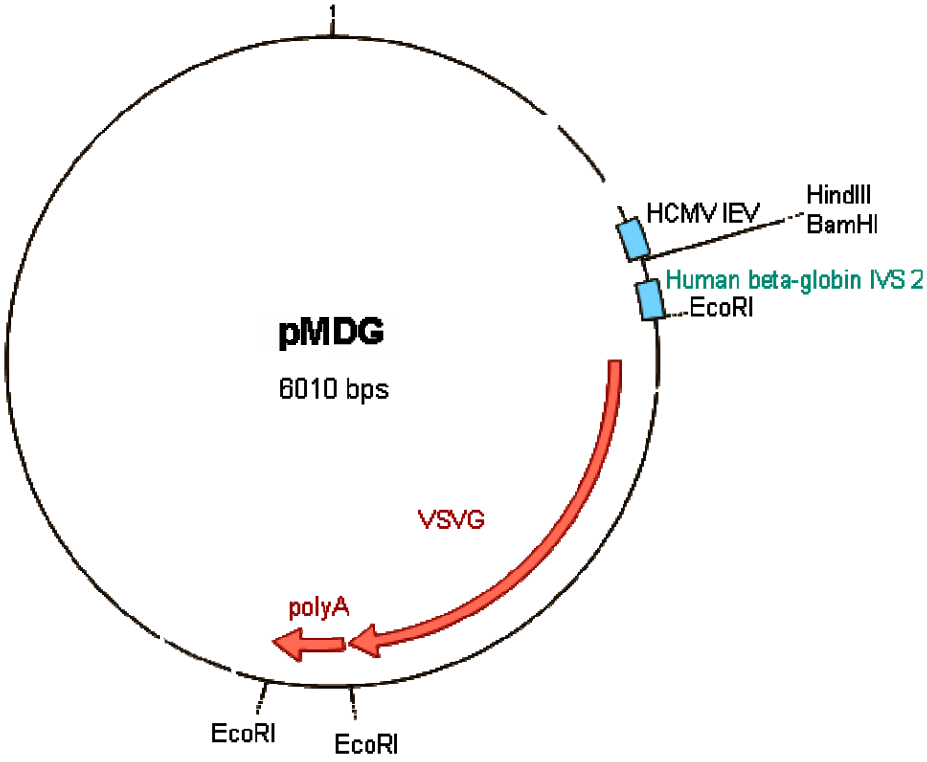

8.1.3 pHIT60 and pCMVΔR8.2

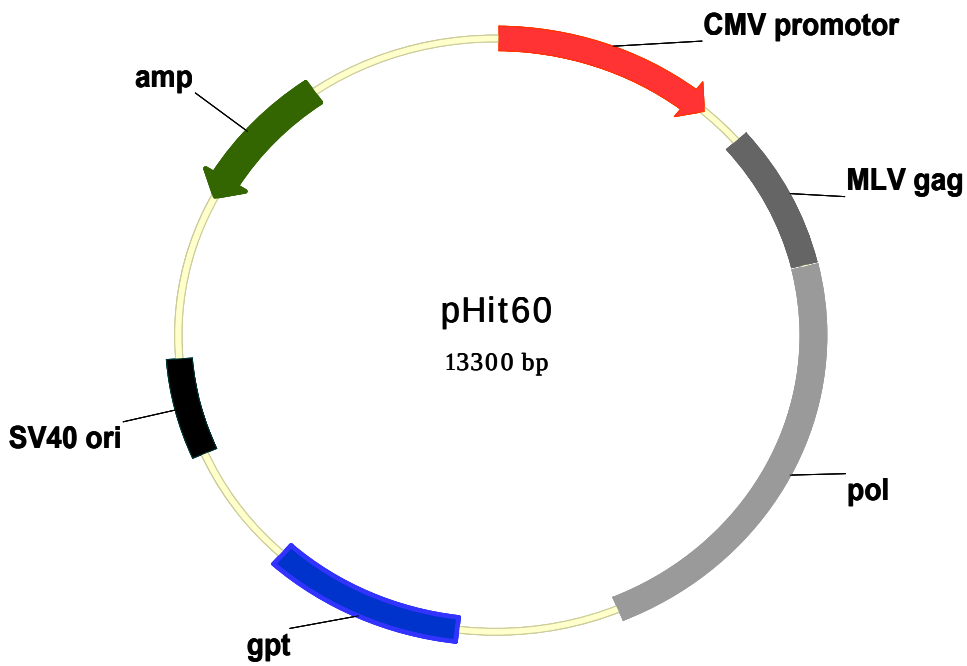

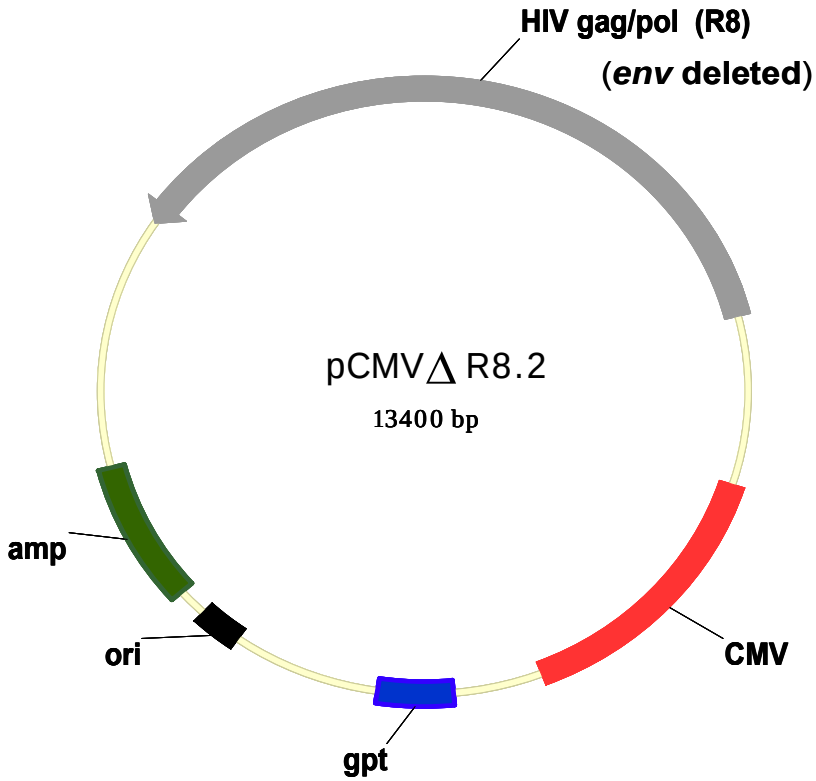

8.1.4 pRSETA mPrP(121-231)

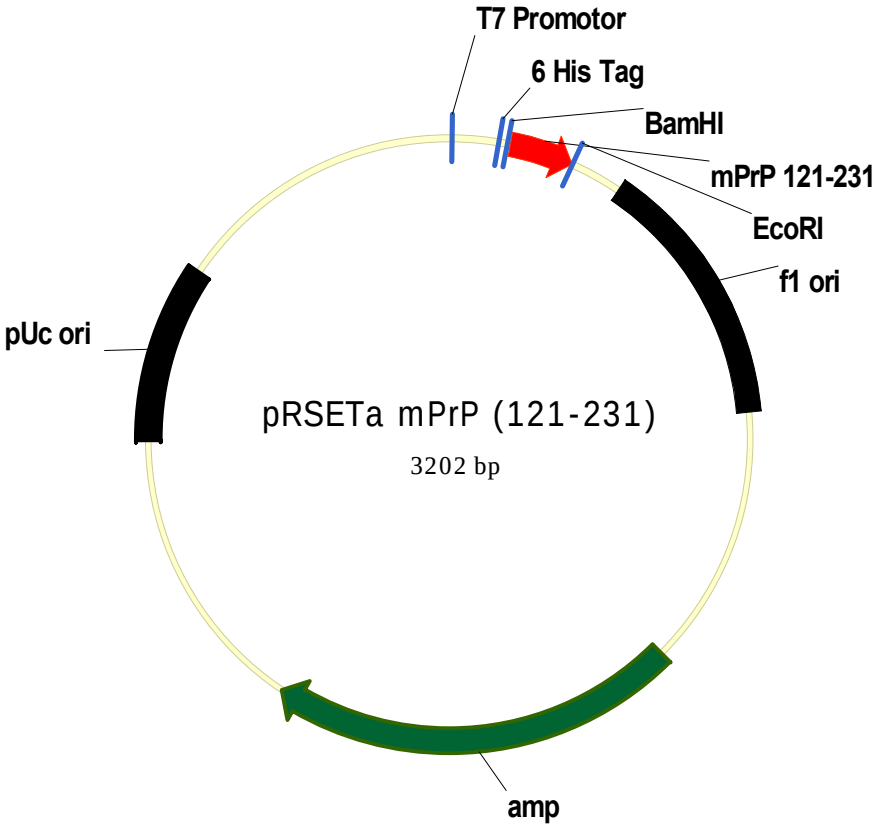

8.2 Abbreviations

%	Percentage
°C	Degree Celsius
µg	Microgram
6H4	PrP^C-specific monoclonal antibody
aa	Amino acid
Ab	Antibody
AD	Alzheimer's disease
APC	Antigen-presenting cell
Aq.dest	Aqua destillata
BCR	B cell receptor
BL/6	C57/BL/6 mice, immunocompetent black wild-type mice
bp	Base pair
BSA	Bovine serum albumin
BSE	Bovine spongiform encephalopathy
CD	Cluster of differentiation
CFA	Complete Freund´s adjuvant
CGG	Chicken gamma globulin
CJD	Creuzfeldt-Jakob disease
CMV	Cytomegali virus
CpG	Unmethylated structural element in DNA: cytidine-phosphate-guanosine
CR	Congo Red
CTL	Cytotoxic T lymphocytes
CWD	Chronic wasting disease
Cy	Cychrome
d	Days
d.p.i.	Days post infection
DC	Dendritic cell
DMEM	Dulbecco's modified Eagle's medium
DMSO	Dimethylsulfoxide
DNA	Desoxyribonucleic acid
E.coli	Escherichia coli
e.g.	For example
ECL	Enhanced Chemiluminescense
EDTA	Ethylenediamintetraacetat
Eenv	Envelope proteins
EGF	Epidermal growth factor
EGF^D	Epidermal growth factor fusion protein with platelet-derived growth factor receptor transmembrane domain
ELISA	Enzyme-linked immunosorbent assay
FACS	Fluorescence-activated cell sorting
FCS	Fetal calf serum
FDC	Follicular dendritic cell
FITC	Fluorescence isothiocyanate
FSC	Forward scatter in FACS, indicates particle size

g	Gram
g	Gravity
Gag	Group-specific antigens
GC	Germinal center
GPI	Glycosyl phosphatidyl inositol
h	Hours
HA	Immunological tag derived from hemagglutinine A
HEK 293FT	Human embryonic kidney cells, fast growing subclone
HEPES	2-(4-(2-Hydroxyetyl)-1piperazinyl) ethanesulfonic
HIV	Human immunodeficient virus
HRP	Horse radish peroxidase
i.c.	Intracerebral
i.e.	That is
i.n.	Intranasal
i.p.	Intraperitoneal
i.v.	Intravenous
IFA	Incomplete Freund’s adjuvant
IFN	Interferon
IFNAR	Interferon-α/ß receptor
Ig	Immunoglobulin
IL	Interleukin
IVC	Individually ventilated cage
kDa	Kilodalton
l	Liter
LD50	Lethal dose
LN	Lymph node
M	Matrix protein of VSV
M	Molar
mA	Milliampere
MACS	Magnetic adsorption cell sorting
mDC	Myeloid dendritic cell
mg	Milligram
MHC	Major histocompatibility complex
min	Minutes
ml	Millilitre
MLV	Murine leukemia virus
mM	Milimolar
mPrP	Murine prion protein
mPrP111	Murine prion protein containing amino acids121 to231
myc	Immunological tag derived from the human c-myc protooncogene
MZ	Marginal zone
MZB	Marginal zone B cell
N2a	Murine neuroblastoma cell line
NK	Natural killer cell
NP	Nuclear protein
N-terminal	Aminoterminal
OD	Optical density

OVA	Ovalbumin
p.a.	Pro analysis
p.c.	Post challenge
p30	MLV-derived capsid protein
PAMP	Pathogen-associated molecular pattern
PCR	Polymerase chain reaction
pDC	Plasmacytoid dendritic cell
PDGFR-TM	Platelet derived growth factor receptor transmembrane domain
PE	Phycoerythin
PEI	Paul-Ehrlich Institut
PFU	Plaque - forming unit
PK	Proteinase K
PNA	Peanut hemagglutinin
Prnp	Prion protein gene
$Prnp^{+/+}$	C57BL/6 wild-type mice
$Prnp^{0/0}$	PrP knockout mice
PrP	Prion protein
PrP^{C}	Cellular prion protein
PrP^{D111}	Prion protein aa121-231 fusion protein with platelet derived growth factor transmembrane domain
PrP^{Sc}	Pathogenic isoform of the prion protein
PVDF	Polyvinylidenedifluoride
REC	Recombinant
RML	Rocky Mountain Laboratory
RNA	Ribonuclei acid
RT	Reverse transcriptase
s.c.	Subcutaneous
SD	Standard deviation
SDS	Sodium dodecyl sulphate
SDS-PAGE	Sodium dodecyl sulphate polyacrylamid gelelectrophoresis
sec	Seconds
SEM	Standard error of the mean
SPF	Specific pathogen-free
SSC	Side scatter in FACS, indicates particle granularity
ssDNA	Single-stranded deoxynucleotide
SU	Soluble unit of the retroviral envelope protein
SV40	Simian virus 40
TBE	Tris borate EDTA
TBS	Tris buffer saline
TBST	Tris buffered saline/Tween 20
TCR	T cell receptor
TD	T cell-dependent
tg	Transgenic
Th	T helper cell
TI	T cell-independent
TLR	Toll-like receptor
TM	Transmembrane domain of the retroviral envelope protein

TSE	Transmissible spongiform encephalopathies
TZ	T cell zone
U	Unit
UK	United kingdom
UV	Ultraviolet
VLP	Virus-like particles
Vs.	Versus
VSV	Vesicular stomatitis virus
VSV-G	Glycoprotein of vesicular stomatitis virus
WT	Wild-type

8.3 Index of tables and figures

Tables:

Figures:

9 References

Abate DA, Watanabe S, Mocarski ES. (2004) Major human cytomegalovirus structural protein pp65 (ppUL83) prevents interferon response factor 3 activation in the interferon response. *J.Virol.* **78**, 10995-11006.

Adelstein S, Pritchard-Briscoe H, Anderson TA, Crosbie J, Gammon G, Loblay RH et al. (1991) Induction of self-tolerance in T cells but not B cells of transgenic mice expressing little self antigen. *Science* **251**, 1223-1225.

Aguzzi A, Heppner FL, Heikenwalder M, Prinz M, Mertz K, Seeger H et al. (2003) Immune system and peripheral nerves in propagation of prions to CNS. *Br.Med.Bull.* **66**, 141-159.

Aguzzi A, Montrasio F, Kaeser PS. (2001) Prions: health scare and biological challenge. *Nat.Rev.Mol.Cell Biol.* **2**, 118-126.

Aichele P, Unsoeld H, Koschella M, Schweier O, Kalinke U, Vucikuja S. (2006) CD8 T cells specific for lymphocytic choriomeningitis virus require type I IFN receptor for clonal expansion
1. *J.Immunol.* **176**, 4525-4529.

Akira S and Takeda K. (2004) Toll-like receptor signalling. *Nat.Rev.Immunol.* **4**, 499-511.

Alper T, Cramp WA, Haig DA, Clarke MC. (1967) Does the agent of scrapie replicate without nucleic acid? *Nature* **214**, 764-766.

Arbel M, Lavie V, Solomon B. (2003) Generation of antibodies against prion protein in wild-type mice via helix 1 peptide immunization. *J.Neuroimmunol.* **144**, 38-45.

Asselin-Paturel C and Trinchieri G. (2005) Production of type I interferons: plasmacytoid dendritic cells and beyond. *J.Exp.Med.* **202**, 461-465.

Aucouturier P, Geissmann F, Damotte D, Saborio GP, Meeker HC, Kascsak R et al. (2001) Infected splenic dendritic cells are sufficient for prion transmission to the CNS in mouse scrapie. *J.Clin.Invest* **108**, 703-708.

Bach EA, Aguet M, Schreiber RD. (1997) The IFN gamma receptor: a paradigm for cytokine receptor signaling. *Annu.Rev.Immunol.* **15**, 563-591.

Bach P, Kamphuis E, Odermatt B, Sutter G, Buchholz CJ, Kalinke U. (2007) Vesicular stomatitis virus glycoprotein displaying retrovirus-like particles induce a type I IFN receptor-dependent switch to neutralizing IgG antibodies. *J.Immunol.* **178**, 5839-5847.

Bachmann MF, Hengartner H, Zinkernagel RM. (1995) T helper cell-independent neutralizing B cell response against vesicular stomatitis virus: role of antigen patterns in B cell induction? *Eur.J.Immunol.* **25**, 3445-3451.

Bachmann MF, Kundig TM, Kalberer CP, Hengartner H, Zinkernagel RM. (1994) How many specific B cells are needed to protect against a virus? *J.Immunol.* **152**, 4235-4241.

Bachmann MF, Odermatt B, Hengartner H, Zinkernagel RM. (1996) Induction of long-lived germinal centers associated with persisting antigen after viral infection. *J.Exp.Med.* **183**, 2259-2269.

Bachmann MF, Rohrer UH, Kundig TM, Burki K, Hengartner H, Zinkernagel RM. (1993) The influence of antigen organization on B cell responsiveness. *Science* **262**, 1448-1451.

Bachmann MF and Zinkernagel RM. (1996) The influence of virus structure on antibody responses and virus serotype formation. *Immunol.Today* **17**, 553-558.

Bachmann MF and Zinkernagel RM. (1997) Neutralizing antiviral B cell responses. *Annu.Rev.Immunol.* **15**, 235-270.

Barchet W, Cella M, Odermatt B, Asselin-Paturel C, Colonna M, Kalinke U. (2002) Virus-induced interferon alpha production by a dendritic cell subset in the absence of feedback signaling in vivo. *J.Exp.Med.* **195**, 507-516.

Barchet W, Krug A, Cella M, Newby C, Fischer JA, Dzionek A et al. (2005) Dendritic cells respond to influenza virus through. *Eur.J.Immunol.* **35**, 236-242.

Berek C, Berger A, Apel M. (1991) Maturation of the immune response in germinal centers. *Cell* **67**, 1121-1129.

Beringue V, Vilette D, Mallinson G, Archer F, Kaisar M, Tayebi M et al. (2004) PrPSc binding antibodies are potent inhibitors of prion replication in cell lines. *J.Biol.Chem.* **279**, 39671-39676.

Bessen RA and Marsh RF. (1994) Distinct PrP properties suggest the molecular basis of strain variation in transmissible mink encephalopathy. *J.Virol.* **68**, 7859-7868.

Boswell HS, Nerenberg MI, Scher I, Singer A. (1980) Role of accessory cells in B cell activation. III. Cellular analysis of primary immune response deficits in CBA/N mice: presence of an accessory cell-B cell interaction defect 221. *J.Exp.Med.* **152**, 1194-1309.

Branca AA and Baglioni C. (1981) Evidence that types I and II interferons have different receptors. *Nature* **294**, 768-770.

Braun D, Caramalho I, Demengeot J. (2002) IFN-alpha/beta enhances BCR-dependent B cell responses

1. *Int.Immunol.* **14**, 411-419.

Bretscher P and Cohn M. (1970) A theory of self-nonself discrimination. *Science* **169**, 1042-1049.

Broderson JR. (1989) A retrospective review of lesions associated with the use of Freund's adjuvant. *Lab Anim Sci.* **39**, 400-405.

Buchholz CJ, Bach P, Nikles D, Kalinke U. (2006) Prion protein-specific antibodies for therapeutic intervention of transmissible spongiform encephalopathies. *Expert.Opin.Biol.Ther.* **6**, 293-300.

Bueler H, Aguzzi A, Sailer A, Greiner RA, Autenried P, Aguet M et al. (1993) Mice devoid of PrP are resistant to scrapie. *Cell* **73**, 1339-1347.

Bueler H, Fischer M, Lang Y, Bluethmann H, Lipp HP, DeArmond SJ et al. (1992) Normal development and behaviour of mice lacking the neuronal cell-surface PrP protein. *Nature* **356**, 577-582.

Cao W and Liu YJ. (2007) Innate immune functions of plasmacytoid dendritic cells. *Curr.Opin.Immunol.* **19**, 24-30.

Chackerian B, Lenz P, Lowy DR, Schiller JT. (2002) Determinants of autoantibody induction by conjugated papillomavirus virus-like particles. *J.Immunol.* **169**, 6120-6126.

Chackerian B, Lowy DR, Schiller JT. (2001) Conjugation of a self-antigen to papillomavirus-like particles allows for efficient induction of protective autoantibodies. *J.Clin.Invest* **108**, 415-423.

Charan S and Zinkernagel RM. (1986) Antibody mediated suppression of secondary IgM response in nude mice against vesicular stomatitis virus. *J.Immunol.* **136**, 3057-3061.

Chen J, Baig E, Fish EN. (2004) Diversity and relatedness among the type I interferons. *J.Interferon Cytokine Res.* **24**, 687-698.

Cohen FE and Prusiner SB. (1998) Pathologic conformations of prion proteins. *Annu.Rev.Biochem.* **67**, 793-819.

Coligan JE, Bierer BE, Margulies DH, Shevach EM, and and Warren Strober. (1991). Current Protocols in Immunology. John Wiley and Sons Inc.

Collinge J and Palmer MS. (1994) Molecular genetics of human prion diseases. *Philos.Trans.R.Soc.Lond B Biol.Sci.* **343**, 371-378.

Colonna M, Trinchieri G, Liu YJ. (2004) Plasmacytoid dendritic cells in immunity. *Nat.Immunol.* **5**, 1219-1226.

Coombes JL, Robinson NJ, Maloy KJ, Uhlig HH, Powrie F. (2005) Regulatory T cells and intestinal homeostasis. *Immunol.Rev.* **204**, 184-194.

Coro ES, Chang WL, Baumgarth N. (2006) Type I IFN receptor signals directly stimulate local B cells early following influenza virus infection. *J.Immunol.* **176**, 4343-4351.

Coutelier JP, van der Logt JT, Heessen FW, Warnier G, Van Snick J. (1987) IgG2a restriction of murine antibodies elicited by viral infections. *J.Exp.Med.* **165**, 64-69.

Creuzfeldt HG. (1920) Über eine eigenartige Erkrankung des Zentralnervensystems. *Vorläufige Mitteilung.Z.f.d.ges.Neurol.und Psych.,* 1-18.

Cronin J, Zhang XY, Reiser J. (2005) Altering the tropism of lentiviral vectors through pseudotyping. *Curr.Gene Ther.* **5**, 387-398.

Dauber B, Heins G, Wolff T. (2004) The influenza B virus nonstructural NS1 protein is essential for efficient viral growth and antagonizes beta interferon induction. *J.Virol.* **78**, 1865-1872.

Deml L, Aigner M, Decker J, Eckhardt A, Schutz C, Mittl PR et al. (2005) Characterization of the Helicobacter pylori cysteine-rich protein A as a T-helper cell type 1 polarizing agent. *Infect.Immun.* **73**, 4732-4742.

Deml L, Speth C, Dierich MP, Wolf H, Wagner R. (2005) Recombinant HIV-1 Pr55gag virus-like particles: potent stimulators of innate and acquired immune responses. *Mol.Immunol.* **42**, 259-277.

Dietschhold B, Rupprecht CE, Fu ZF, and Koprowski H. (1996). Rhabdoviruses. Fields, B. N., Knipe D.M., and Howley P.M. Lippincott-Raven Publishers, Philadelphia.

DiPerna G, Stack J, Bowie AG, Boyd A, Kotwal G, Zhang Z et al. (2004) Poxvirus protein N1L targets the I-kappaB kinase complex, inhibits signaling to NF-kappaB by the tumor necrosis factor superfamily of receptors, and inhibits NF-kappaB and IRF3 signaling by toll-like receptors. *J.Biol.Chem.* **279**, 36570-36578.

Donofrio G, Heppner FL, Polymenidou M, Musahl C, Aguzzi A. (2005) Paracrine inhibition of prion propagation by anti-PrP single-chain Fv miniantibodies. *J.Virol.* **79**, 8330-8338.

Ehrlich P. and Morgenroth J. (1957) On haemolysins. *The Collected Papers of Paul-Ehrlich* **2**, 246-255.

Enari M, Flechsig E, Weissmann C. (2001) Scrapie prion protein accumulation by scrapie-infected neuroblastoma cells abrogated by exposure to a prion protein antibody. *Proc.Natl.Acad.Sci.U.S.A* **98**, 9295-9299.

Fagarasan S and Honjo T. (2000) T-Independent immune response: new aspects of B cell biology. *Science* **290**, 89-92.

Fehr T, Bachmann MF, Bucher E, Kalinke U, Di Padova FE, Lang AB et al. (1997) Role of repetitive antigen patterns for induction of antibodies against antibodies. *J.Exp.Med.* **185**, 1785-1792.

Feraudet C, Morel N, Simon S, Volland H, Frobert Y, Creminon C et al. (2005) Screening of 145 anti-PrP monoclonal antibodies for their capacity to inhibit PrPSc replication in infected cells. *J.Biol.Chem.* **280**, 11247-11258.

Fink K, Lang KS, Manjarrez-Orduno N, Junt T, Senn BM, Holdener M et al. (2006) Early type I interferon-mediated signals on B cells specifically enhance antiviral humoral responses. *Eur.J.Immunol.*

Fischer M, Rulicke T, Raeber A, Sailer A, Moser M, Oesch B et al. (1996) Prion protein (PrP) with amino-proximal deletions restoring susceptibility of PrP knockout mice to scrapie. *EMBO J.* **15**, 1255-1264.

Fontenot JD and Rudensky AY. (2005) A well adapted regulatory contrivance: regulatory T cell development and the forkhead family transcription factor Foxp3. *Nat.Immunol.* **6**, 331-337.

Ford MJ, Burton LJ, Morris RJ, Hall SM. (2002) Selective expression of prion protein in peripheral tissues of the adult mouse. *Neuroscience* **113**, 177-192.

Foy E, Li K, Wang C, Sumpter R, Jr., Ikeda M, Lemon SM et al. (2003) Regulation of interferon regulatory factor-3 by the hepatitis C virus serine protease. *Science* **300**, 1145-1148.

Freund J. (1956) The mode of action of immunologic adjuvants. *Bibl.Tuberc.* 130-148.

Gajdusek DC. (1977) Unconventional viruses and the origin and disappearance of kuru. *Science* **197**, 943-960.

Gatto D, Ruedl C, Odermatt B, Bachmann MF. (2004) Rapid response of marginal zone B cells to viral particles. *J.Immunol.* **173**, 4308-4316.

Gavin AL, Hoebe K, Duong B, Ota T, Martin C, Beutler B et al. (2006) Adjuvant-enhanced antibody responses in the absence of toll-like receptor signaling. *Science* **314**, 1936-1938.

Gay D, Saunders T, Camper S, Weigert M. (1993) Receptor editing: an approach by autoreactive B cells to escape tolerance. *J.Exp.Med.* **177**, 999-1008.

Gerstmann J, Straussler E, and Schenker I. (1936) Über eine eigenartige hereditär-familiäre Erkrankung des Zentralnervensystems. Zugleich ein Beitrag

zur Frage des vorzeitigen lokalen Alterns. *Zeitschrift für die gesamte Neurologie und Psychiatrie* **154**, 736-762.

Gilch S, Wopfner F, Renner-Muller I, Kremmer E, Bauer C, Wolf E et al. (2003) Polyclonal anti-PrP auto-antibodies induced with dimeric PrP interfere efficiently with PrPSc propagation in prion-infected cells. *J.Biol.Chem.* **278**, 18524-18531.

Gobet R, Cerny A, Ruedi E, Hengartner H, Zinkernagel RM. (1988) The role of antibodies in natural and acquired resistance of mice to vesicular stomatitis virus. *Exp.Cell Biol.* **56**, 175-180.

Goni F, Knudsen E, Schreiber F, Scholtzova H, Pankiewicz J, Carp R et al. (2005) Mucosal vaccination delays or prevents prion infection via an oral route. *Neuroscience* **133**, 413-421.

Goodnow CC, Crosbie J, Adelstein S, Lavoie TB, Smith-Gill SJ, Brink RA et al. (1988) Altered immunoglobulin expression and functional silencing of self-reactive B lymphocytes in transgenic mice. *Nature* **334**, 676-682.

Goodnow CC, Sprent J, Fazekas de St GB, Vinuesa CG. (2005) Cellular and genetic mechanisms of self tolerance and autoimmunity. *Nature* **435**, 590-597.

Griffith JS. (1967) Self-replication and scrapie. *Nature* **215**, 1043-1044.

Hammarstedt M and Garoff H. (2004) Passive and active inclusion of host proteins in human immunodeficiency virus type 1 gag particles during budding at the plasma membrane. *J.Virol.* **78**, 5686-5697.

Hammarstedt M, Wallengren K, Pedersen KW, Roos N, Garoff H. (2000) Minimal exclusion of plasma membrane proteins during retroviral envelope formation. *Proc.Natl.Acad.Sci.U.S.A* **97**, 7527-7532.

Hanan E, Goren O, Eshkenazy M, Solomon B. (2001) Immunomodulation of the human prion peptide 106-126 aggregation. *Biochem.Biophys.Res.Commun.* **280**, 115-120.

Hanan E, Priola SA, Solomon B. (2001) Antiaggregating antibody raised against human PrP 106-126 recognizes pathological and normal isoforms of the whole prion protein. *Cell Mol.Neurobiol.* **21**, 693-703.

Handisurya A, Gilch S, Winter D, Shafti-Keramat S, Maurer D, Schatzl HM et al. (2007) Vaccination with prion peptide-displaying papillomavirus-like particles induces autoantibodies to normal prion protein that interfere with pathologic prion protein production in infected cells. *FEBS J.* **274**, 1747-1758.

Hartley SB, Crosbie J, Brink R, Kantor AB, Basten A, Goodnow CC. (1991) Elimination from peripheral lymphoid tissues of self-reactive B lymphocytes recognizing membrane-bound antigens. *Nature* **353**, 765-769.

Head MW and Ironside JW. (2000) Inhibition of prion-protein conversion: a therapeutic tool? *Trends Microbiol.* **8**, 6-8.

Hebeis BJ, Klenovsek K, Rohwer P, Ritter U, Schneider A, Mach M et al. (2004) Activation of virus-specific memory B cells in the absence of T cell help. *J.Exp.Med.* **199**, 593-602.

Heikenwalder M, Polymenidou M, Junt T, Sigurdson C, Wagner H, Akira S et al. (2004) Lymphoid follicle destruction and immunosuppression after repeated CpG oligodeoxynucleotide administration. *Nat.Med.* **10**, 187-192.

Heppner FL and Aguzzi A. (2004) Recent developments in prion immunotherapy. *Curr.Opin.Immunol.* **16**, 594-598.

Heppner FL, Musahl C, Arrighi I, Klein MA, Rulicke T, Oesch B et al. (2001) Prevention of scrapie pathogenesis by transgenic expression of anti-prion protein antibodies. *Science* **294**, 178-182.

Holan V, Kohno K, Minowada J. (1991) Natural human interferon-alpha augments interleukin-2 production by a direct action on the activated IL-2-producing T cells. *J.Interferon Res.* **11**, 319-325.

Hornshaw MP, McDermott JR, Candy JM. (1995) Copper binding to the N-terminal tandem repeat regions of mammalian and avian prion protein 2. *Biochem.Biophys.Res.Commun.* **207**, 621-629.

Isaacs A and Lindenmann J. (1987) Virus interference. I. The interferon. By A. Isaacs and J. Lindenmann, 1957. *J.Interferon Res.* **7**, 429-438.

Jacob J, Kelsoe G, Rajewsky K, Weiss U. (1991) Intraclonal generation of antibody mutants in germinal centres. *Nature* **354**, 389-392.

Jego G, Palucka AK, Blanck JP, Chalouni C, Pascual V, Banchereau J. (2003) Plasmacytoid dendritic cells induce plasma cell differentiation through type I interferon and interleukin 6. *Immunity.* **19**, 225-234.

Kalinke U, Bucher EM, Ernst B, Oxenius A, Roost HP, Geley S et al. (1996) The role of somatic mutation in the generation of the protective humoral immune response against vesicular stomatitis virus. *Immunity.* **5**, 639-652.

Kamphuis E, Junt T, Waibler Z, Forster R, Kalinke U. (2006) Type I interferons directly regulate lymphocyte recirculation and cause transient blood lymphopenia. *Blood* **108**, 3253-3261.

Kato H, Sato S, Yoneyama M, Yamamoto M, Uematsu S, Matsui K et al. (2005) Cell type-specific involvement of RIG-I in antiviral response. *Immunity.* **23**, 19-28.

Kawai T and Akira S. (2006) Innate immune recognition of viral infection. *Nat.Immunol.* **7**, 131-137.

Kawai T and Akira S. (2006) [Role of IPS-1 in type I IFN induction]. *Nippon Rinsho* **64**, 1231-1235.

Kawai T and Akira S. (2007) Antiviral signaling through pattern recognition receptors. *J.Biochem.(Tokyo)* **141**, 137-145.

Kim CL, Karino A, Ishiguro N, Shinagawa M, Sato M, Horiuchi M. (2004) Cell-surface retention of PrPC by anti-PrP antibody prevents protease-resistant PrP formation. *J.Gen.Virol.* **85**, 3473-3482.

Klaus SJ, Berberich I, Shu G, Clark EA. (1994) CD40 and its ligand in the regulation of humoral immunity. *Semin.Immunol.* **6**, 279-286.

Klein MA, Frigg R, Flechsig E, Raeber AJ, Kalinke U, Bluethmann H et al. (1997) A crucial role for B cells in neuroinvasive scrapie. *Nature* **390**, 687-690.

Kocisko DA, Come JH, Priola SA, Chesebro B, Raymond GJ, Lansbury PT et al. (1994) Cell-free formation of protease-resistant prion protein. *Nature* **370**, 471-474.

Koller MF, Grau T, Christen P. (2002) Induction of antibodies against murine full-length prion protein in wild-type mice. *J.Neuroimmunol.* **132**, 113-116.

Kolumam GA, Thomas S, Thompson LJ, Sprent J, Murali-Krishna K. (2005) Type I interferons act directly on CD8 T cells to allow clonal expansion and memory formation in response to viral infection. *J.Exp.Med.* **202**, 637-650.

Kozlovska TM, Cielens I, Vasiljeva I, Strelnikova A, Kazaks A, Dislers A et al. (1996) RNA phage Q beta coat protein as a carrier for foreign epitopes. *Intervirology* **39**, 9-15.

Kretzschmar HA. (1993) Human prion diseases (spongiform encephalopathies). *Arch.Virol.Suppl* **7**, 261-293.

Laemmli UK. (1970) Cleavage of structural proteins during the assembly of the head of bacteriophage T4. *Nature* **227**, 680-685.

Lahl K, Loddenkemper C, Drouin C, Freyer J, Arnason J, Eberl G et al. (2007) Selective depletion of Foxp3+ regulatory T cells induces a scurfy-like disease. *J.Exp.Med.* **204**, 57-63.

Lamken P, Lata S, Gavutis M, Piehler J. (2004) Ligand-induced assembling of the type I interferon receptor on supported lipid bilayers. *J.Mol.Biol.* **341**, 303-318.

Le Bon A, Durand V, Kamphuis E, Thompson C, Bulfone-Paus S, Rossmann C et al. (2006a) Direct stimulation of T cells by type I IFN enhances the CD8+ T cell response during cross-priming
9. *J.Immunol.* **176**, 4682-4689.

Le Bon A, Etchart N, Rossmann C, Ashton M, Hou S, Gewert D et al. (2003) Cross-priming of CD8+ T cells stimulated by virus-induced type I interferon. *Nat.Immunol.* **4**, 1009-1015.

Le Bon A, Schiavoni G, D'Agostino G, Gresser I, Belardelli F, Tough DF. (2001) Type i interferons potently enhance humoral immunity and can promote isotype switching by stimulating dendritic cells in vivo. *Immunity.* **14**, 461-470.

Le Bon A, Thompson C, Kamphuis E, Durand V, Rossmann C, Kalinke U et al. (2006) Cutting edge: enhancement of antibody responses through direct stimulation of B and T cells by type I IFN. *J.Immunol.* **176**, 2074-2078.

Leist TP, Cobbold SP, Waldmann H, Aguet M, Zinkernagel RM. (1987) Functional analysis of T lymphocyte subsets in antiviral host defense. *J.Immunol.* **138**, 2278-2281.

Lund JM, Alexopoulou L, Sato A, Karow M, Adams NC, Gale NW et al. (2004) Recognition of single-stranded RNA viruses by Toll-like receptor 7. *Proc.Natl.Acad.Sci.U.S.A* **101**, 5598-5603.

Lutfalla G, Gardiner K, Proudhon D, Vielh E, Uze G. (1992) The structure of the human interferon alpha/beta receptor gene. *J.Biol.Chem.* **267**, 2802-2809.

MacLennan IC. (1994) Germinal centers. *Annu.Rev.Immunol.* **12**, 117-139.

Malmgaard L, Salazar-Mather TP, Lewis CA, Biron CA. (2002) Promotion of alpha/beta interferon induction during in vivo viral infection through alpha/beta interferon receptor/STAT1 system-dependent and -independent pathways. *J.Virol.* **76**, 4520-4525.

Marrack P, Kappler J, Mitchell T. (1999) Type I interferons keep activated T cells alive. *J.Exp.Med.* **189**, 521-530.

Marsh RF and Bessen RA. (1993) Epidemiologic and experimental studies on transmissible mink encephalopathy. *Dev.Biol.Stand.* **80**, 111-118.

Martin F and Kearney JF. (2000) B-cell subsets and the mature preimmune repertoire. Marginal zone and B1 B cells as part of a "natural immune memory". *Immunol.Rev.* **175**, 70-79.

McAdam AJ, Farkash EA, Gewurz BE, Sharpe AH. (2000) B7 costimulation is critical for antibody class switching and CD8(+) cytotoxic T-lymphocyte generation in the host response to vesicular stomatitis virus. *J.Virol.* **74**, 203-208.

McCluskie MJ, Wen YM, Di Q, Davis HL. (1998) Immunization against hepatitis B virus by mucosal administration of antigen-antibody complexes. *Viral Immunol.* **11**, 245-252.

McGowan JP. (1922) Scrapie in sheep. *Scott J.Agric* **5**, 365-375.

Merten CA, Engelstaedter M, Buchholz CJ, Cichutek K. (2003) Displaying epidermal growth factor on spleen necrosis virus-derived targeting vectors. *Virology* **305**, 106-114.

Meylan E, Tschopp J, Karin M. (2006) Intracellular pattern recognition receptors in the host response. *Nature* **442**, 39-44.

Miyamoto K, Nakamura N, Aosasa M, Nishida N, Yokoyama T, Horiuchi H et al. (2005) Inhibition of prion propagation in scrapie-infected mouse neuroblastoma cell lines using mouse monoclonal antibodies against prion protein. *Biochem.Biophys.Res.Commun.* **335**, 197-204.

Mond JJ, Lees A, Snapper CM. (1995) T cell-independent antigens type 2. *Annu.Rev.Immunol.* **13**, 655-692.

Muller U, Steinhoff U, Reis LF, Hemmi S, Pavlovic J, Zinkernagel RM et al. (1994) Functional role of type I and type II interferons in antiviral defense. *Science* **264**, 1918-1921.

Naldini L, Blomer U, Gallay P, Ory D, Mulligan R, Gage FH et al. (1996) In vivo gene delivery and stable transduction of nondividing cells by a lentiviral vector. *Science* **272**, 263-267.

Nemazee DA and Burki K. (1989) Clonal deletion of B lymphocytes in a transgenic mouse bearing anti-MHC class I antibody genes. *Nature* **337**, 562-566.

Nikles D, Bach P, Boller K, Merten CA, Montrasio F, Heppner FL et al. (2005) Circumventing tolerance to the prion protein (PrP): vaccination with PrP-displaying retrovirus particles induces humoral immune responses against the native form of cellular PrP. *J.Virol.* **79**, 4033-4042.

Nishida N, Harris DA, Vilette D, Laude H, Frobert Y, Grassi J et al. (2000) Successful transmission of three mouse-adapted scrapie strains to murine neuroblastoma cell lines overexpressing wild-type mouse prion protein. *J.Virol.* **74**, 320-325.

Nossal GJ. (1994) Differentiation of the secondary B-lymphocyte repertoire: the germinal center reaction. *Immunol.Rev.* **137**, 173-183.

Ochsenbein AF, Pinschewer DD, Odermatt B, Carroll MC, Hengartner H, Zinkernagel RM. (1999) Protective T cell-independent antiviral antibody responses are dependent on complement
218. *J.Exp.Med.* **190**, 1165-1174.

Paramithiotis E, Pinard M, Lawton T, LaBoissiere S, Leathers VL, Zou WQ et al. (2003) A prion protein epitope selective for the pathologically misfolded conformation. *Nat.Med.* **9**, 893-899.

Parry HB. (1983). Historical, clinical, epidemiological, pathological and practical aspects of the natural disease. Academic Press, London.

Pasare C and Medzhitov R. (2005) Control of B-cell responses by Toll-like receptors. *Nature* **438**, 364-368.

Peretz D, Williamson RA, Kaneko K, Vergara J, Leclerc E, Schmitt-Ulms G et al. (2001) Antibodies inhibit prion propagation and clear cell cultures of prion infectivity. *Nature* **412**, 739-743.

Perrier V, Solassol J, Crozet C, Frobert Y, Mourton-Gilles C, Grassi J et al. (2004) Anti-PrP antibodies block PrPSc replication in prion-infected cell cultures by accelerating PrPC degradation. *J.Neurochem.* **89**, 454-463.

Pestka S, Krause CD, Walter MR. (2004) Interferons, interferon-like cytokines, and their receptors. *Immunol.Rev.* **202**, 8-32.

Petricoin EF, III, Ito S, Williams BL, Audet S, Stancato LF, Gamero A et al. (1997) Antiproliferative action of interferon-alpha requires components of T-cell-receptor signalling. *Nature* **390**, 629-632.

Ploegh HL. (1998) Viral strategies of immune evasion. *Science* **280**, 248-253.

Polymenidou M, Heppner FL, Pellicioli EC, Urich E, Miele G, Braun N et al. (2004) Humoral immune response to native eukaryotic prion protein correlates with anti-prion protection. *Proc.Natl.Acad.Sci.U.S.A* **101 Suppl 2**, 14670-14676.

Proietti E, Bracci L, Puzelli S, Di Pucchio T, Sestili P, De Vincenzi E et al. (2002) Type I IFN as a natural adjuvant for a protective immune response: lessons from the influenza vaccine model. *J.Immunol.* **169**, 375-383.

Prusiner SB, Bolton DC, Groth DF, Bowman KA, Cochran SP, McKinley MP. (1982) Further purification and characterization of scrapie prions. *Biochemistry* **21**, 6942-6950.

Pumpens P and Grens E. (2001) HBV core particles as a carrier for B cell/T cell epitopes. *Intervirology* **44**, 98-114.

Pyra H, Boni J, Schupbach J. (1994) Ultrasensitive retrovirus detection by a reverse transcriptase assay based on product enhancement. *Proc.Natl.Acad.Sci.U.S.A* **91**, 1544-1548.

Raeber AJ, Sailer A, Hegyi I, Klein MA, Rulicke T, Fischer M et al. (1999) Ectopic expression of prion protein (PrP) in T lymphocytes or hepatocytes of PrP knockout mice is insufficient to sustain prion replication. *Proc.Natl.Acad.Sci.U.S.A* **96**, 3987-3992.

Richt JA, Kasinathan P, Hamir AN, Castilla J, Sathiyaseelan T, Vargas F et al. (2007) Production of cattle lacking prion protein. *Nat.Biotechnol.* **25**, 132-138.

Riek R, Hornemann S, Wider G, Billeter M, Glockshuber R, Wuthrich K. (1996) NMR structure of the mouse prion protein domain PrP(121-321). *Nature* **382**, 180-182.

Roost HP, Haag A, Burkhart C, Zinkernagel RM, Hengartner H. (1996) Mapping of the dominant neutralizing antigenic site of a virus using infected cells. *J.Immunol.Methods* **189**, 233-242.

Rosset MB, Ballerini C, Gregoire S, Metharom P, Carnaud C, Aucouturier P. (2004) Breaking Immune Tolerance to the Prion Protein Using Prion Protein Peptides Plus Oligodeoxynucleotide-CpG in Mice. *J.Immunol.* **172**, 5168-5174.

Rudyk H, Vasiljevic S, Hennion RM, Birkett CR, Hope J, Gilbert IH. (2000) Screening Congo Red and its analogues for their ability to prevent the formation of PrP-res in scrapie-infected cells. *J.Gen.Virol.* **81**, 1155-1164.

Sakaguchi S. (2005) Naturally arising Foxp3-expressing CD25+CD4+ regulatory T cells in immunological tolerance to self and non-self. *Nat.Immunol.* **6**, 345-352.

Samuel CE. (2001) Antiviral actions of interferons. *Clin.Microbiol.Rev.* **14**, 778-809, table.

Schatzl HM, Da Costa M, Taylor L, Cohen FE, Prusiner SB. (1995) Prion protein gene variation among primates. *J.Mol.Biol.* **245**, 362-374.

Schneider P. (2005) The role of APRIL and BAFF in lymphocyte activation. *Curr.Opin.Immunol.* **17**, 282-289.

Schwarz A, Kratke O, Burwinkel M, Riemer C, Schultz J, Henklein P et al. (2003) Immunisation with a synthetic prion protein-derived peptide prolongs survival times of mice orally exposed to the scrapie agent. *Neurosci.Lett.* **350**, 187-189.

Sethi S, Lipford G, Wagner H, Kretzschmar H. (2002) Postexposure prophylaxis against prion disease with a stimulator of innate immunity. *Lancet* **360**, 229-230.

Shevach EM. (2000) Regulatory T cells in autoimmmunity*. *Annu.Rev.Immunol.* **18**, 423-449.

Sigurdsson B. (1954) Ride-a chronic encephalitis of sheep-with general remarks on infections which develop slowly and some of their special charateristics. *Br.Vet.J.* **110**, 341-354.

Sigurdsson EM, Brown DR, Daniels M, Kascsak RJ, Kascsak R, Carp R et al. (2002) Immunization delays the onset of prion disease in mice. *Am.J.Pathol.* **161**, 13-17.

Sigurdsson EM, Sy MS, Li R, Scholtzova H, Kascsak RJ, Kascsak R et al. (2003) Anti-prion antibodies for prophylaxis following prion exposure in mice. *Neurosci.Lett.* **336**, 185-187.

Snapper CM, Yamaguchi H, Moorman MA, Sneed R, Smoot D, Mond JJ. (1993) Natural killer cells induce activated murine B cells to secrete Ig 220. *J.Immunol.* **151**, 5251-5260.

Soneoka Y, Cannon PM, Ramsdale EE, Griffiths JC, Romano G, Kingsman SM et al. (1995) A transient three-plasmid expression system for the production of high titer retroviral vectors. *Nucleic Acids Res.* **23**, 628-633.

Souan L, Tal Y, Felling Y, Cohen IR, Taraboulos A, Mor F. (2001) Modulation of proteinase-K resistant prion protein by prion peptide immunization. *Eur.J.Immunol.* **31**, 2338-2346.

Stahl N and Prusiner SB. (1991) Prions and prion proteins. *FASEB J.* **5**, 2799-2807.

Stojdl DF, Lichty BD, tenOever BR, Paterson JM, Power AT, Knowles S et al. (2003) VSV strains with defects in their ability to shutdown innate immunity are potent systemic anti-cancer agents. *Cancer Cell* **4**, 263-275.

Strengell M, Julkunen I, Matikainen S. (2004) IFN-alpha regulates IL-21 and IL-21R expression in human NK and T cells. *J.Leukoc.Biol.* **76**, 416-422.

Takaoka A, Mitani Y, Suemori H, Sato M, Yokochi T, Noguchi S et al. (2000) Cross talk between interferon-gamma and -alpha/beta signaling components in caveolar membrane domains. *Science* **288**, 2357-2360.

Takeda K and Akira S. (2003) Toll receptors and pathogen resistance. *Cell Microbiol.* **5**, 143-153.

Tato CM, Laurence A, O'Shea JJ. (2006) Helper T cell differentiation enters a new era: le roi est mort; vive le roi! *J.Exp.Med.* **203**, 809-812.

Thomsen AR, Nansen A, Andersen C, Johansen J, Marker O, Christensen JP. (1997) Cooperation of B cells and T cells is required for survival of mice infected with vesicular stomatitis virus. *Int.Immunol.* **9**, 1757-1766.

Thormar H. (1971) Slow infections of the central nervous system. II. *Z.Neurol.* **199**, 151-166.

Tiegs SL, Russell DM, Nemazee D. (1993) Receptor editing in self-reactive bone marrow B cells. *J.Exp.Med.* **177**, 1009-1020.

Tobler I, Gaus SE, Deboer T, Achermann P, Fischer M, Rulicke T et al. (1996) Altered circadian activity rhythms and sleep in mice devoid of prion protein. *Nature* **380**, 639-642.

van den Broek MF, Muller U, Huang S, Zinkernagel RM, Aguet M. (1995) Immune defence in mice lacking type I and/or type II interferon receptors. *Immunol.Rev.* **148**, 5-18.

Walker LS, Gulbranson-Judge A, Flynn S, Brocker T, Lane PJ. (2000) Co-stimulation and selection for T-cell help for germinal centres: the role of CD28 and OX40. *Immunol.Today* **21**, 333-337.

Warren HS, Vogel FR, Chedid LA. (1986) Current status of immunological adjuvants. *Annu.Rev.Immunol.* **4**, 369-388.

Weeratna RD, Brazolot Millan CL, McCluskie MJ, Davis HL. (2001) CpG ODN can re-direct the Th bias of established Th2 immune responses in adult and young mice. *FEMS Immunol.Med.Microbiol.* **32**, 65-71.

Weissmann C. (2004) The state of the prion. *Nat.Rev.Microbiol.* **2**, 861-871.

Weissmann C and Flechsig E. (2003) PrP knock-out and PrP transgenic mice in prion research. *Br.Med.Bull.* **66**, 43-60.

Wells GA, Scott AC, Johnson CT, Gunning RF, Hancock RD, Jeffrey M et al. (1987) A novel progressive spongiform encephalopathy in cattle. *Vet.Rec.* **121**, 419-420.

White AR, Enever P, Tayebi M, Mushens R, Linehan J, Brandner S et al. (2003) Monoclonal antibodies inhibit prion replication and delay the development of prion disease. *Nature* **422**, 80-83.

Will RG, Ironside JW, Zeidler M, Cousens SN, Estibeiro K, Alperovitch A et al. (1996) A new variant of Creutzfeldt-Jakob disease in the UK. *Lancet* **347**, 921-925.

Williams ES. (2002) The transmissible spongiform encephalopathies: disease risks for North America. *Vet.Clin.North Am.Food Anim Pract.* **18**, 461-473.

Williams ES and Miller MW. (2003) Transmissible spongiform encephalopathies in non-domestic animals: origin, transmission and risk factors. *Rev.Sci.Tech.* **22**, 145-156.

Williams ES and Young S. (1980) Chronic wasting disease of captive mule deer: a spongiform encephalopathy. *J.Wildl.Dis.* **16**, 89-98.

Wolniak KL, Shinall SM, Waldschmidt TJ. (2004) The germinal center response. *Crit Rev.Immunol.* **24**, 39-65.

Zahn R, von Schroetter C, Wuthrich K. (1997) Human prion proteins expressed in Escherichia coli and purified by high-affinity column refolding. *FEBS Lett.* **417**, 400-404.

Zhang CC, Steele AD, Lindquist S, Lodish HF. (2006) Prion protein is expressed on long-term repopulating hematopoietic stem cells and is important for their self-renewal. *Proc.Natl.Acad.Sci.U.S.A* **103**, 2184-2189.

Zhang X, Sun S, Hwang I, Tough DF, Sprent J. (1998) Potent and selective stimulation of memory-phenotype CD8+ T cells in vivo by IL-15. *Immunity.* **8**, 591-599.

10 Curriculum Vitae

Patricia Bach

Paul-Ehrlich-Institut
Abteilung Immunologie
Paul-Ehrlich-Strasse 51-59
D-63225 Langen, Deutschland

Telefon:	+49-6103-775104
Fax:	+49-6103-771253
E-mail:	bacpa@pei.de

Persönliche Daten

Name:	Patricia Bach
Geburtsdatum:	02.01.1978
Geburtsort:	Offenbach am Main
Staatsangehörigkeit:	deutsch

Schulausbildung

1984-1988:	Grundschule „Johannes Gutenberg“, Hainburg
1988-1997:	„Einhardgymnasium“, Seligenstadt und „Claus von Stauffenberg-Gymnasium“, Rodgau, Erlangung der allgemeinen Hochschulreife

Studium

10/1997-09/1999:	Grundstudium der Biologie (Diplom) an der Johann Wolfgang Goethe-Universität Frankfurt/Main
09/1999-07/2002:	Hauptstudium der Biologie (Diplom) an der Johann Wolfgang Goethe-Universität Frankfurt/Main
10/2001-07/2002:	Diplomarbeit am Paul-Ehrlich-Institut in der Abteilung Virologie unter der Leitung von Fr. Dr. Roswitha Löwer und Fr. Prof. Dr. A. Starzinski-Powitz mit dem Thema: „Vergleichende Studien zur Expression der Leptinrezeptor-Isoformen in humanen und animalen Geweben“ Abschluß mit Diplom
Seit 11/2002:	Promotion am Paul-Ehrlich Institut in der Abteilung Immunologie unter der Leitung von Herrn Dr. U. Kalinke Thema der Promotion: „Immunogenicity of antigen-displaying virus-like particles and their use as a potential vaccine against prion diseases“ im Rahmen des EU Projektes „PRIOVAX“

Hainburg den 24.07.2007

Patricia Bach

11 Konferenzteilnahmen mit Posterpräsentationen

09/2003: GfV Workshop „Immunobiology of Viral Infections“, Zeilitzheim
“Vaccination against prion disease” (Talk)

10/2003: “International Prion Conference”, München
„Induction of prion protein-specific antibody responses using PrP-retroparticles” (Poster)

10/2005: “International Prion Conference Prion 2005”, Düsseldorf
„PrP-displaying retroparticles as a novel tool for mapping the fine specificity of antibodies binding to the cellular form of the prion protein” (Poster)

03/2006: “B cell Meeting”, Kloster Banz
„The impact of virus-induced Type I interferon on anti-viral antibody cell responses“ (Poster)

09/2006: “16th European Congress of Immunology”, Paris
“Virus-induced Type I interferon is required to promote IgG switch of neutralizing antibody cell responses” (Poster)

12 Publikationen

Bach P, Kamphuis E, Odermatt B, Sutter G, Buchholz CJ, Kalinke U. (**2007**) Vesicular stomatitis virus glycoprotein displaying retrovirus-like particles induce a type I IFN receptor-dependent switch to neutralizing IgG antibodies. *J.Immunol.* 178, 5839-5847.

Buchholz CJ, **Bach P**, Nikles D, Kalinke U. (**2006**) Prion protein-specific antibodies for therapeutic intervention of transmissible spongiform encephalopathies. *Expert.Opin.Biol.Ther.* 6, 293-300.

Kalinke U, **Bach P,** Konig M, Buchholz CJ. (**2006**) Vaccination against prion diseases. *Discov.Med.* 6, 29-34.

Nikles D*, **Bach P***, Boller K, Merten CA, Montrasio F, Heppner FL et al. (**2005**) Circumventing tolerance to the prion protein (PrP): vaccination with PrP-displaying retrovirus particles induces humoral immune responses against the native form of cellular PrP. *J.Virol.* 79, 4033-4042.

Dominguez D, Tournoy J, Hartmann D, Huth T, Cryns K, Deforce S, Serneels L, Camacho I E, Marjaux E, Craessaerts K, Roebroek A J, SchwakeM, D'Hooge R, **Bach P**, Kalinke U et al. (**2005**) Phenotypic and biochemical analyses of BACE1- and BACE2-deficient mice. *J.Biol.Chem.* **280**, 30797-30806.

***authors contributed equally to this work

13 Patente

“Vaccination against amyloid diseases using retrovirus-like particles displaying amyloid peptides” (submitted by PD Dr. Christian Buchholz, Dr. Ulrich Kalinke, Patricia Bach and Prof. Dr. Ulrike Müller, 2007)

14 Danksagung

Mein besonderer Dank geht an Herrn Dr. Ulrich Kalinke für die Überlassung des Themas und für die Möglichkeit am Paul-Ehrlich-Institut meine Doktorarbeit durchführen zu können, sowie für die hervorragenden Arbeitsbedingungen und die gute Ausbildung. Seine Motivationsfähigkeit und die Begeisterung für die Forschung haben mir die Tür zum wissenschaftlichen Arbeiten geöffnet.

Des Weiteren möchte ich mich bei Prof. Dr. Michael A. Klein für die Betreuung meiner Arbeit an der Julius-Maximilian Universität Würzburg bedanken.
Herrn Prof. Dr. Thomas Raabe danke ich für die Übernahme des Zweitgutachtens dieser Arbeit.

Ich bedanke mich bei Herrn PD Dr. Christian Buchholz, Dr. Daphne Nikles und bei Gundi Braun für die außerordentlich gute Zusammenarbeit und Diskussionen bezüglich unterschiedlicher Projekte. Bei Dr. Fabio Montrasio bedanke ich mich in diesem Zusammenhang für viele fachliche Ratschläge sowie für die Hilfestellung bei allen Scrapie Inokkulationsexperimenten.

Nur der umfangreichen Zucht und fachgerechter Tierpflege durch Dorothea Kreuz und vielen Tierpflegern ist es zu verdanken, dass für die verschiedenen Experimenten genügend gesunde Tiere zur Verfügung standen. Dafür ein ganz großes Dankeschön.

Weiterhin möchte ich mich bei Wilfried Dreher und Dr. Klaus Boller für die Unterstützung bei mikroskopischen Angelegenheiten bedanken. Herrn Kay-Martin Hanschmann danke ich für die statistische Auswertung der Experimente.

Allen jetzigen und früheren Kollegen der Abteilung „Immunologie 3/0“ danke ich für die angenehme Atmosphäre und die schöne Zeit im Labor, die ich auch weiterhin genießen darf. Insbesondere danke ich Elisabeth Kamphuis für die

nette Zeit die wir in der Anfangsphase als „Erstdoktoranden“ in der Abteilung Immunologie hatten, Martin König als „Prionenkollege“ für den Spaß innerhalb und außerhalb des Labors, Claudia Detje für die Unterstützung insbesondere in der letzten Phase des Zusammenschreibens, Sven Flindt, unserem „Labormanager“ für die zahlreichen Hilfestellungen am FACS und für Gespräche bezüglich unterschiedlicher Methoden und natürlich dem Rest der „Rosa Labor-Fraktion“ Martina Anzahge, Stefanie Bauer, Thereasa Frenz, Kathrin Gibbert, Suse Roederstein, Linda Sender und Dr. Zoe Waibler.

Allen Doktorandenkollegen, sowie TA´s und anderen Mitarbeitern des Institutes danke ich für die Zusammenarbeit und die sehr gute Atmosphäre innerhalb und außerhalb des Instituts.

Nicht zuletzt danke ich all meinen Freunden, die mich während dieser Zeit auch bei der Bewältigung von schwierigen Lebensphasen ständig aufgemuntert und unterstützt haben. Ein ganz großer Dank geht an Christina Hartz, die mir in vielen Lebenslagen beiseite stand und immer ein offenes Ohr für mich hatte.

Zum Schluß möchte ich mich bei meinen Eltern Norma und Otto Bach ganz besonders bedanken, da Sie mich während des Studiums und der Promotionszeit in jeglicher Form unterstützt haben. Ich widme diese Arbeit meinen Eltern, weil ohne sie dies alles nicht möglich gewesen wäre.

Erklärung:

Hiermit erkläre ich ehrenwörtlich, dass ich diese Dissertation selbständig angefertigt und keine anderen als die von mir angegebenen Hilfsmittel und Quellen benutzt habe.
Zudem erkläre ich, dass diese Dissertation weder in gleicher noch in anderer Form bereits in einem Prüfungsverfahren vorgelegen hat.
Ich habe früher, außer den mit dem Zulassungsgesuch urkundlichen Graden, keine weiteren akademischen Grade erworben oder zu erwerben versucht.

Hainburg den 24.07.2007

Patricia Bach